

NASA Technical Memorandum 86687

(NASA-TM-86687) ROTORCRAFT RESEARCH TESTING  
IN THE NATIONAL FULL-SCALE AERODYNAMICS  
COMPLEX AT NASA AMES RESEARCH CENTER (NASA)  
90 p HC A05/MF A01 CSCI 01C

N85-27854

UNCLASSIFIED  
G3/05 21502

---

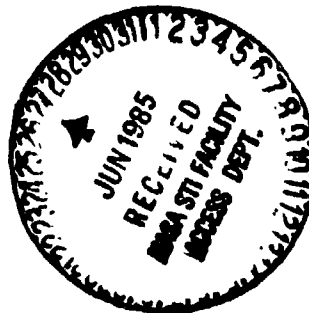
# Rotorcraft Research Testing in the National Full-Scale Aerodynamics Complex at NASA Ames Research Center

---

William Warmbrodt, Charles A. Smith, and  
Wayne Johnson

---

May 1985



---

# **Rotorcraft Research Testing in the National Full-Scale Aerodynamics Complex at NASA Ames Research Center**

---

William Warmbrodt  
Charles A. Smith  
Wayne Johnson, Ames Research Center, Moffett Field, California

May 1985

**NASA**

National Aeronautics and  
Space Administration

**Ames Research Center**  
Moffett Field, California 94035

## SUMMARY

The unique capabilities of the National Full-Scale Aerodynamics Complex (NFAC) for testing rotorcraft systems are described. The test facilities include the 40- by 80-Foot Wind Tunnel, the 80- by 120-Foot Wind Tunnel, and the Outdoor Aerodynamic Research Facility. The Ames 7- by 10-Foot Subsonic Wind Tunnel is also used in support of the rotor research programs conducted in the NFAC. Detailed descriptions of each of the facilities, with an emphasis on helicopter rotor test capability, are presented. The special purpose rotor test equipment used in conducting helicopter research is reviewed. Test rigs to operate full-scale helicopter main rotors, helicopter tail rotors, and tilting prop-rotors are available, as well as full-scale and small-scale rotor systems for use in various research programs. The specialized data-acquisition and analysis systems used in rotorcraft experiments in these facilities are reviewed. Special test equipment, including several laser Doppler velocimeters (LDVs), are briefly described. Lastly, the test procedures used in conducting rotor experiments are discussed together with representative data obtained from previous test programs. Specific examples are given for rotor performance, loads, acoustics, system interactions, dynamic and aeroelastic stability, and advanced technology and prototype demonstration models.

## INTRODUCTION

The National Full-Scale Aerodynamics Complex (NFAC) at Ames Research Center provides the United States the capability to perform helicopter wind-tunnel research at full- and large-scale. This unique national facility includes the 40- by 80-Foot Wind Tunnel, the 80- by 120-Foot Wind Tunnel, and the Outdoor Aerodynamic Research Facility (fig. 1). The helicopter research conducted in the NFAC encompasses a wide range of investigations into helicopter aerodynamics, dynamics, and acoustics, as well as studies of technology demonstrator rotorcraft and their systems. To realize maximum benefit from the full-scale test programs, small-scale rotor research experiments are also performed to provide insight into the basic physics and guidance in establishing the approach and data measurements necessary for full-scale investigations. To this end, the Ames 7- by 10-Foot Subsonic Wind Tunnel (fig. 2) is utilized to support the full-scale research programs.

Many helicopter-related tests have been performed in the NFAC. The first, which dates back to 1953, was a test of an XV-1 compound helicopter with a pusher propeller (fig. 3(a)). The first helicopter main-rotor test was conducted in 1957 when a three-bladed Boeing Vertol helicopter rotor, using boundary-layer control for improved performance, was tested using a unique three-strut/drive system arrangement

(fig. 3(b)). Some of the major rotorcraft experiments performed in the Ames full-scale wind tunnel and ground-based hover facility are given in table 1. Many of these models were tested in the wind tunnel with more than one test entry. The dates listed are for each model's first tunnel occupancy. These tests have included use of special test equipment to investigate specific advanced technologies applied to helicopter rotor systems (boundary layer control, jet flap and multicyclic control, circulation control, bearingless rotor hubs, and advanced airfoils and planforms). Other tests have documented overall rotorcraft vehicle performance (XV-1, XV-3, UH-1, OH-6, XH-56, and XV-15). Installation photographs of several of these tests are also shown in figure 3. Tests have also been performed on technology demonstrator rotor systems aircraft (tilting prop-rotor aircraft, coaxial hingeless rotors, and stoppable circulation-controlled rotor systems).

Since the first rotor tests in the 40- by 80-Foot Wind Tunnel, the capability has been developed to perform a wide variety of full-scale tests using unique equipment and test techniques. This capability includes special test equipment to operate full-scale helicopter main rotors, tail rotors, and tilting prop-rotors in both an outdoor ground-based hover environment and in a wind-tunnel; a comprehensive data-acquisition and reduction system developed to analyze helicopter rotor operation; several full-scale and small-scale model helicopter rotor systems; several special-purpose digital data analysis systems for on-line, real-time dynamics testing; and nonintrusive laser velocimeter flow-measurement systems.

The test facilities and equipment afforded by the NFAC for helicopter research are described in detail. How these systems are used in the helicopter research programs, using specific examples and representative test results, is discussed, and test procedures for full-scale investigations of helicopter rotor performance, acoustics, and dynamics are reviewed. Where appropriate, the effect on these test procedures of the unique requirements of full-scale tests is assessed. Results from several representative tests demonstrate the research results of full-scale, ground-based hover and forward flight helicopter testing in the NFAC.

## FACILITIES

### 40- by 80-Foot Wind Tunnel

The Ames 40- by 80-Foot Wind Tunnel was first used for research testing in 1944. As mentioned above, the first rotorcraft test was performed in it in 1953. The wind tunnel has a closed 40- by 80-ft test section with semicircular sides with radii of 20 ft, and a closed-circuit air return passage. The test section is lined with 6 in. of sound absorptive material to improve the quality of acoustic measurements. Figure 4 shows the test section with the acoustic lining installed. Beneath the lining, the walls have 0.625-in. to 1.25-in. thick armor plating for purposes of safety. The test section (net dimensions) is now 39 ft high, 79 ft wide, and 80 ft long. Models are installed through overhead doors in the test section, 78.5 ft wide by 49 ft long. The test section is located on the third deck of the facility. The

control room for the 40- by 80-foot Wind Tunnel test section is located immediately adjacent to the room on the second deck which houses the wind-tunnel scale system.

The air is driven by six 40-ft-diam fans, each powered by a three-phase synchronous motor rated at 12 MW (18,000 hp) continuous with a 2-hr 20% overload capacity. The motor-generator system that supplies power to the fan drive motors may be operated continuously at any power output up to a maximum of 106 MW. The fan speed is variable from 36 to 180 rpm, and the fan-blade pitch angles are variable from  $-18^{\circ}$  to  $52^{\circ}$ . The speed range of the tunnel is 0 to about 300 knots, continuously variable. The tunnel stagnation pressure is atmospheric. The tunnel stagnation temperature is uncontrolled, and depends on atmospheric conditions and the energy production of the model. An air exchanger, upstream of the fans, can provide up to 10% of the air (5% at full speed), which does offer some temperature control.

The primary model support system consists of three movable struts mounted on a turntable. The height of the two forward struts is variable between 2 and 20 ft, and the struts may be adjusted laterally to accommodate different model treads (8 to 20 ft). A single telescoping tail strut may be adjusted longitudinally to accept models of varying tail length (8.2 to 20 ft). Model angle of attack is varied during testing by varying the length of the tail strut; the angle-of-attack range is typically  $20^{\circ}$ . Model angle of yaw is varied during testing by rotating the turntable ( $290^{\circ}$  range). Each strut is shielded from the airstream by a fairing, which is mounted independently of the struts to a nonmetric floor turntable. The struts themselves are mounted on a strut turntable, which in turn is mounted to the wind-tunnel balance. As the turntable is rotated, the strut fairings are rotated also so that they remain aligned with the windstream. Alternative support systems, including semispan and sting mounts, are available. Mechanical lever systems transmit the model loads to seven scales located beneath the floor of the tunnel. The capability of each scale (2 front lift, 2 rear lift, 1 drag force, 2 side force) is shown in table 2. Accuracies of the resulting force measurements are shown in table 3; they range from 0.01% of full scale for lift to 0.09% of full scale for pitch moment.

The wind-tunnel balance system may be operated completely free or with eight viscous dampers installed (two on each side of the balance frame). The dampers, which are mechanically installed, significantly increase the damping of the balance-system modes. A hydraulic snubber system can also be activated during testing if large balance-system vibrations occur. When this snubber system is activated, the balance system is locked, and scale data cannot be acquired.

Helicopter main and tail rotors are frequently powered by electric motors during wind tunnel testing. Two variable-frequency (0 to 150 Hz) motor-generator sets are available, with maximum power of 3000 hp at 150 Hz. Two additional variable-frequency (0 to 400 Hz) motor-generator sets are available, with maximum power of 900 hp at 400 Hz.

Several enhancement projects have been conducted in the last decade: replacement of the balance and strut system; replacement of the scales; expansion of the control room and computer room; replacement of the data-acquisition computers, and expansion of the data-acquisition software; and installation of test section

acoustic treatment. Currently in progress is a major modification project that involves repowering the wind tunnel and adding a new open-circuit leg with an 80- by 120-ft test section.

### 80- by 120-Foot Wind Tunnel

The world's largest wind tunnel is soon to be part of the NFAC helicopter research program. The 80- by 120-Foot Wind Tunnel is scheduled to begin operational research testing in 1987. It is an open-circuit tunnel and uses the same 106-MW drive system as the 40- by 80-Foot Wind Tunnel. By opening and closing appropriate vane sets and exit louvers (fig. 5) located within the closed-circuit portion of the tunnel, air can be drawn in through the rectangular inlet, through the test section, deflected to pass through the drive system, and then caused to exit through louvers located in the tunnel wall. The wind tunnel will have a maximum airspeed capability of about 100 knots. A scaled-up design of the 40- by 80-Foot Wind Tunnel turntable, T-frame, and balance system is used. The capacities of the individual scale-heads are given in table 2, and the anticipated accuracies listed in table 3. Single-, dual-, and three-strut mountings will be used for model installation. Model pitch can be changed using a telescoping tail strut similar to that of the 40- by 80-ft design. Access to the test section is provided by two large doors (60 ft wide, 80 ft high), which are located on the east side of the tunnel test section (fig. 6). A 75-ton-capacity gantry crane, which can be operated within the wind-tunnel test section, is used for installing and removing models. The gantry crane runs on a rail system located outside and directly beneath the test section, allowing the crane to span the test section turntable. There is no acoustic liner on the walls of the test section, which are made of metal sheeting with limited armor plating. A dedicated set of model utilities (oil, water, air, fuel, electric power) is available for model operation.

As a result of the tunnel design, the wind-tunnel test section is located on the third deck of the facility. The tunnel control room is located on the first deck, immediately adjacent to the room housing the wind tunnel balance system. The control room includes all controls for operating the wind tunnel, for controlling the helicopter model, and for controlling the model's required utility systems. A full array of on-line instrumentation monitoring equipment is available. A computer room next to the control room houses the data-acquisition computer system.

Because of its size, the 80- by 120-ft tunnel will provide a unique opportunity to test very large helicopter rotor systems. During test operation, the helicopter rotor will be 30 to 50 ft above the ground. For the first time, this will make it possible to test full-scale rotor systems at very low forward flight speeds in ground-based tests without significant wind-tunnel wall or floor effects.

### Outdoor Aerodynamic Research Facility

The Outdoor Aerodynamic Research Facility can be used to obtain a wide variety of ground-based hover data on full-scale or small-scale rotorcraft. It can also be

used as an area for checking out the systems of a model before the model is installed in the wind tunnel (fig. 7). The test facility consists of a 100- by 100-ft concrete pad. A strut mounting T-frame, sized for the 40- by 80-ft test section, is located beneath the center of the test pad. No integral balance system exists. Model forces and moments are measured in a typical installation by using a balance within the model itself or by using several one-, two-, or three-component load cells mounted between the metric portion of the model and the supporting strut system. The facility is sufficiently remote from other buildings at Ames so that accurate near- and far-field acoustic data can be obtained. A 30- by 40-ft control room, partially underground, contains model controls, monitoring equipment, and closed-circuit television; the control room is located immediately adjacent to the test area. A complete data system for monitoring and recording data is available. A second underground room houses the 150- and 400-cycle variable-frequency electric power supplies. A 75-ton-capacity overhead crane, identical to that available in the 80- by 120-Foot Wind Tunnel, is used for positioning models. It moves on a rail system to straddle the test area or can be positioned away from the test area.

#### 7- by 10-Foot Subsonic Wind Tunnel

Small-scale helicopter research experiments are performed in the Ames 7- by 10-Foot Subsonic Wind Tunnel (fig. 8). It is one of two low-speed, closed-circuit, atmospheric 7- by 10-ft tunnels at Ames. The test section velocities are continuously variable from 0 to 220 knots with a maximum Reynolds number of  $2.3 \times 10^6/\text{ft}$ . This airflow is produced by a single, eight-blade, fixed-pitch, 28-ft-diam fan, driven by a 1.34-MW (1600 hp) variable-speed electric motor. Maximum tunnel speed is obtained at a fan rotation rate of 360 rpm. The wind-tunnel cross legs are treated to reduce the background noise in the test section, which results from both the drive fan and outside noise entering through the air exchanger.

Models are generally supported on a single or dual pair of vertical struts, each with a trailing link which provides remote pitch control (fig. 9). Semispan models can attach directly to the wind-tunnel turntable/balance system or may include an integral balance within the model. Model test stands can mount directly to the wind-tunnel turntable. A high-pressure 3000-lb/in.<sup>2</sup> air system is available for model use. Electric power to the model is supplied by a 100-kW, 400-cycle, variable-frequency power system. A 2-ton ceiling crane allows for installation and removal of tunnel models through the tunnel ceiling.

The external six-component balance system is typically used to measure model forces and moments. Three lift scales (two front, one rear), two side-force scales (front and rear), a drag scale, and dynamic pressure scale are used. Scale capacities are listed in table 2. Overall scale-system accuracies are listed in table 3.

The tunnel can be operated in three different modes: closed test section with hard walls; closed test section with soft walls; and an open test section with the floor remaining in place. The closed test section with hard walls is the basic configuration for aerodynamic testing. Each of the two side walls of the test section is composed of five removable panels. The 3- by 7-ft panels are latched in place

and can be easily removed for access to the test section. Personnel access doors are also located in each wall. The closed test section with soft walls is used for acoustic research. Sound absorbent wall and ceiling panels are composed of 3-in. foam glued to an open mesh that is suspended 3 in. from a back wall. Each panel is 3 ft wide and is positioned such that the internal dimensions of the test section remain 7 by 10 ft exclusive of any foam treatment. With the treatment installed, the maximum airspeed of the test section is reduced to approximately 170 knots. The open test section allows for aero-acoustic helicopter research without tunnel walls or ceiling to allow microphone placement in the far-field outside the airflow. A three-sided collector attaches to the diffuser inlet to capture the jet. In this configuration, maximum tunnel speed is about 130 knots. A gust generator capable of producing sinusoidal lateral or longitudinal gusts is available for any tunnel configuration. The gust generator utilizes harmonic circulation control of twin parallel airfoils to achieve the harmonic lift variation required for gust generation.

## DATA SYSTEMS

### Wind-Tunnel Data-Acquisition System

Each site of the NFAC has a distributed computed-based data-acquisition system (fig. 10). The basic data path begins at the model, where the measurements include, for instance, balance forces, pressures (via scanivalves), and blade loads from strain gages. A Kernel System provides signal conditioning, digitizing, multiplex/demultiplex, and control of other data-acquisition hardware. The principal parts of the Kernel System are the remote multiplexer/demultiplexer units (RMDUs) and RMDU control units (RCUs). The RMDUs can be configured in many ways, using various plug-in card configurations for low-level or high-level analog or digital signals as required. The maximum number of channels possible with the present hardware for one RMDU is 352 high-level analog signals. The RMDU handles digitization and multiplexing of the data, sending a pulse-code-modulated (PCM) signal to the RCU. The RMDU can be located on the model, so the PCM format greatly reduces the number of wires between the model and the control room. The present RMDUs are not suitable for installation on a rotor hub, but it is planned to acquire RMDUs that are small, can handle about 200 low-level analog channels, and can be used in the rotating frame.

The RCUs control acquisition of the PCM data from the RMDUs, under the direction of the Kernel System (a DEC PDP 11/34 computer in the 40- by 80-ft and 80- by 120-ft tunnel data systems). The RCU is capable of a scan rate (aggregate sample rate) of 250 Hz to 125 kHz. The azimuth and N-per-rev (AZ/NPR) pulse from the rotor can be used to initiate the data-acquisition process and trigger each data scan, respectively.

The Data Gathering Processor (DGP) receives data in digital form from the Kernel System. The DGP, which is a DEC PDP 11/70 computer in the 40- by 80-ft and 80- by 120-ft tunnels, controls data acquisition, records data, computes reduced



data in real time, and displays the computed data for model/tunnel parameter control. The DGP receives data in two modes: static (total rate 40-62 K/sec) and dynamic (total rate 75-125 K/sec). Static data are averaged by the DGP, and only the averaged values are stored in the static data base. Other parameters can also be obtained from the static channels, such as minimum, maximum, or rms values. For dynamic data, the entire time-history is recorded by the DGP. If there are too many channels to be sampled simultaneously within the above data rates, the data are acquired in more than one pass (a single channel can be sampled in each of the passes, or in both the dynamic and static modes). The DGP sends the data in digital form to the Real-time Executive Processor (REP). The REP, which is a DEC VAX 11/780 computer in the 40- by 80-ft and 80- by 120-ft tunnel data systems, is used on-line to reduce data as required to aid the conduct of the test, and is used to reduce all the static data at the end of a run.

For historical reasons, the 40- by 80-Foot Wind Tunnel (however, not the other NFAC sites) also has a High-Speed Data-Acquisition System (HSDAS), which can simultaneously sample 60 analog channels and send the dynamic data in digital form directly to the DGP. The DGP writes the data to disk and to a digital magnetic tape for postrun processing. Both the DGP and the REP have printers for output during and after a run. The REP can also send the static data base to a Display Processor System (DPS), for plotting data during or after a run. The REP has an Array Processor, which provides it direct access to the Kernel System PCM data during a run; this link is useful particularly as a diagnostic tool for the data system. The Signal Analysis System (SAS) can digitize and analyze up to 181 channels of analog data. The SAS is used during a run for damping measurements in flutter testing, and for general diagnostics of the model and data system. The SAS is also used for posttest reduction of the acoustic data.

Acoustics measurements generally form an entirely separate data path, because the frequency content of the data signals is so much higher than that of the other measurements. The microphone signals are recorded on analog tape for posttest reduction. An interface is available, however, to send dBA measurements to an RMDU, to be included directly in the static data base.

The data system also provides information for control and monitoring of the test. The DGP can perform real-time computations using the static data, and display up to 32 parameters on a cathode-ray tube (CRT) in the control room (typically updated every 2 sec). These parameters would normally include the tunnel speed or advance ratio; the rotor speed or tip Mach number; the rotor lift, drag, hub moment, or power in coefficient form; control positions and shaft angle. A system for real-time monitoring of dynamic measurements accepts up to two PCM streams from the Kernel System and 32 analog channels. This monitor system includes a 50-channel bar-chart display (for mean, maximum, minimum, half peak-to-peak, or rms), eight channels of oscilloscope display, and 18 channels of oscillograph display (eventually to be replaced by brush recorders).

Common data-acquisition software is used for all of the NFAC sites (and in fact all other wind tunnels at Ames). The data systems for all NFAC sites are identical in overall structure, but there are significant differences in the hardware. The

40- by 80-ft and the 80- by 120-ft tunnels are very similar, except for the absence of the HSDAS at the latter. The Outdoor Aerodynamic Research Facility and the 7- by 10-ft tunnel have less capability. These two sites have more limited dynamic monitoring capability, and do not have an REP (and with it the array processor and display processor system), although the intention is to connect them to the REPs at the other sites through fiber optic links. The 7- by 10-ft tunnel has a DEC PDP 11/34 as a DGP. Lacking a DMA70 interface, the dynamic data are limited to the same rate as the static data acquisition. However, the overall rate limit is more important for small-scale testing, in which the rotor rotational speeds are typically 6 to 7 times those for full-scale models.

### Rotor Data Reduction System

Rotor testing is notable for the great quantity of dynamic data that is acquired, as well as the existence of fairly standard requirements for basic reduction of the static and dynamic data. Hence, a Rotor Data Reduction System (RDRS) has been developed (fig. 11). This system reads the data tapes generated by the wind-tunnel data-acquisition system; performs the primary data reduction, and creates the data base; and controls output of the data by various means. The structure of the system has been governed by the nature of the hardware and software of the wind-tunnel data-acquisition system, and by the nature of wind-tunnel testing of helicopter rotors. The software is largely interactive, and is resident on a DEC VAX 11/780 computer with four 256-Mbyte RM05 disks dedicated to the system (one for software and three for data).

The basic data path involves reading the digital magnetic tapes, reducing the data, and forming the data base. The data base resides in direct access files on disks. The data base includes static, dynamic, acoustic, and scanivalve data types. Raw data are kept on disk to facilitate re-reduction; however, because of the great quantity of dynamic data, only the reduced dynamic data are included.

The basic data-reduction process is based on converting measurements from a linear transducer to engineering units. A zero, measured at the beginning of the run, is subtracted from the raw data obtained during a run. The conversion factor is preferably obtained using a calibration step measured at the beginning of each run. For the static data, standard equations are used for reduction of the rotor forces, power, etc. Usually, there is also a large test-dependent part of the static data-reduction program. Typically, the static data base consists of 50 to 250 reduced parameters per data-acquisition point. An identical program is executed off-line on the REP of the wind-tunnel data system to reduce the static data immediately after a run.

Dynamic data are typically sampled synchronously with the rotor rotation at 64 samples per rotor revolution. They are converted to engineering units, using the zero and calibration data as described above. Then, a Fourier transform of eight revolutions of data is performed; the data are smoothed and averaged by dropping subharmonics and higher harmonics in the frequency domain; the data are corrected for analog filters and PCM sampling time skew in the frequency domain; and the

corrected signal is reconstructed, using an inverse fast Fourier transform. Mean, half peak-to-peak, and harmonic data are normally used from the corrected signal. For dynamic pressure data, it is also useful to create new dynamic channels of integrated aerodynamic load, by summing the measured channels over the chord or the planform. A generalized normalization procedure is available, allowing output of all the data normalized with measurements from the static data base (such as air density, tunnel dynamic pressure, or rotor tip speed).

The analog tapes of acoustic data are reduced using the SAS. Digital time-histories of the rotor noise data are obtained directly from the SAS. The acoustic information transmitted to the RDRS for incorporation in the data base includes the overall sound pressure level, dBA, PNdB, blade-passage harmonics, minimum and maximum pressure, and 1/3-octave spectra. The acoustic data are also corrected for wind-tunnel background noise by the RDRS.

Output is available in standard forms on various devices. The output includes listings and plots. Plots are available for time-histories, harmonics, and pressures, and in polar, x-y, contour, and carpet-plot format. Interface programs are available to read the data base for test-dependent output format, such as preparation of data reports.

## TEST EQUIPMENT

### Rotor Test Apparatus

The Rotor Test Apparatus (RTA) is a special-purpose drive and support system for operating helicopter rotors in the NFAC (fig. 12). It has been used in numerous wind-tunnel tests with articulated, hingeless, and bearingless rotor systems. It houses two 1500 hp, 150-cycle electric motors. The use of electric power to operate rotor systems is preferred in the various facilities for wider rotational speed control and to reduce the possibility of accidents involving flammable fuels. Two transmission gearboxes are available: a high-speed transmission (6.9:1; 437 maximum rotor rpm) and a low-speed transmission (11.05:1; 271 maximum rotor rpm). The RTA has hydraulic servo actuators for the primary control system (blade collective, longitudinal, and lateral cyclic pitch) to establish rotor trim operating conditions. It also has a dynamic control system, which is capable of introducing dynamic perturbations to the nonrotating swashplate (collective and tilt), at frequencies up to 30 Hz. This dynamic control system can be used for both transient excitation of the rotor system for aeroelastic stability testing and for N-per-rev multicyclic control testing.

The RTA control console allows for external control of the dynamic control system by the Multicyclic Computer Control System (MCCS) (see next section). The rotor console operator has individual toggle switches for changes in rotor collective and cyclic pitch. Displayed information to the operator includes a resolved blade-flap measurement for coning and cyclic flapping, a resolved blade-pitch measurement for collective and cyclic pitch, and displays of the commanded pitch from

the console for collective and cyclic pitch. Blade-pitch and flap measurements can be obtained from angulators located within a blade's flap and pitch bearing or hinge. In some cases, particularly for hingeless or bearingless hub designs, strain gages are used to provide indirect measures of flapping motion.

A typical test installation in the 40- by 80-Foot Wind Tunnel is shown in figure 13. To install a rotor system onto the RTA, new swashplate hardware (non-rotating and rotating) and hub-adapting hardware are required. Model utility leads and instrumentation lines are run down inside the main struts. Various strut systems are available for mounting the rig in the wind tunnel. Each uses a different set of strut tips to locate the rotor hub approximately at the center line of the tunnel. Similar installations can be used in the 80- by 120-Foot Wind Tunnel and in the Outdoor Aerodynamic Research Facility.

#### Model 576 Test Stand

The Model 576 Test Stand is the second general-purpose test apparatus used to test full-scale rotors in the NFAC. It is a body of revolution (consequently, it is called the "Easter Egg" (EE)) with a profile of a NACA 0030-74 (mod) airfoil. A typical installation in the 40- by 80-Foot Wind Tunnel is shown in figure 14 with a strut system no longer in use. It houses a 7.81:1 transmission and one 1500 hp, 150-cycle electric drive motor. The maximum rotor rotation rate is 383 rpm. The test stand was originally designed (by virtue of its transmission/control-system design) to operate two-bladed helicopter rotor systems. Three recent modifications to this stand make it ideally suited for rotor/fuselage interaction tests. First, the fuselage frame itself is mounted on load cells so that both rotor and fuselage loads can be determined. Complete system performance can be determined from the wind-tunnel balance system; body loads can be determined from the load cells. Second, two new modified front noses for the rig were designed and fabricated. These will make it possible to investigate basic changes in the body configuration on body forces and rotor performance and airloads. Third, 108 pressure taps have been added to the external fairing in circumferential rings at 12 axial stations to provide static and dynamic body pressure measurements. This will provide details of the effect of the rotor wake on the test stand fuselage.

#### Tail-Rotor Test Rig

The tail-rotor test rig was designed to test full-scale tail rotors in the wake of a main rotor in the NFAC (fig. 15). The test rig would be positioned behind the main-rotor/test-apparatus installation in the wind-tunnel test section. The rig is mounted to a traversing system that allows the tail-rotor column to be moved laterally and longitudinally in the wind tunnel on a system of rails. Vertical motion is accomplished by raising or lowering the pylon pod's position on the vertical column. A separate, three-component balance with a capacity of 1000 lb of thrust and 570 ft-lb of torque is installed in the pylon; it measures tail-rotor performance independently of the main rotor. The horizontal drive pod contains a 250 hp drive

motor and a right-angle gearbox. Maximum rotor rotation speed is 1850 rpm (37:19 gearbox). The vertical column is 27 ft high and is enclosed in a set of telescoping fairings. As the drive pod rises or descends on the vertical support, these fairings ride over each other.

#### Prop Test Rig

Large- and full-scale tilting prop-rotor systems can be tested in hover and forward flight using the prop test rig (fig. 16). The rig houses two 1500-hp, 150-cycle electric motors and a 4:1 gearbox. Maximum output is 3000 hp at a rotor rate of 750 rpm. A rotor hub balance can be used that has an exceptionally high sensitivity to rotor thrust with minimal interactions, owing to other forces, moments, and thermal effects. With this balance, rotor thrust up to 16,000 lb can be measured to within 0.3% full range. A drive shaft load cell, accurate to 0.2% full range, has a 21,000 ft-lb capacity. For wind-tunnel testing, the rig is installed on two main struts. The angle of incidence of the pylon to the oncoming wind is varied by yawing the turntable. Hover performance can be obtained with the prop test rig at the Outdoor Aerodynamic Research Facility. For such a test, the rig is mounted on a rigid A-frame, which is in turn supported by a three-point strut system. Three-component load cells can be used at strut attachment points to provide a second, redundant set of rotor performance measurements accurate to within about 1% of full range in thrust. The use of the A-frame support can allow for the positioning of a bluff body in the rotor wake, clear of the supporting struts, when performing large-scale investigations of rotor/body aerodynamic interactions and when studying wing download in a tilting prop-rotor hover mode.

#### Model Rotor Test Rig

To support the full-scale test programs, a small-scale rotor test rig is used for hover and forward flight experiments (fig. 17). The rig is a general purpose test stand which can be used to test Mach-scaled two- to seven-bladed rotor systems up to 7 ft in diameter. The 110 hp, 400-cycle electric motor drives through a gearbox with twin output shaft for maximum rotor rotation rates of either 2800 (5:1) or 2000 (3.57:1) rpm. Rotation rates in either clockwise or counterclockwise directions are possible. Rotor thrust can be either up or down, depending on the particular experiment. The rig has a 102-channel slip-ring assembly. A body gimbal, which allows pitch and roll motion about a point on the drive shaft approximately 12 in. below the rotor hub, has springs and viscous dampers which can be used to tune the fixed system dynamics to minimize coupled rotor/body dynamic problems.

Rotor swashplate control is by three low-speed electromechanical actuators for rotor trim setting. High-speed electrohydraulic actuators provide the capability for high-frequency blade pitch inputs up to  $\pm 1^\circ$  at 40 Hz. Remote setting of the shaft angle of attack,  $\pm 15^\circ$ , is possible. A six-component hub balance is horizontally located in the fuselage body. Capabilities of the hub balance are as follows:

Lift force	±2,000 lb
Side force	±1,000 lb
Propulsive force	±400 lb
Roll moment	5,000 in.-lb
Pitch moment	15,000 in.-lb
Yaw moment	6,000 in.-lb

A torque load cell (3800 in.-lb maximum) located at the gearbox drive shaft measures shaft power.

The control console includes resolved blade-pitch and blade-flap displays for mean and once-per-revolution motion plus commanded pitch displays. The rotor operator has direct control over collective and cyclic pitch or may command all three of the primary control actuators or any one of them. The dynamic actuators may be commanded at the console or from an external source. A CRT display of blade in-plane and out-of-plane motion is provided for monitoring rotor/test-stand dynamics. A 32-channel data logger is also installed in the console for monitoring and recording the status of the model drive and utility systems.

#### Rotors for Full-Scale and Small-Scale Tests

Much of the rotorcraft testing in the NFAC involves unique hardware, particularly development tests of new rotor designs and new aircraft configurations. In addition, many rotors are available for general purpose or more basic research. Table 4 shows the rotor systems available for use in basic research programs.

The Ames Rotor Test Apparatus (RTA) was originally delivered with an H-34 hub, and in several of the first tests on the RTA that hub was used. The Sikorsky H-34 is out of date technically, but it remains useful for research for two reasons: it is a large rotor (but still within the capabilities of the RTA), and the blades are available commercially at a very reasonable price. The 56-ft-diam H-34 is about as large a rotor as can be tested in the 40- by 80-ft tunnel without concern about wall effects. A large rotor is desired for research in which low rotational speed is important, notably vibration-control studies.

The Bell 412 rotor was obtained as part of the interactional aerodynamics program. The Model 576 Test Stand or Easter Egg (EE) was chosen as the test module for that program because 1) it could be devoted solely to the program; 2) the body shell had been designed to measure aerodynamic loads; and 3) the body itself is fairly short. The design work had already been accomplished by Bell for an interface between the transmission and the Bell 412 rotor before acquisition of the rotor.

Acquisition of the Sikorsky S-76 rotor and installation of the Bell 412 rotor on the RTA is an attempt to obtain current-technology rotor systems that are a good match to the RTA for general use in future research programs. These rotors are about the ideal size for the load and performance capability of the RTA--radius 22-23 ft, chord 1.3 ft, and design thrust 10,000-12,000 lb. These rotors require

only about two thirds of the available power, with the electric motors operated at about two thirds of full rpm. In addition, this rotor diameter is a good match with the size of the 40- by 80-Foot Wind Tunnel. The installation of the Bell 412 on the RTA in addition to the EE was desired because of the greater power and higher harmonic control capability of the RTA (design and fabrication of the interface hardware is not a major project). These two rotors and hubs will provide the capability for much future research in aerodynamics and vibration reduction.

The installation hardware and the initial testing of the MBB BO-105 were obtained as part of a bearingless-rotor research program. As a proven hingeless rotor system, this rotor will provide the capability for future research in dynamics.

Recently, small-scale rotors have been obtained that are models of the Sikorsky S-76 and Bell 412 rotors. Since our small-scale programs are often either preludes to or investigations of more fundamental aspects of the full-scale tests, it is desirable to conduct them using models of the full-scale rotors. In addition, these rotors will provide the capability for direct research on scale effects.

#### Special Purpose Test Equipment

Several systems are available for use in support of helicopter testing. Worth special mention are the special purpose digital data computation systems and the nonintrusive laser Doppler velocimeter (LDV) flow-measurement systems.

The Multicyclic Computer Control System (MCCS) is a dedicated array-processor-based computer system for rotorcraft dynamics and control testing. The computer system is designed for real-time data acquisition and computation, data storage, and display, as well as for coordinating a host of other activities related to user interaction, file management, and data reduction. The computer architecture is designed into two subsystems--the executive processor and the loop processor (fig. 18). The executive processor (a PDP 11/60 computer) serves as the basic operating system and loop processor controller, and performs all non-real-time tasks. The loop processor (a Floating Point Systems AP-120B) is dedicated to the execution of all real-time computation functions (for example, parameter identification and control). The system provides 64-channel data acquisition and eight channels of analog data output capability. The complete computer system includes 20-Mbyte and 80-Mbyte disk memory units and an intelligent terminal with a printer/plotter unit.

A second general-purpose, on-line computational system is the Signal Analysis System (SAS). It is a Fortran-programmable PDP 11-34 computer with 181 analog channel sampling capability. Up to 16 channels may be sampled simultaneously at rates up to 160 kHz. It has 128K installed memory and 10 Mbyte rigid disk storage. It is used for a wide variety of applications including on-line time-series analysis, transfer function calculations, and transient dynamics analysis for aeroelastic stability testing. It is also used off-line for dynamics analysis and for

initial acoustic data digitization and reduction from acoustic data recorded on analog tape.

Laser velocimetry technology as applied to rotorcraft experiments in the NFAC has been pursued for many years (ref. 1). Using two-dimensional LDV systems, spanwise lift distributions on a hovering rotor blade, the formation of the trailed vorticity in the rotor wake, and the generation and roll-up of a tip vortex have been measured (fig. 19). These systems have automated digital data acquisition and reduction; high-resolution, on-line graphics display; and computer feedback to the signal conditioning electronics to enhance the LV signal-to-noise ratios. Position control is also automated by means of a five-motor digital controller interfaced to the minicomputer.

Two additional laser velocimeter systems have been recently developed and demonstrated for potential use in rotorcraft experiments: a three-dimensional LV system for use in the 7- by 10-Foot Wind Tunnel and a two-dimensional, long-range laser velocimeter for use in the NFAC (fig. 20). The three-dimensional laser velocimeter measures all three velocity components by means of three independent dual-beam channels that operate in the backscatter direction. Lateral positioning of the system's focal point within the wind-tunnel test section is accomplished by tilting and zooming the upper (off-axis) channel to follow the lower two-channel optics as they zoom across the test section. Vertical and streamwise motions are accomplished by moving the entire system package on a digitally controlled platform. The velocimeter optics and electronics are interfaced to a dedicated high-speed minicomputer with peripheral and input/output capability.

The long-range laser velocimeter can be used for flow measurements in the full-scale wind tunnels. The entire optical package is mounted within the tunnel test section on lateral rails that are located at a selected longitudinal position. Test-point positioning is accomplished through a combination of lateral motion along the rails, mechanical rotation of the upper tabular section, a variable focusing by means of zoom optics within the package. All of the LDV systems are stand-alone data-acquisition and analysis systems. The minicomputer controller/processor is programmed for each particular experiment. In a typical experiment, the LDV processor is not directly interfaced with the wind-tunnel data system or the rotor data reduction system.

## TEST PROCEDURES AND TYPICAL RESULTS

### Typical Full-Scale Helicopter Rotor Tests

As a result of more than 30 years of testing in the 40- by 80-Foot Wind Tunnel, many standard procedures for routine helicopter rotor tests have been developed. The typical test plan is a matrix of advance ratio and tip Mach number, obtained by setting the appropriate uncorrected tunnel dynamic pressure and rotor rotational speed (taking into account the influence of tunnel temperature in particular). At each operating condition (tunnel and rotor speed), a set of data points is defined



by a matrix of shaft angle-of-attack and rotor collective pitch, with the rotor flapping relative to the shaft (or hub moment) always kept near zero, using the rotor cyclic pitch. Variations of cyclic pitch are made at selected conditions to measure the influence of control. Using the real-time display of the data-acquisition system, it is also possible to fly the rotor to specific thrust and propulsive force conditions, such as 1-g flight. When a full performance map is to be obtained, however, it is faster to use the shaft angle and collective pitch matrix.

Results from a 40- by 80-Foot Wind Tunnel test of a Sikorsky S-76 rotor on the Ames rotor test apparatus are presented (fig. 21) as an example of a full-scale helicopter rotor test (ref. 2). Rotor performance (figs. 22 and 23) was obtained, using the wind-tunnel balance to measure the forces and a shaft torque gage to measure the rotor power. An aerodynamic tare is subtracted from the scale forces. This tare is obtained by measuring the loads on the test module without the rotor blades installed. The rotor hub is installed and is rotating during the tare measurements. When properly calibrated, the shaft torque parameter is a more accurate measurement of the rotor power than the wind-tunnel balance yaw moment, since the latter includes a measurable influence of the rotor wake on the test module. The accuracy of the performance measurements depends then primarily on the repeatability of the test condition and on the level of unsteadiness of the wind-tunnel flow. Standard fixed-wing wind tunnel-wall corrections provide an estimate of the effective shaft angle-of-attack, hence a correction for the measured propulsive force. This correction is very crude, but no better method has been developed. At high speed, the angle-of-attack correction is small for the disk loadings typical of helicopter rotors, and at low speeds the rotor performance is not very sensitive to angle of attack.

In the past, the emphasis in tests in the 40- by 80-ft tunnel has always been on high-speed characteristics, so the exact lower speed limit for flow breakdown in this tunnel is not known. A significant influence of flow breakdown has never been observed, but neither has much testing been conducted at very low speeds. Hover testing can be done in the wind tunnel (fig. 24). Hover tests are performed with the overhead doors open and the rotor tilted forward 10°. In this configuration, there is considerable unsteady recirculation in the test section, but little ground effect. The accuracy of this test procedure has been established (for rotors with diameters up to 44-ft) by making comparisons with data from other facilities.

Rotor-blade loads (fig. 25) are measured using strain gages, calibrated in terms of moment or force. The signals are typically samples at 64/rev by the data-acquisition system. Data analysis typically involves 1) conversion to engineering units (using a resistance calibration (real) step at the beginning of a run to obtain the conversion factor), 2) averaging over eight revolutions (although the signals are very steady--periodic--in most operating conditions), 3) making a harmonic analysis, and 4) making corrections for the filtering and time skew in the data system. Typically the oscillating (one-half peak-to-peak) loads are of most interest, reflecting both the importance of the oscillatory loads to the structural design, and the current inability to reliably predict the time-history or harmonics.

Rotor noise is measured using several microphones installed three to five rotor radii from the hub, usually upstream. The acoustic pressure signals are recorded in analog form. An interface is available to send dBA measurements to the wind-tunnel data-acquisition system, but the high-frequency content of the noise signals precludes recording them digitally during the test. After the test, the noise signals are digitally analyzed, and the resulting information transferred to the data base with the performance and loads information. The noise is corrected for the wind-tunnel background noise, subtracted on a 1/3-octave basis. At high speed, rotor noise is often dominated by impulsive noise, which is well measured in the wind tunnel (fig. 26) (ref. 3). The impulsive noise is much greater than the background noise, and is seldom contaminated by reflections, because of its extremely narrow directivity pattern. At low thrust or high speed without impulsive noise, the tunnel previously had a background noise level that prevented measuring the rotor noise (fig. 27).

The reduced background noise level in the modified wind tunnel (primarily because of the lower tip speed of the new wind-tunnel fans), together with improved microphone stands, should provide the capability to measure the rotor noise at all conditions. With the test section acoustic treatment installed, the noise measurements above about 150 Hz, as well as integrated metrics such as dBA and PNdB, should reliably represent free-field conditions. For tail rotors or small-scale rotors, the acoustic treatment will be active for the entire range of the noise spectrum. For full-scale rotors, however, the rotational noise begins, typically, at 20 Hz. It will never be practical to treat the wind tunnel to eliminate reverberations at such low frequencies--that would require an open test section, with absorbing wedges about 6 ft tall. Hence, it will be necessary to rely on empirical or theoretical corrections to the full-scale rotational noise.

### Helicopter Rotor Dynamics Testing

Helicopter dynamics testing can have two objectives: identifying the inherent dynamic characteristics of the rotor, and using control inputs to modify the dynamics of the complete rotor system. Both of these types of testing are performed in the NFAC.

Dynamics testing requires a number of unique test considerations. Coupled rotor/body dynamics in the wind tunnel are not identical to a helicopter's flight dynamics for a large number of reasons, including the large inertias of the model/strut/balance system. The fundamental low-frequency modes of the support system yield primarily translational motions of the rotor hub without significant pitch and roll motions, unlike a helicopter in flight. Yet in some cases this allows for, effectively, an isolated rotor dynamics test condition. It has been shown that the dynamic characteristics of a helicopter rotor, together with the influence of the support system dynamics, can be accurately measured in the tunnel for use in validating analytical prediction codes.

Since the rotor system is never allowed to have free-body modes, as would a helicopter in a hover- or forward flight-state, the dynamic influence of the body

modes has an important influence on system dynamics for all test regimes in the wind tunnel, including forward flight. This is particularly critical when considering ground-resonance-type stability in which inplane damping of the rotor blades at the fundamental edgewise bending frequency may be reduced because of the superimposed once-per-revolution inplane motion induced by the tunnel's airspeed. In typical cases for conventional articulated rotors with nonlinear hydraulic dampers with pressure relief valves, maximum once-per-revolution inplane motion limits are established to guarantee that adequate rotor inplane damping will exist.

The philosophy of rotor stability testing in the NFAC is to evaluate the system damping levels as a function of operating condition. Often, rotor hub parameter changes that affect rotor damping (i.e., reduced control system stiffness or blade sweep) are investigated. The balance system dynamics may also be altered by installing or disconnecting the eight viscous balance dampers mentioned previously. It is not the intent of the test program to actually identify system stability boundaries by acquiring data at neutrally stable or unstable operating conditions. In the interest of personnel and facility safety, known regions of rotor instability are avoided. Should a test condition result in an unstable rotor system, test procedures are used that would quickly return the rotor system to a safe and well-damped operating state.

Most rotor stability investigations are performed with the rotor system installed on the RTA. Rotor-blade motions and bending moments and fuselage body accelerations are analyzed during operation in response to external excitation. For helicopter rotors, the best aeroelastic stability determinations are obtained when analyzing transient decay records obtained after sudden termination of time-dependent cyclic pitch inputs. A moving-block transient analysis is used in an on-line process to determine system dynamic characteristics in a matter of a few minutes during rotor/tunnel operation.

To acquire rotor system damping data, the desired wind-tunnel operating conditions are established, and the rotor is trimmed as in normal rotor testing. A steady-state data point is taken for rotor performance, loads, and acoustics. The dynamic control system of the RTA is then used to oscillate the rotor cyclic pitch (producing a forward "wobble" of the nonrotating swashplate) at the proper rotor excitation frequency. This is typically the regressing rotor inplane bending frequency ( $\omega_r < \Omega$ ). This is equivalent to stick stirring, which is often used in flight testing. The amplitude of the oscillation is increased until either an adequate signal at the forcing frequency is obtained in the blade edgewise bending moment, or until a load limit is reached at any instrumented blade station. Abrupt termination of the excitation yields an edgewise bending-moment signal which is digitally recorded on the SAS. Outputs from accelerometers located in various positions on the RTA can also be used. However, these signals typically have poorer signal-to-noise characteristics. Data analysis records are typically 5-10 sec in length, depending on the rotor operation state and the data sampling rate. The signal analysis system operator immediately reviews the recorded data to determine if an adequate transient decay signal was acquired and recorded. After identification of the modal frequency, a moving-block analysis is performed by the system

operator. By interactively identifying the length of the data record and the size of the moving block to be used in the analysis, the operator then identifies the portion of the natural logarithm of the Fourier coefficient magnitude versus time plot for fitting a straight line. From this straight-line curve fit, modal damping is calculated and displayed to the operator. The displayed output to the operator for a typical data analysis is shown in figure 28. Forward flight stability characteristics for the Boeing Vertol bearingless main rotor as a function of airspeed and shaft angle are shown in figure 29 (ref. 4). After successful determination of the system damping a given operating condition, three or more transient decay records are digitally recorded on the SAS for off-line reduction after the run. This provides a reasonable estimate of the inherent variability in determining the system's dynamic characteristics.

Hover stability data are obtained in a similar manner, using the hover test procedures described previously. Representative rotor stability results from a recent BO-105 hingeless rotor hover test in the 40- by 80-Foot Wind Tunnel test section are shown in figure 30 (ref. 5). The quality of these results is considered to be excellent. The scatter at higher rotor thrusts is similar to small-scale model test data. These particular results also compare very well with whirl tower data obtained in a free-field outdoor environment, as shown in the figure.

Helicopter rotor multicyclic testing is similar in approach to stability testing. After acquisition of trimmed performance data, high-frequency blade-pitch inputs are introduced into the rotor system by the MCCS operator. During this process, all system loads and vibration levels are again closely monitored on-line to avoid exceeding previously established safe operating limits. Once the pitch input has been fully introduced, a second data-acquisition point is taken, which includes static mean performance parameters as well as dynamic, steady-state loads and vibrations. Since the blade-pitch inputs have only rotor rate harmonic content, the dynamic data-acquisition and reduction processes for normal dynamic data are sufficient. A number of different data records are typically taken for one single trimmed operating condition. Analysis of the data is performed both on-line and after each run.

#### Rotor/Body Aerodynamic Interactions

A series of small-scale wind-tunnel tests has been conducted to help quantify one type of helicopter aerodynamic interaction--that between a rotor and a fuselage. A major full-scale wind-tunnel test program is also planned. The small-scale test program provides the opportunity to investigate the basic phenomena of these interactions and to provide data that will be useful in establishing the direction of full-scale rotor/body investigations. The model installation for a small-scale test in the 7- by 10-Foot Subsonic Wind Tunnel is shown in figure 31. The rotor rig is mounted onto the wind-tunnel turntable. The body (a 1/7th-scale model of the RTA shown) is independently mounted from the tunnel test-section ceiling with a six-component balance within the body. This makes it possible to measure both the

individual and combined loads of the rotor and body. There is no physical connection between the body and the rotor system; the rotor shaft between the fuselage and hub is not simulated. Data are obtained for the isolated body, isolated rotor, and combined body/rotor configurations. During a particular test run, only rotor thrust is varied, using collective pitch. Orientation of the tip-path plane, determined from blade-flapping measurements, is held constant, using cyclic pitch control. Rotor-shaft angle and tip Mach number, although possible test matrix variables, have been held constant throughout these tests to date. Body position is adjusted as its angle of attack is varied, so that the location of the hub relative to the body remains constant.

These tests have shown that the effect of the rotor on the body is much larger than the effect of the body on the rotor, particularly for thicker bodies. Also, the locations of the rotor wake and the hub are the important factors in determining the interaction on the body. From figure 32, the body loads such as lift, when normalized by rotor thrust, scale with a single wake parameter (ref. 6). Such results are providing insight into the governing physics of this problem and are being used to guide the planning, currently in progress, for a series of full-scale wind-tunnel tests of rotor/body aerodynamic interactions, using the Bell 412 rotor system and the EE test module.

#### Laser Velocimetry

The accurate measurement of flow-field velocities in and around the rotor wake has always been an important requirement for understanding and predicting rotor behavior. Laser velocimetry provides a nonintrusive method by which this information can be acquired. Previous tests have measured the radial distribution of circulation and the local section lift coefficient by the circulation box technique using a two-dimensional, dual-beam backscatter-type laser. Briefly, this technique is based on the definition of circulation as the line integral of the tangential velocity around a closed contour. Thus, by measuring the tangential flow velocities on the sides of a rectangular contour (box) surrounding a wing or rotor section, the bound circulation at the section and the local lift coefficient can be calculated. The size of the circulation box, relative to the local airfoil section, is shown in figure 33. Velocity measurements at 26 points along each side of the box are typically used. A mineral oil mist is used to seed the airflow. Testing in the 7- by 10-ft tunnel with seeding for the laser system can be performed, with the tunnel's air exchangers open without significantly reducing the data-acquisition rate.

Experimental studies have included the flow surrounding a small-scale, two-bladed rotor in hover (ref. 7). Data samples were taken only during an acceptance time of 60  $\mu$ sec after the blade had reached the prescribed azimuth. This time corresponds to a blade rotation of  $0.25^\circ$ , representing a blade movement at the tip of 6% of the chord and a corresponding lesser amount at inboard radial locations. The radial distribution of the blade circulation was obtained by the circulation-box technique described above. The blade sectional loading measured for an ogee tip using this technique is shown in figure 34. The velocity induced by the tip vortex

(+)

can also be measured. Measurements are made immediately behind the generating blade and immediately before the encounter with the following blade. Typical results are shown in figure 35 for a rectangular tip. After 180° of rotor azimuth displacement (fig. 35(b)), the trailing vortex has been displaced radially inward, which indicates the wake contraction. However, more importantly, these data reveal any changes in the vortex structure. In this case, the velocity structure demonstrates the extent to which vorticity has diffused outward from the vortex center.

In other LDV applications, the spanwise distribution of bound circulation on a semispan wing and the flow velocities in its wake were measured in forward flight (fig. 36) in the 7- by 10-ft tunnel. The wing was mounted on a splitter plate, which in turn was mounted to the tunnel floor. However, the splitter plate is not directly connected to the tunnel turntable for measuring balance loads. Instead, the wing tip contains a six-component internal balance. The data from the balance are acquired at steady operating conditions. Integrated loads from the LDV measurements are then compared with the swing-tip balance to verify proper data-acquisition and reduction software. Particular attention was given to documenting the flow velocities in and around the developing tip vortex. The spanwise variation in section lift loading and the induced velocity structure of the tip vortex at various stations along the wake are shown in figure 37 (ref. 8). Changes in peak velocity, motion inward of the vortex center, and vorticity diffusion can be seen in the results.

#### Full-Scale Tilt-Rotor Performance

Acquiring tilt-rotor performance data in the wind tunnel is similar to helicopter rotor performance testing. Previous tests have included isolated tilting prop-rotor test configurations and tests of an entire tilt-rotor aircraft with rotor systems (fig. 38). For isolated rotor testing, special-purpose drive systems are used, for example, the prop-rotor test rig described previously. For dynamics testing, the rotor can be mounted on a dynamically semispan wing, without a powered drive system in the model. Model excitation for dynamics testing can be performed through dynamic actuators changing blade pitch at the proper frequency or through a movable aerodynamic control surface (flap, winglet) located on the pylon or the wing. Isolated tilting prop-rotor tests usually require that the pylon angle of attack be changed by rotating the wind-tunnel turntable relative to the oncoming wind. For complete system performance and stability testing, the entire flight aircraft is installed in the 40- by 80-Foot Wind Tunnel (e.g., the XV-3 and XV-15 airplanes). Performance maps are obtained by establishing a test matrix of aircraft and pylon angle of attack, tunnel airspeed, tip Mach number, and rotor thrust (fig. 39). As with helicopter rotors, once-per-revolution rotor flapping is minimized, using cyclic pitch input.

Full-scale isolated tilt-rotor hover performance and acoustics can be obtained outdoors to eliminate the possibility of wind-tunnel walls affecting performance measurements (fig. 16(b)). As in wind-tunnel testing, the rotor is tested with its rotation axis horizontal to avoid ground effects. To acquire very accurate thrust

(+)

and torque measurements and to avoid operational (thermal) problems with the prop test rig rotor balance, special test procedures have been established. After the test rig is assembled, but before it is installed in the facility, motor/gearbox running is conducted without the rotor to measure thermal effects on the indicated thrust and torque. These effects have been shown to be less than 0.2% full-scale in measured thrust and less than 0.3% full-scale in measured torque. These thermal effects are further minimized by conducting 5-min warmup runs each day before beginning data runs; this is to allow the system to stabilize thermally. To verify accurate performance measurements, simultaneous thrust and torque check loadings are performed on the installed rig at the test site (without blades on) before research testing. Since rotor performance can be significantly affected by even light winds, all performance data taken outdoors are obtained in winds of less than 3 knots. The best time of day for finding such light winds is just after dawn. Consequently, only 2 to 3 hr of desirable testing time is available on a daily basis. A theoretical correction for ambient winds to a pure hover condition is made, taking into account both wind amplitude and direction. The resulting rotor performance data (fig. 40) (ref. 9) have excellent repeatability, and are some of the most accurate data that have been obtained on full-scale rotor systems.

#### Advanced Technology Demonstrations

Because of the unique capability of the NFAC, it is not unusual to test new, emerging technologies in critical test environments. Over the years, such technologies as rotor airfoil boundary-layer control, tip jet propulsion, and circulation control airfoil blowing, have been investigated. In addition, advanced full-scale rotorcraft systems are often tested in the NFAC before final flight-test evaluation to understand the vehicles' performance in a controlled and measured environment (e.g., the XV-15 aircraft and the ABC rotor system). Such unique tests require innovative test approaches and procedures. Model propulsion, instrumentation, control system, and utility support are typically one-of-a-kind installations. However, the NFAC has developed the capability to perform tunnel tests under these highly demanding circumstances within a general testing approach, using the facilities, test hardware, data-acquisition and data-reduction systems, and special test equipment described in this paper.

A typical instance of such a test program was the forward flight investigation of the 25-ft-diam X-Wing technology demonstrator (fig. 41). During the test, the most complex portion of the X-Wing flight regime, the conversion from rotary-wing to fixed-wing and back, was investigated. This flight condition requires maintaining sufficient lift for flight and ensuring that a moment balance acts across the rotor disk. A hub-moment feedback control system was tested in the 40- by 80-ft tunnel to determine the ability to maintain trimmed flight. Control stability measurements were collected during both fixed- and rotary-wing modes, and open-loop Bode plots were obtained for the pitch- and roll-moment control loops. Each loop was tested for stability with the other loop open or, later in the test program, closed. Having established the stability of the hub-moment feedback control system,

conversion-mode testing was performed (ref. 10). Figure 42 presents transient time-histories from one such conversion test from rotary-wing to fixed-wing mode at 180 knots. From this test, the technology required for rotary-wing circulation control airfoils for a stoppable rotor was demonstrated in large scale.

#### CONCLUDING REMARKS

Rotorcraft research testing in the National Full-Scale Aerodynamics Complex over the past quarter century has played a critical role in developing the technology for today's helicopters. Future research, using the facilities, data systems, and test equipment described here, will continue to contribute to the advancement of helicopter and advanced rotorcraft system technology in many technical areas and for many years.



## REFERENCES

1. Orloff, K. L., Snyder, P. K., and Reinath, M. S., "Laser Velocimetry in the Low Speed Wind Tunnels at Ames Research Center," NASA TM-85885, Jan. 1984.
2. Johnson, W., "Performance and Loads Data from a Wind Tunnel Test of a Full-Scale Rotor with Four Blade Tip Planforms," NASA TM-81229, Sept. 1980.
3. Mosher, M., "Acoustic Measurements of a Full-Scale Rotor with Four Tip Shapes," NASA TM-85878, Apr. 1984.
4. Warmbrodt, W. and McCloud, J. L., "A Full-Scale Wind Tunnel Investigation of a Helicopter Bearingless Main Rotor," NASA TM-81321, Aug. 1981.
5. Peterson, R. L. and Warmbrodt, W., "Hover Test of a Full-Scale Hingeless Helicopter Rotor: Aeroelastic Stability, Performance, and Loads Data," NASA TM-85892, Jan. 1984.
6. Smith, C. A. and Betzina, M. D., "A Study of the Aerodynamic Interaction between a Main Rotor and a Fuselage," Proceedings of the 39th Annual Forum of the American Helicopter Society, May 1983.
7. Ballard, J. D., Orloff, K. L., and Luebs, A. B., "Effect of Tip Planform on Blade Loading Characteristics for a Two-Bladed Rotor in Hover," NASA TM-78615, Nov. 1979.
8. Felker, F. F., Piziali, R. A., and Gall, J. K., "Spanwise Loading Distribution and Wake Velocity Surveys of a Semi-Span Wing," NASA TM-84213, Feb. 1982.
9. Felker, F. F., Maisel, M. D., and Betzina, M. D., "Full Scale Tilt Rotor Performance," Proceedings of the 41st Annual Forum of the American Helicopter Society, May 1985.
10. Ballard, J. D., McCloud, J. L., and Forsyth, T. J., "An Investigation of a Stoppable Helicopter Rotor with Circulation Control," NASA TM-81218, Aug 1980.

TABLE 1.- PARTIAL LIST OF LARGE-SCALE/FULL-SCALE  
 ROTORCRAFT RESEARCH TESTS IN THE NATIONAL  
 FULL-SCALE AERODYNAMICS COMPLEX

Model	Year
McDonnell Convertiplane	1953
BLC to Helicopter Rotor	1957
XV-3 Tilt Rotor	1957
Bell UH-1 Helicopter	1961
Lockheed Rigid Rotor	1962
Bell High Speed Rotor	1964
Sikorsky H-34 Rotor	1964
Jet Flap Rotor	1965
Lockheed Stoppable Rotor	1965
Hughes LOH OH-6	1968
AH-56 Helicopter	1969
Sikorsky ABC Rotor	1970
Bell Folding Prop Rotor	1972
Semi-Span Tilt Rotor Model	1972
Powered Tilt Rotor Performance	1972
Kaman Controllable Twist Rotor	1975
Sikorsky S-76 Rotor	1977
Bell 222 Helicopter Fuselage	1977
XV-15 Tilt Rotor	1978
Kaman Circulation Control Rotor	1978
Lockheed 25-ft X-Wing Rotor	1979
Boeing Vertol Bearingless Main Rotor	1980
Sikorsky ABC Model	1980
MBB BO-105 Hover Dynamics	1983
Bell/Boeing JVX Rotor Hover Performance	1984

TABLE 2.- WIND-TUNNEL BALANCE SYSTEM CAPABILITIES  
 (range in 1000 lb)

	40- by 80-Foot Wind Tunnel	80- by 120-Foot Wind Tunnel	7- by 10-Foot Wind Tunnel
<b>Lift</b>			
Front	100	150	1.8
Rear	100	150	.8
<b>Drag</b>	16	50	.5
<b>Side force</b>			
Front	8	30	2
Rear	8	30	.5

TABLE 3.- RESULTANT MEASUREMENT ACCURACIES FROM WIND-TUNNEL  
BALANCE SYSTEMS

	40- by 80-Foot Wind Tunnel	80- by 120-Foot Wind Tunnel	7- by 10-Foot Wind Tunnel
Lift, lb	±10	±100	±8
Drag, lb	±5	±25	±1
Side force, lb	±10	±50	±3
Pitch moment, ft-lb	±320	±1840	±12
Roll moment, ft-lb	±170	±1840	±30
Yaw moment, ft-lb	±122	±1300	±6

TABLE 4.- ROTORS AVAILABLE FOR GENERAL RESEARCH

Rotor system	Test module
Sikorsky H-34	Rotor Test Apparatus
Bell 412	Rotor Test Apparatus and Easter Egg
Sikorsky S-76	Rotor Test Apparatus
MBB BO-105	Rotor Test Apparatus
Small-scale Bell 412	Rotor Test Rig
Small-scale Sikorsky S-76	Rotor Test Rig



(a) 40- by 80-Foot Wind Tunnel.

Figure 1.- National Full-Scale Aerodynamics Complex.

ORIGINAL PAGE IS  
OF POOR QUALITY



(b) 80- by 120-Foot Wind Tunnel.

Figure 1.- Continued.



(c) Outdoor Aerodynamic Research Facility.

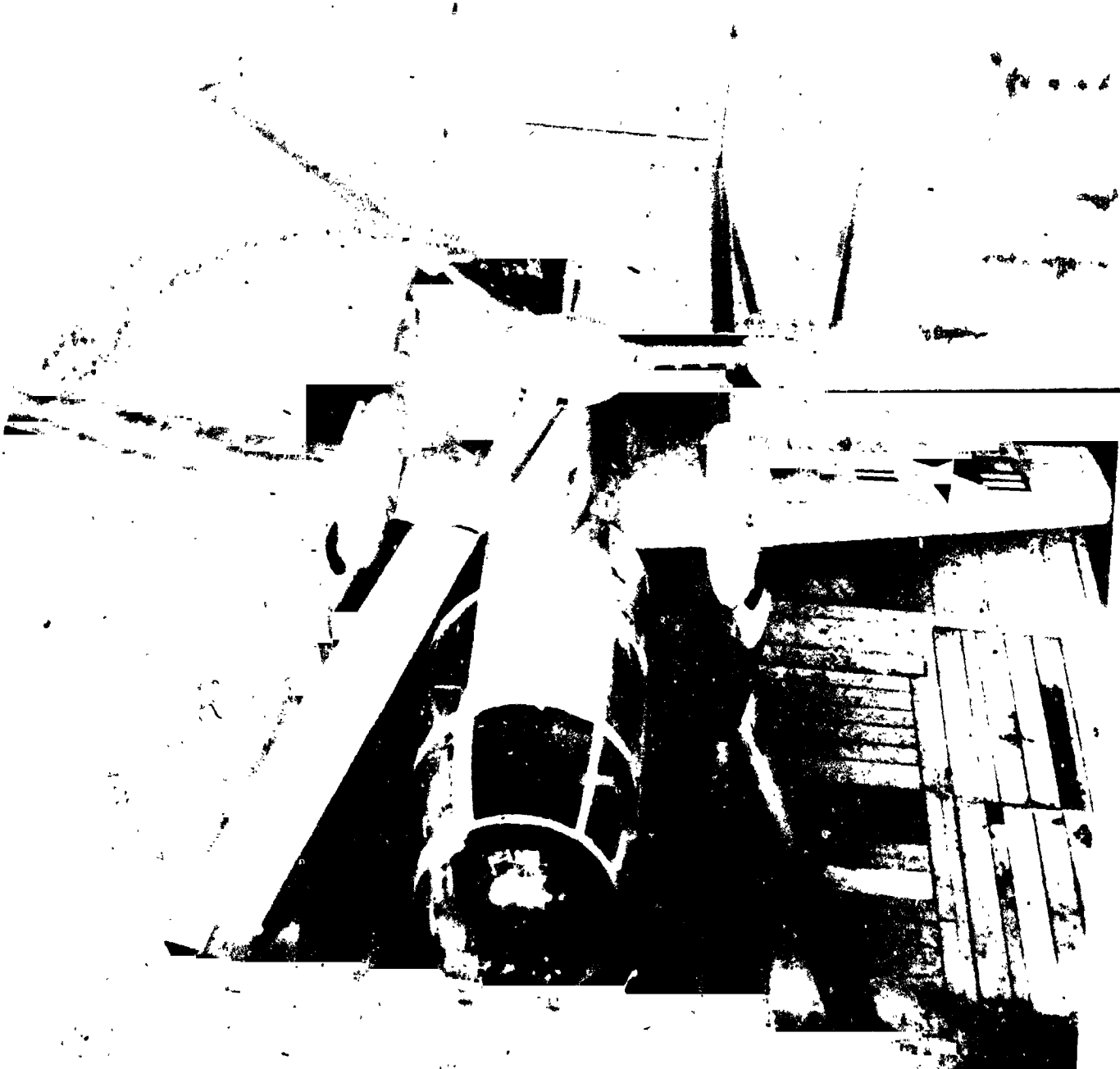
Figure 1.- Concluded.

ORIGINAL PAGE IS  
OF POOR QUALITY



Figure 2.- Ames 7- by 10-Foot Subsonic Wind Tunnel

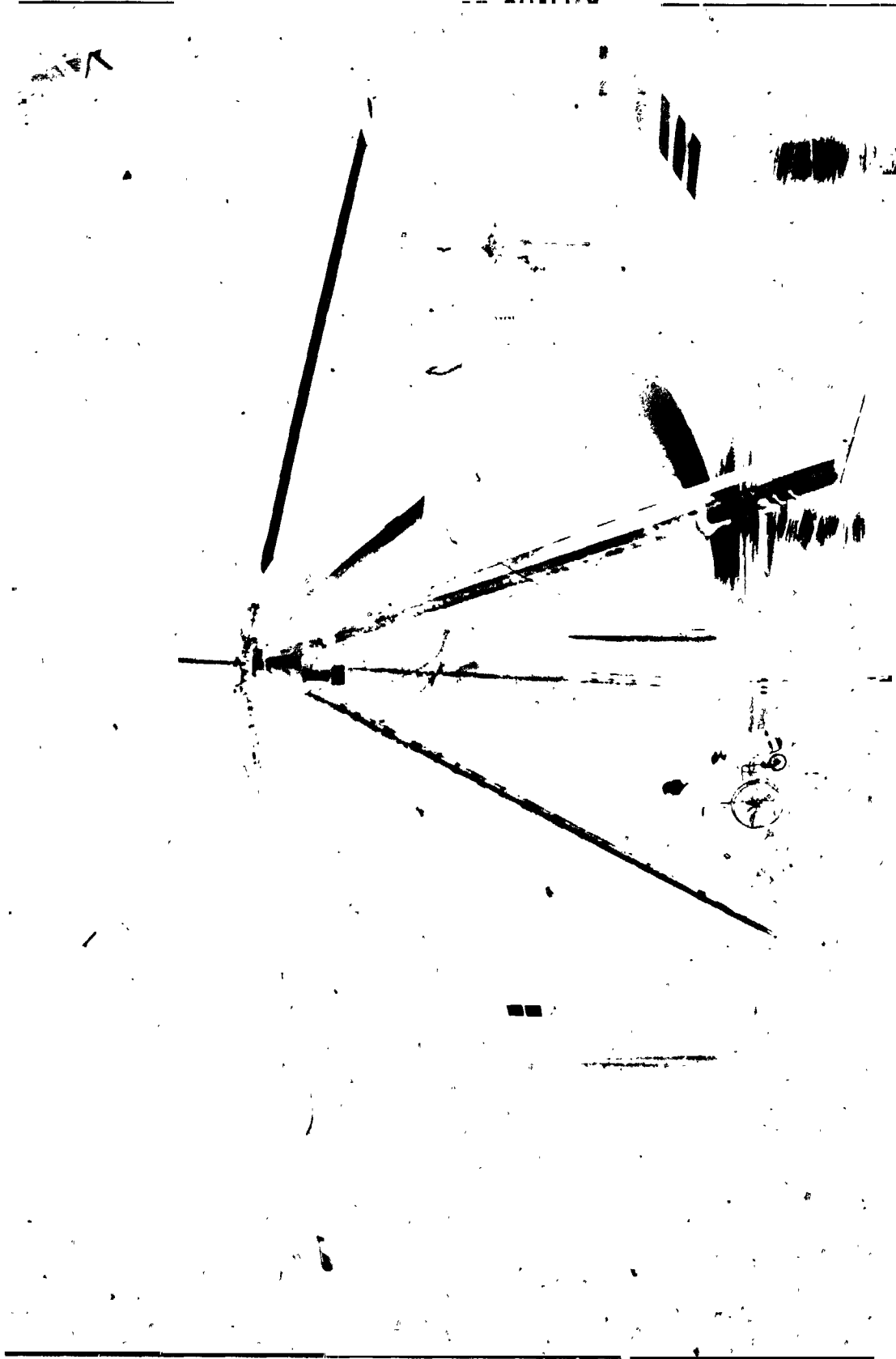
ORIGINAL PAGE IS  
OF POOR QUALITY



(a) XV-1 compound rotorcraft (1953).

Figure 3.- First rotorcraft tests in the 40- by 80-Foot Wing Tunnel.





(b) First helicopter main rotor test (1957).

Figure 3.- Continued.



(c) XV-3 tilting prop-rotor aircraft (1958).

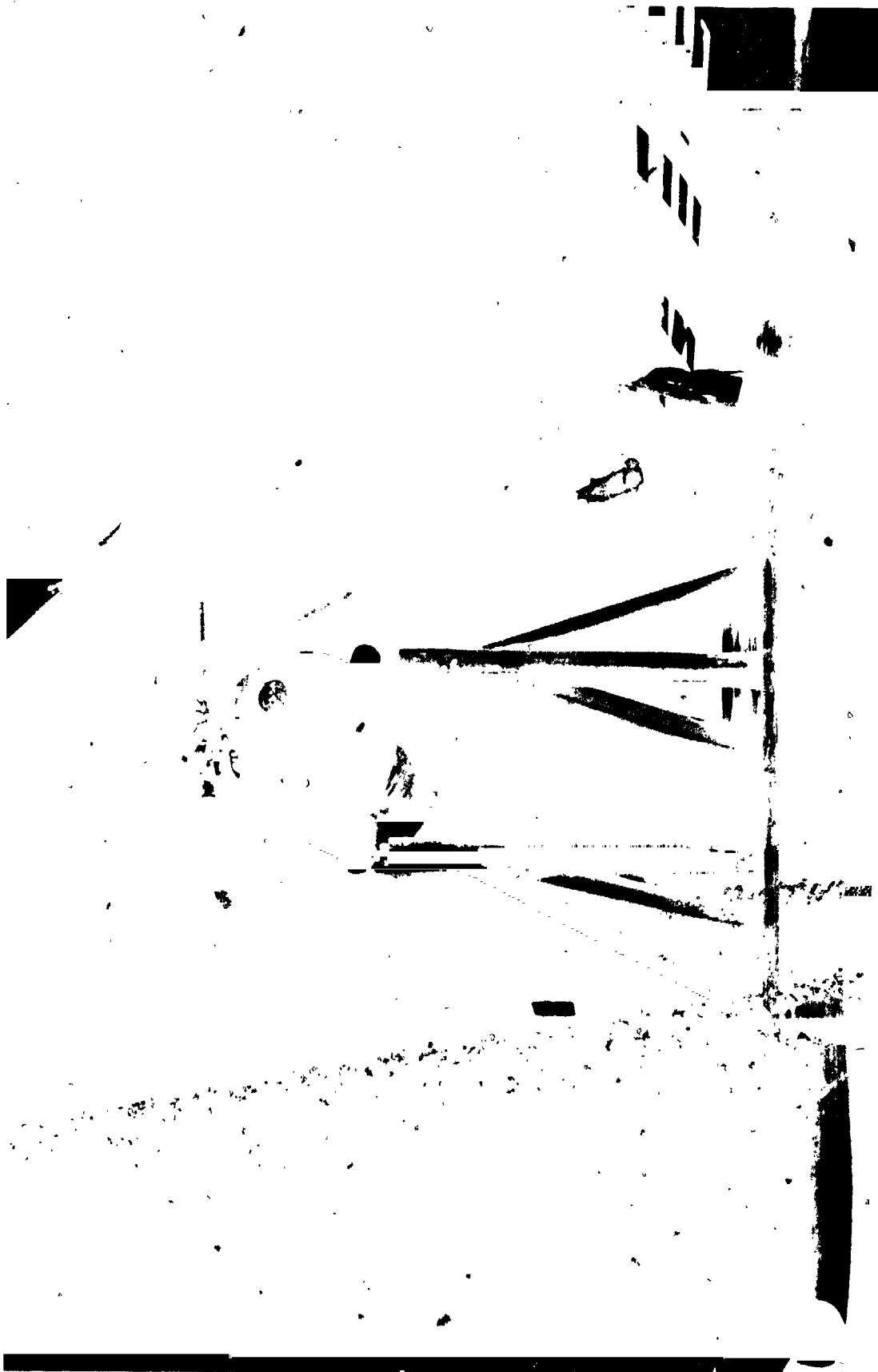
Figure 3.- Continued.

ORIGIN OF  
OF POOR QUALITY



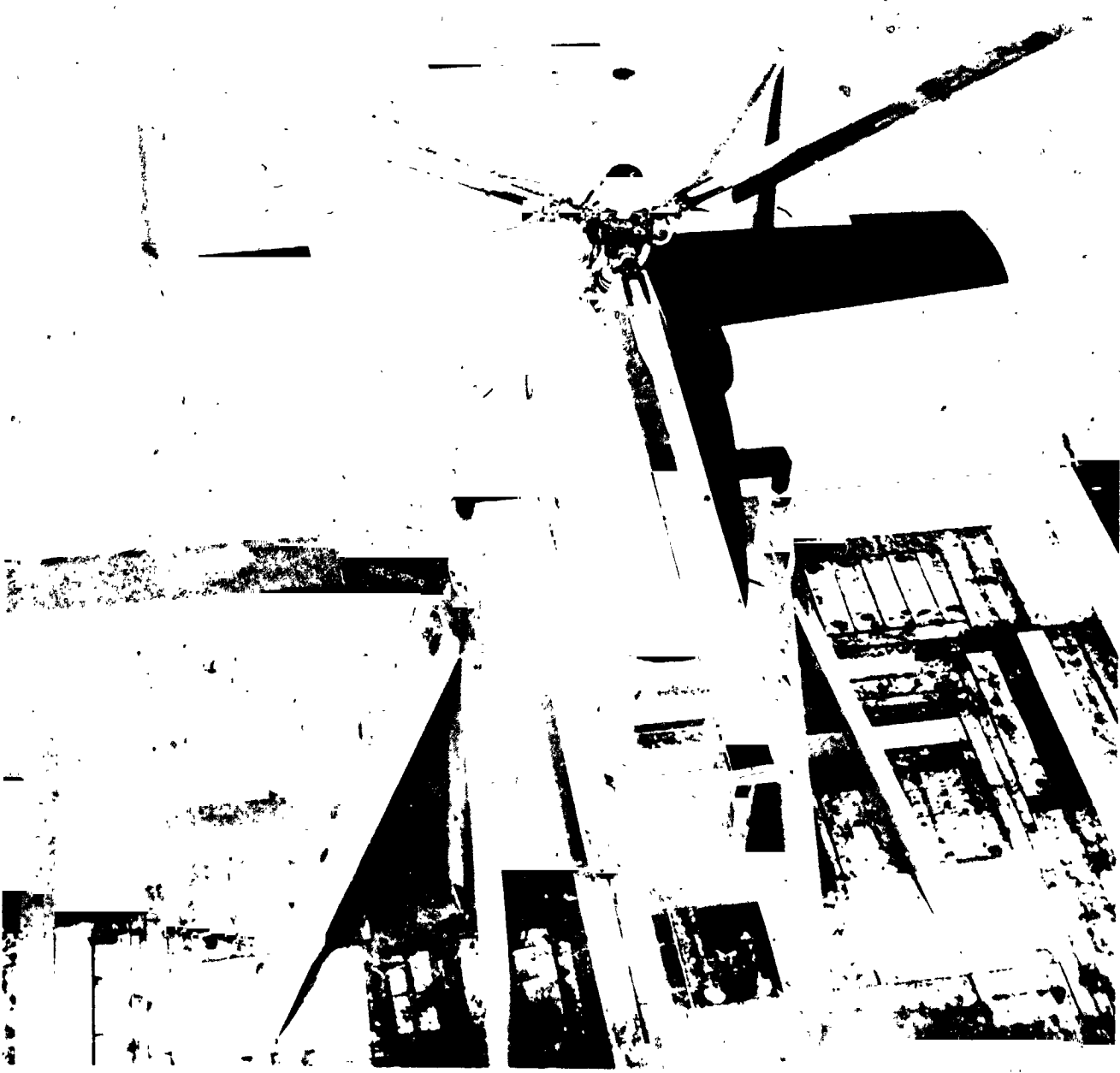
(d) UH-1 helicopter (1961).

Figure 3.- Continued.



(e) Instrumented H-34 rotor system (1964).

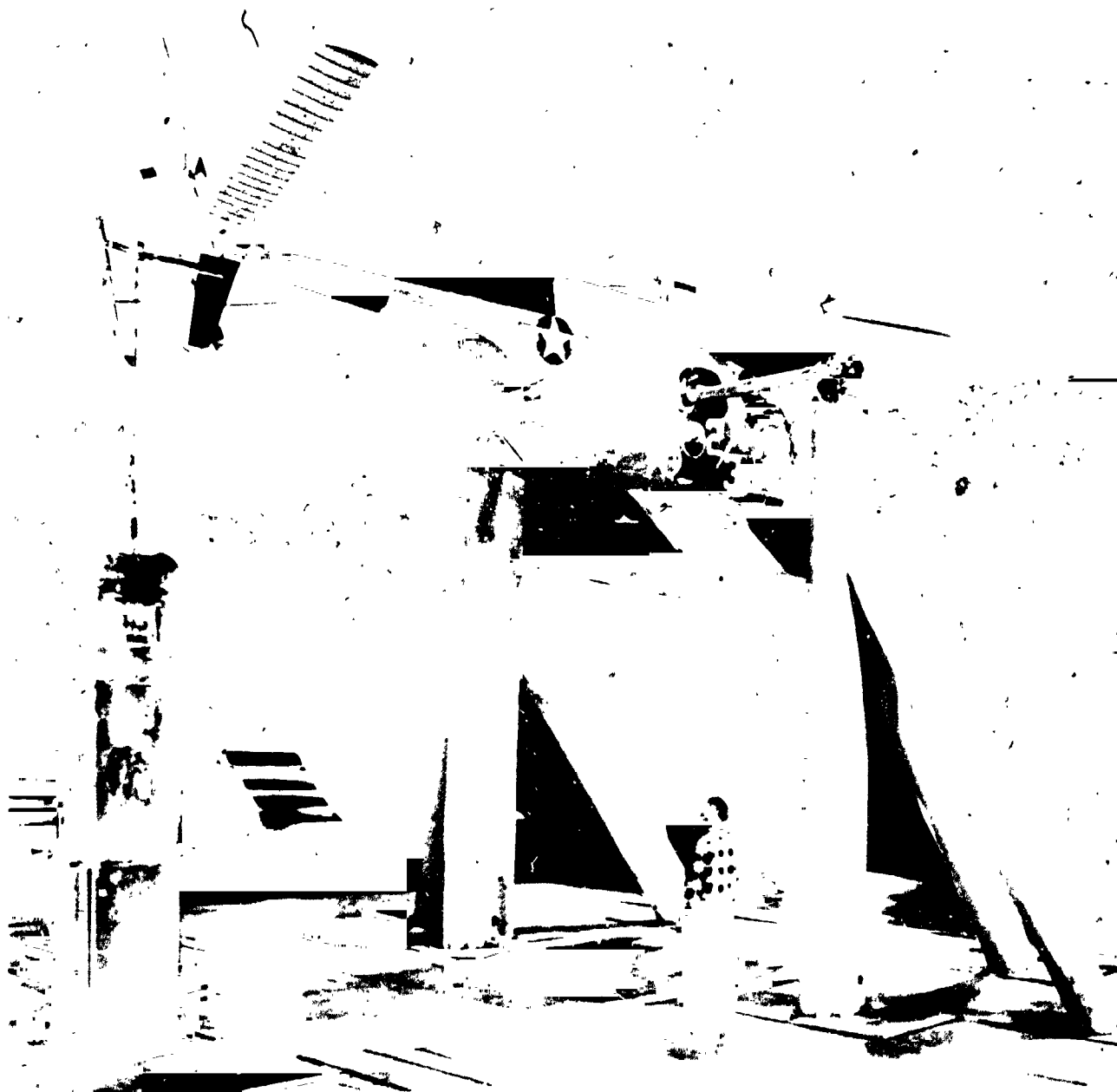
Figure 3.- Continued.



(f) Lockheed stoppable rotor (1965).

Figure 3.- Continued.

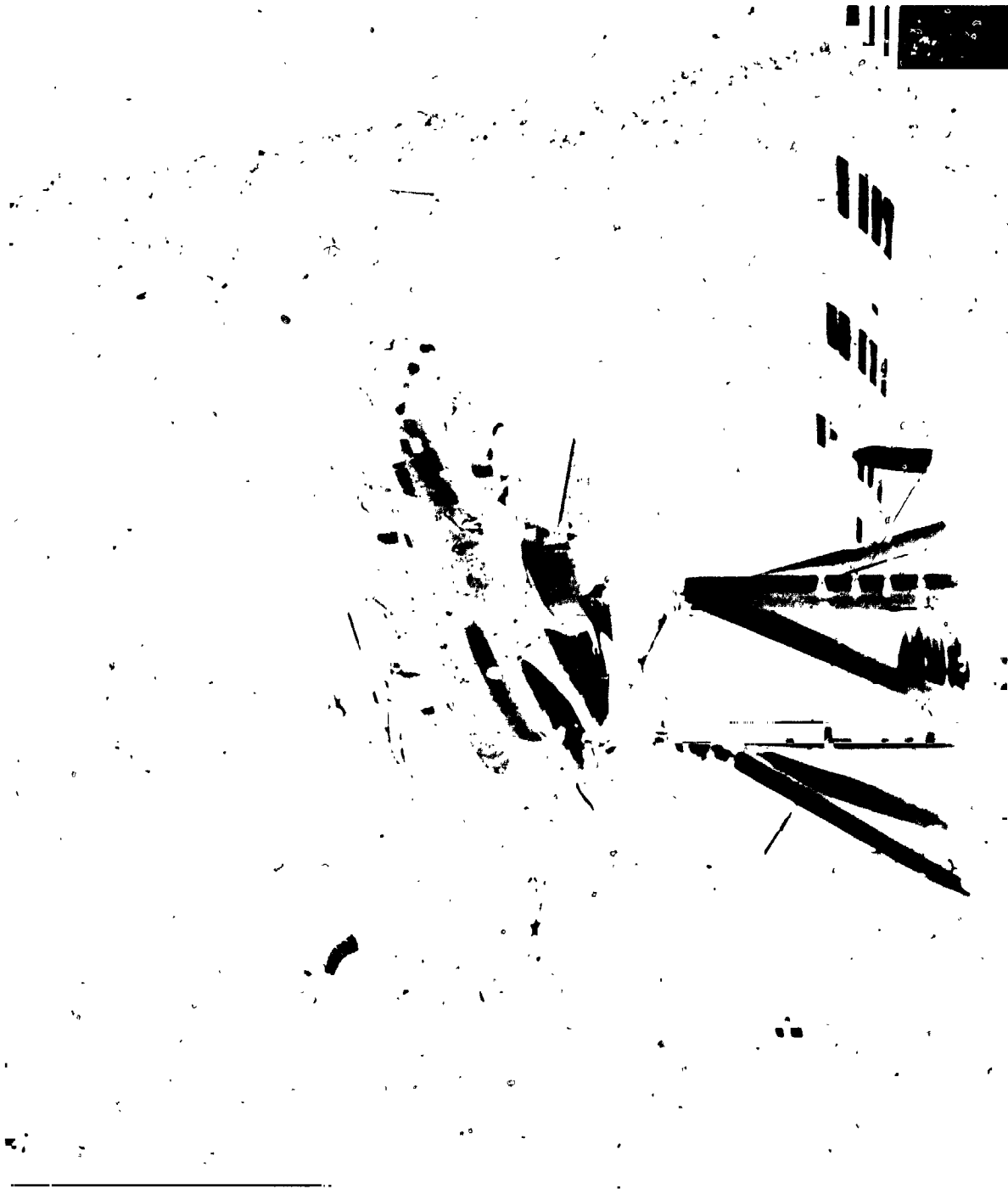
ORIGINAL PAGE IS  
OF POOR QUALITY



(g) OH-6A helicopter (1968).

Figure 3.- Continued.

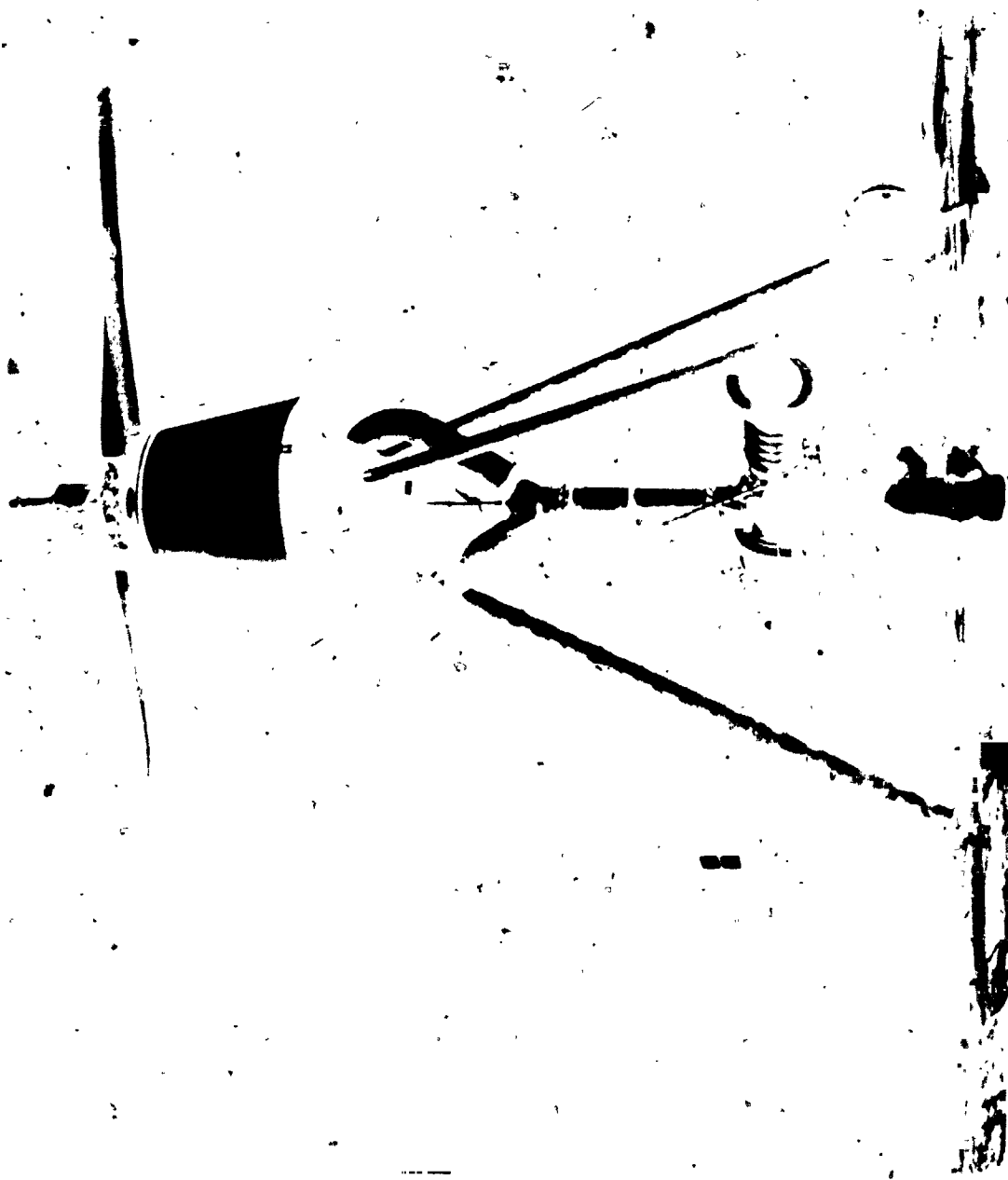
ORIGINAL PAGE IS  
OF POOR QUALITY.



(h) AH-56 helicopter (1969).

Figure 3.- Continued.

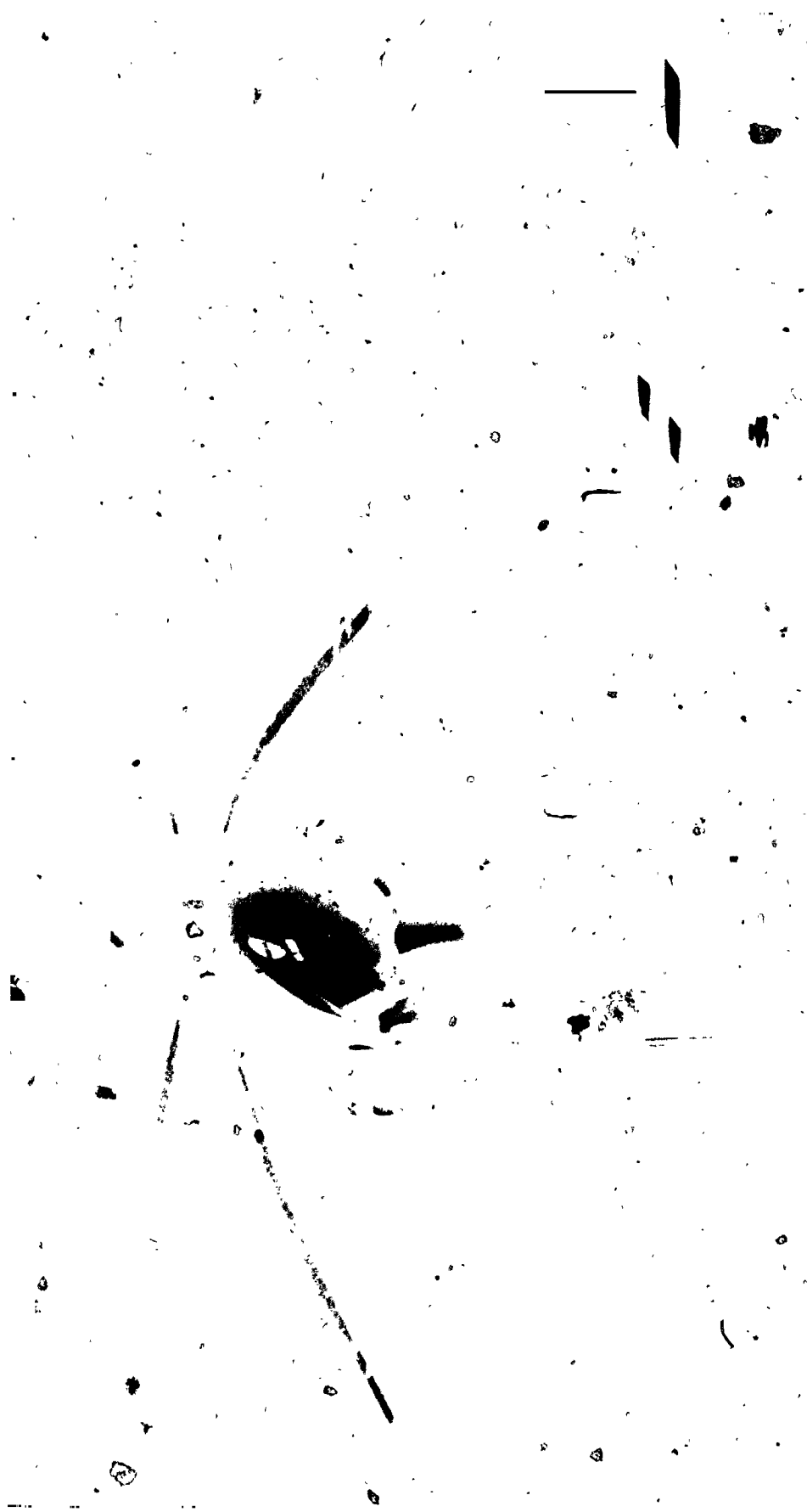
ORIGINAL FORM  
OF POOR QUALITY



(i) Jet flap rotor (1971).

Figure 3.- Continued.





(J) Controllable twist rotor (1976).

Figure 3.- Continued.

ORIGINAL PART  
OF POOR QUALITY



(k) Helicopter Model 222 airframe (1977).

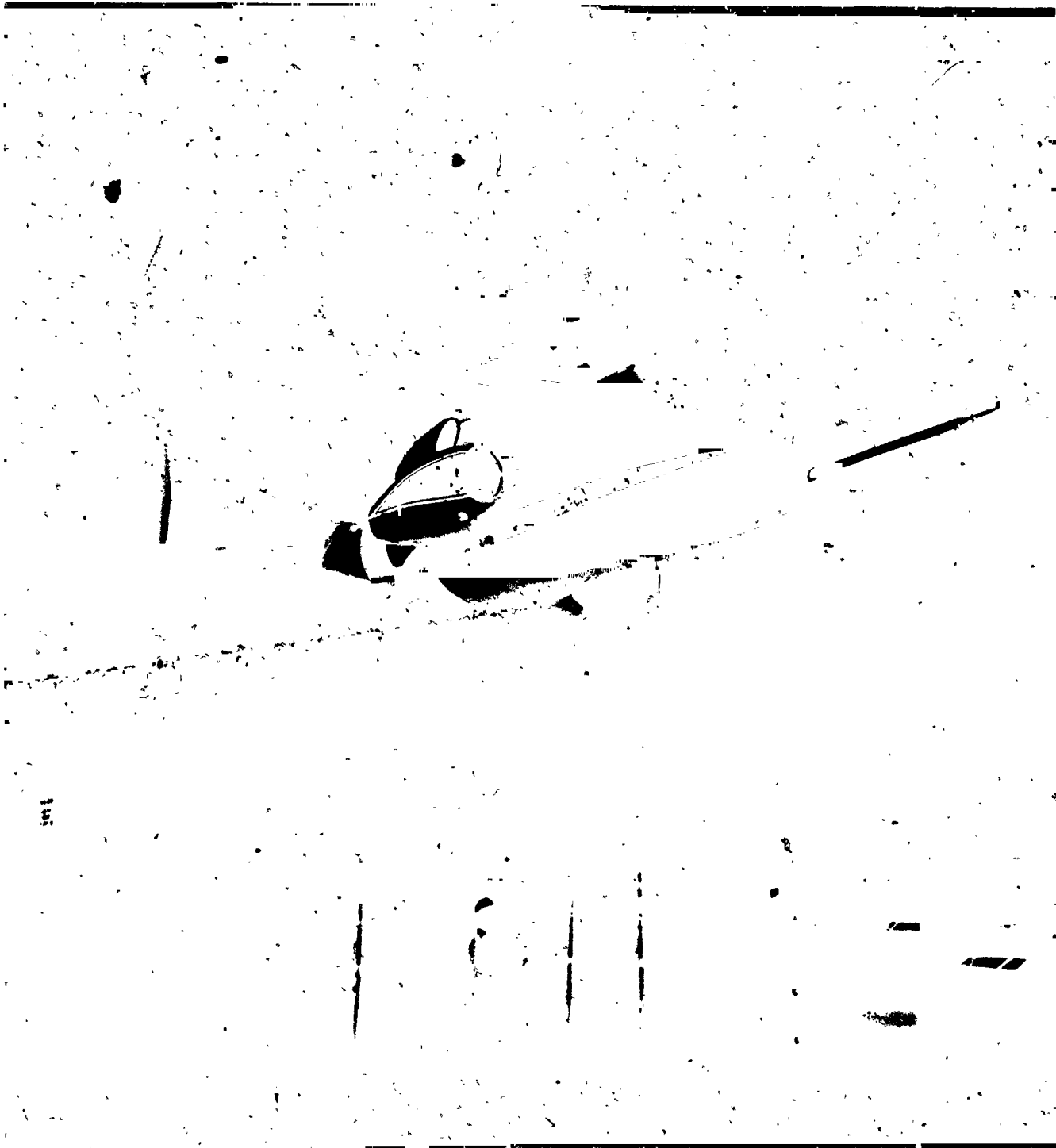
Figure 3.- Continued.



(1) Circutation control rotor (1978).

Figure 3.- Continued.

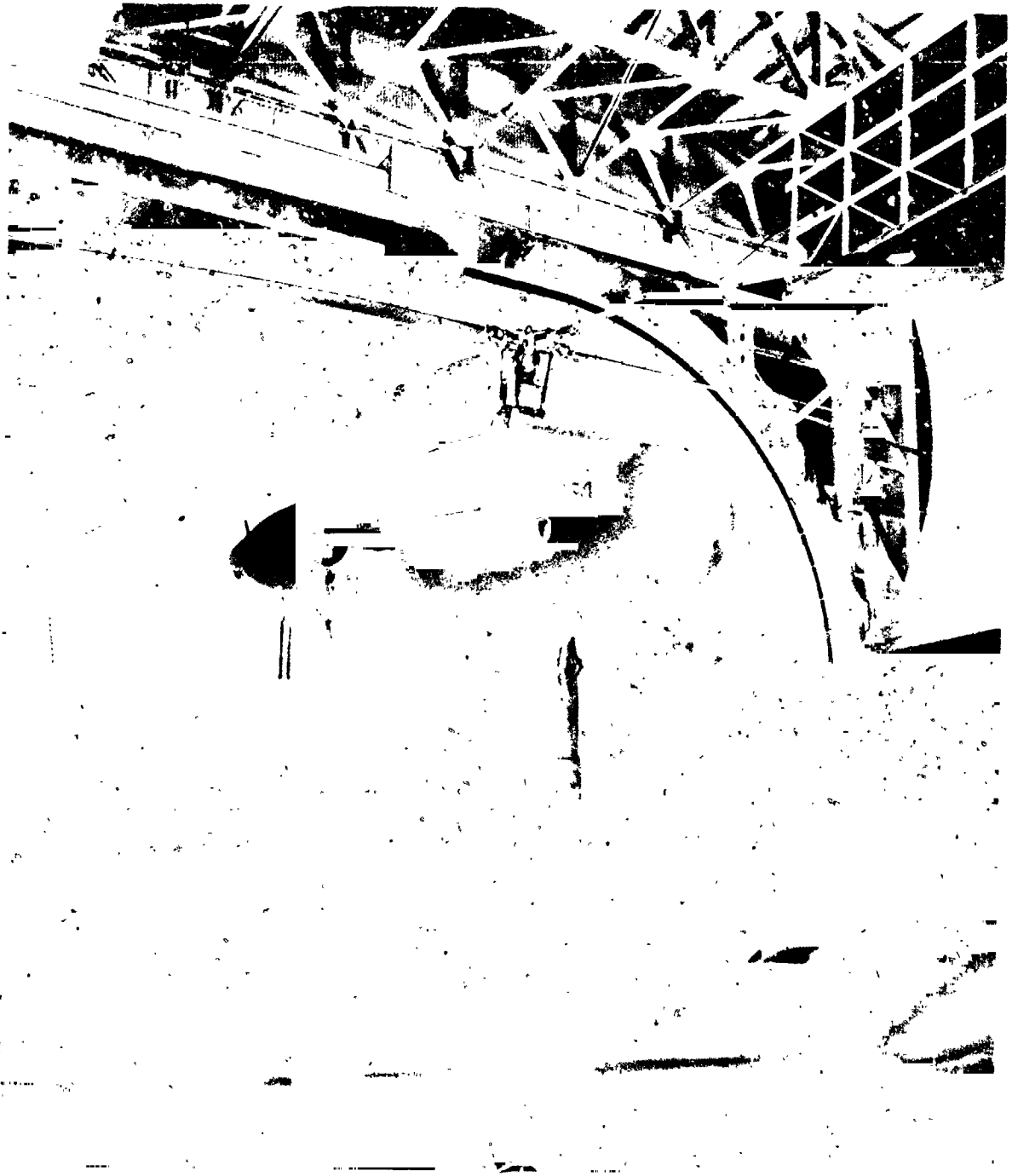
ORIGINAL FIGURE  
OF POOR QUALITY



(m) ABC model (1980).

Figure 3.- Continued.

ORIGINAL PAGE IS  
OF POOR QUALITY



(n) BO-105 rotor (1983).

Figure 3.- Concluded.

ORIGINAL PAGE IS  
OF POOR QUALITY

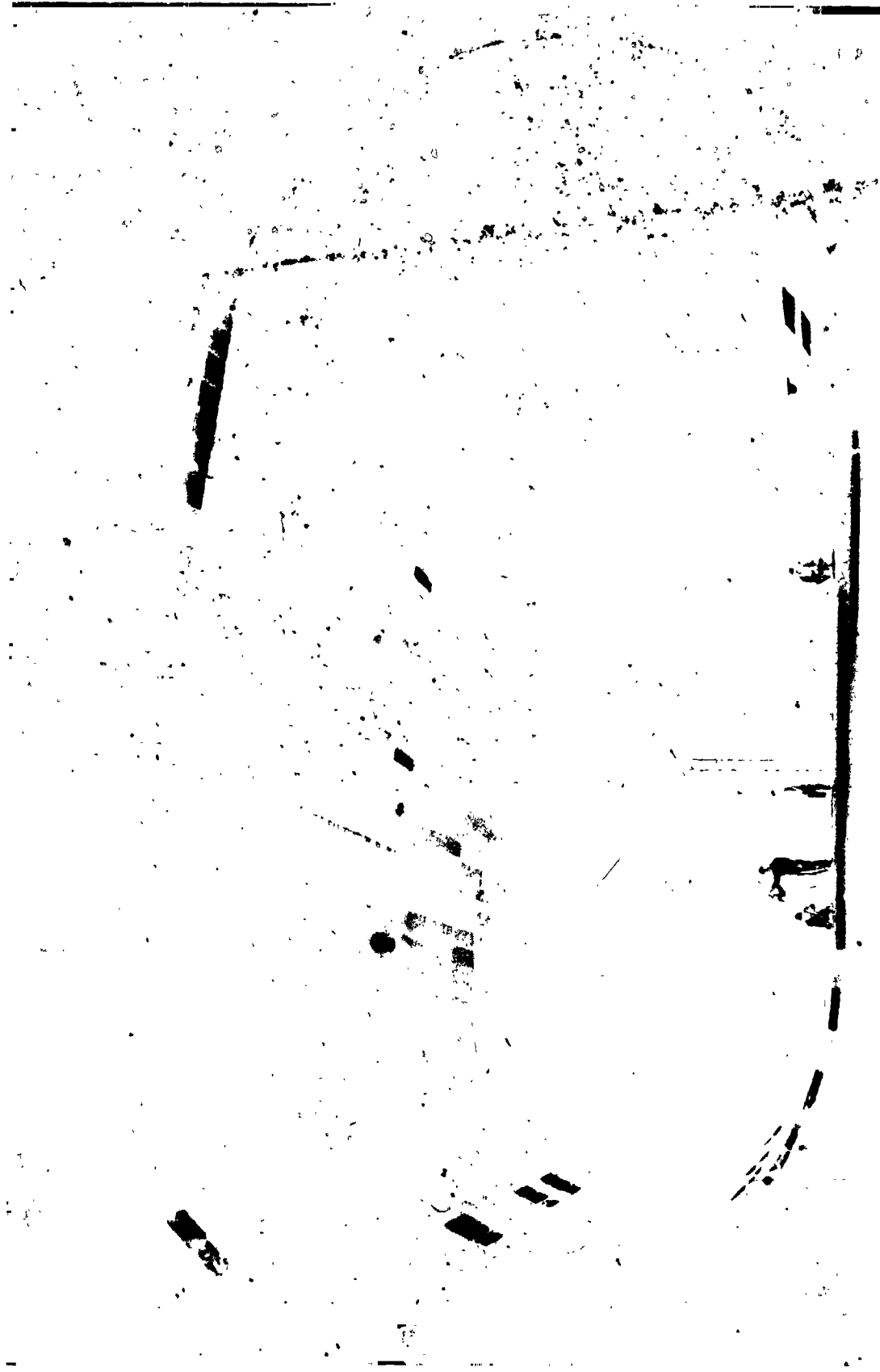


Figure 4.- The 40- by 80-Foot Wind Tunnel test section.

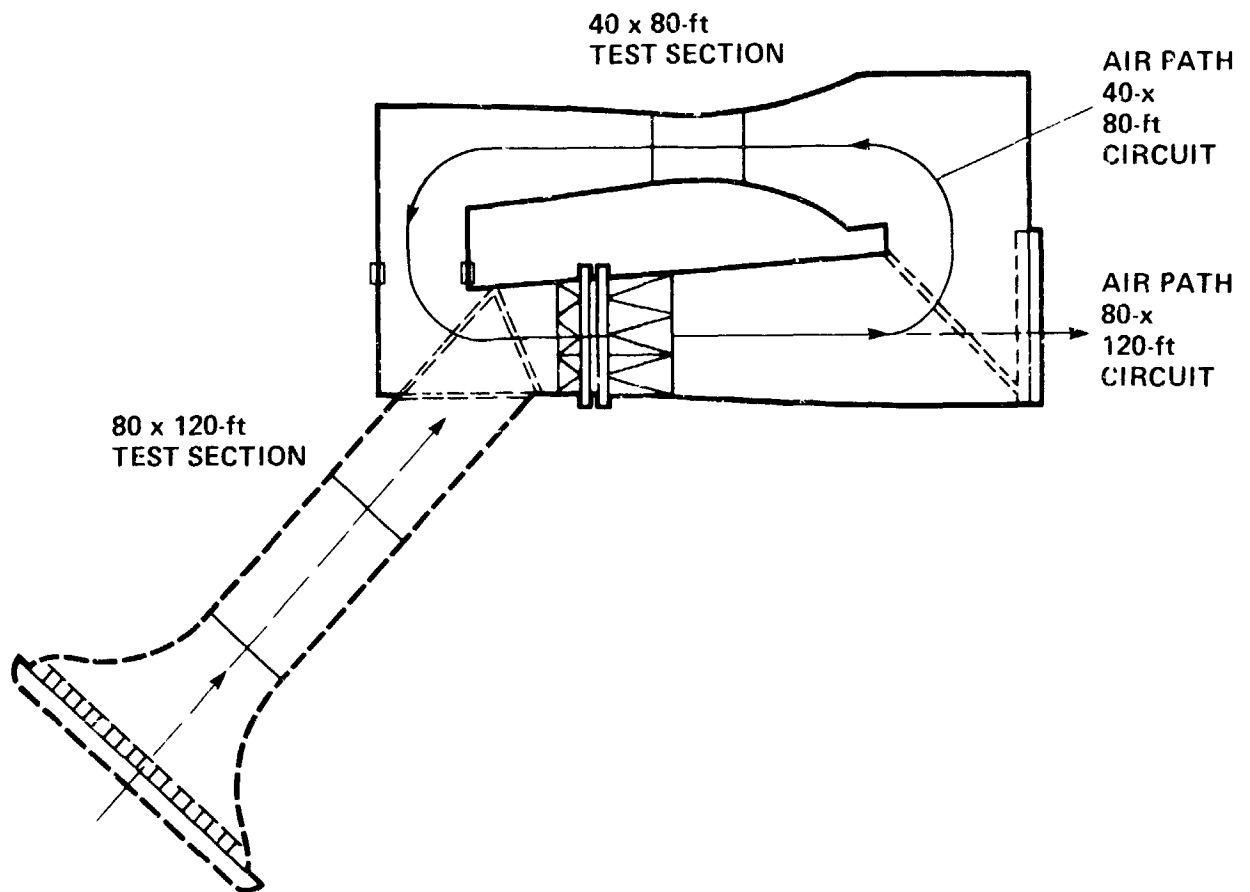


Figure 5.- Plan view of 40- by 80-/80- by 120-Foot Wind Tunnel facility.

ORIGINAL DRAWING  
OF POOR QUALITY

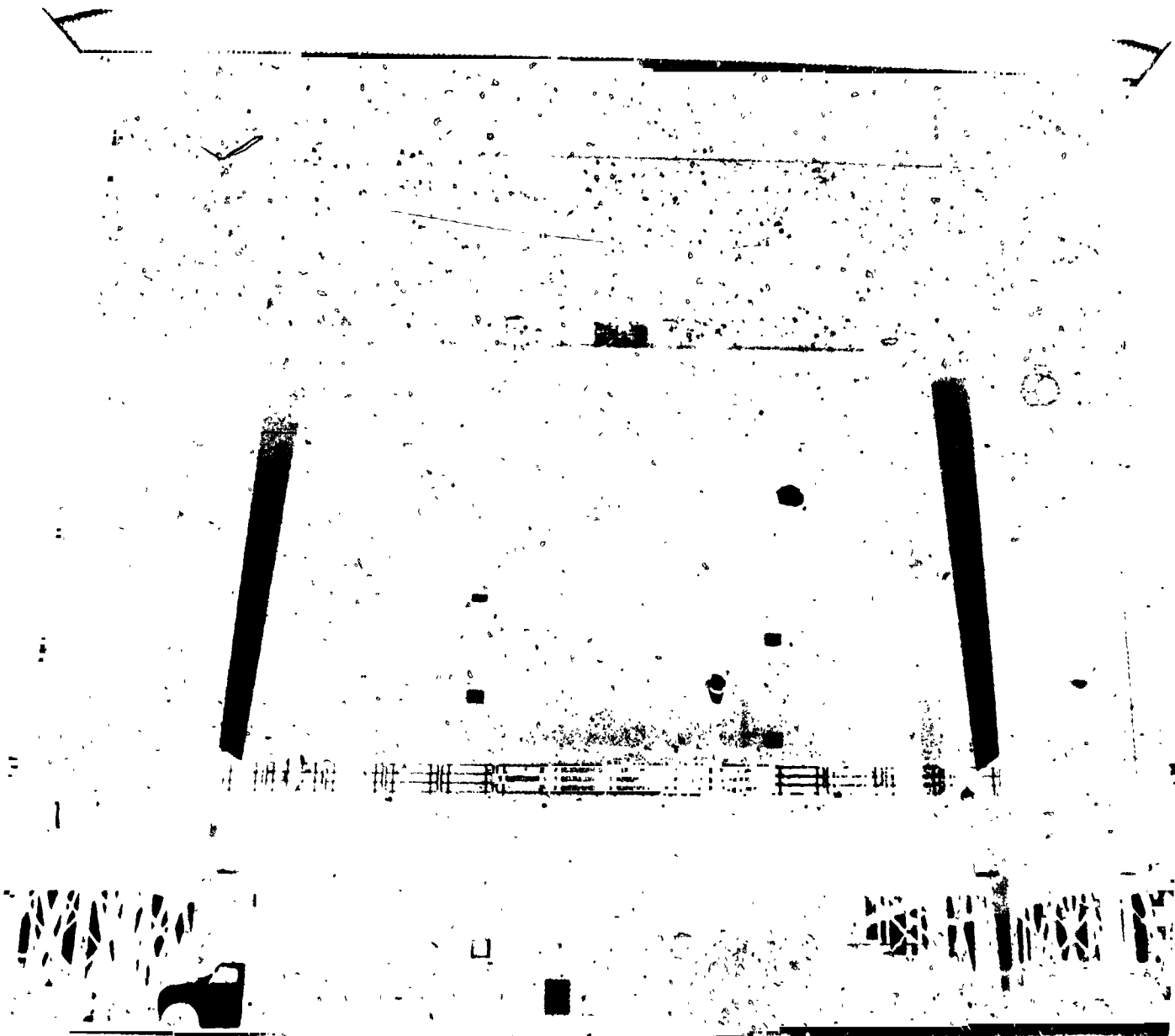


Figure 6.- 80- by 120-Foot Wind Tunnel test section entrance.





Figure 7.- Advancing Blade Concept (ABC) aircraft model under pretest checkout at the Outdoor Aerodynamic Research Facility.

AIR EXCHANGER

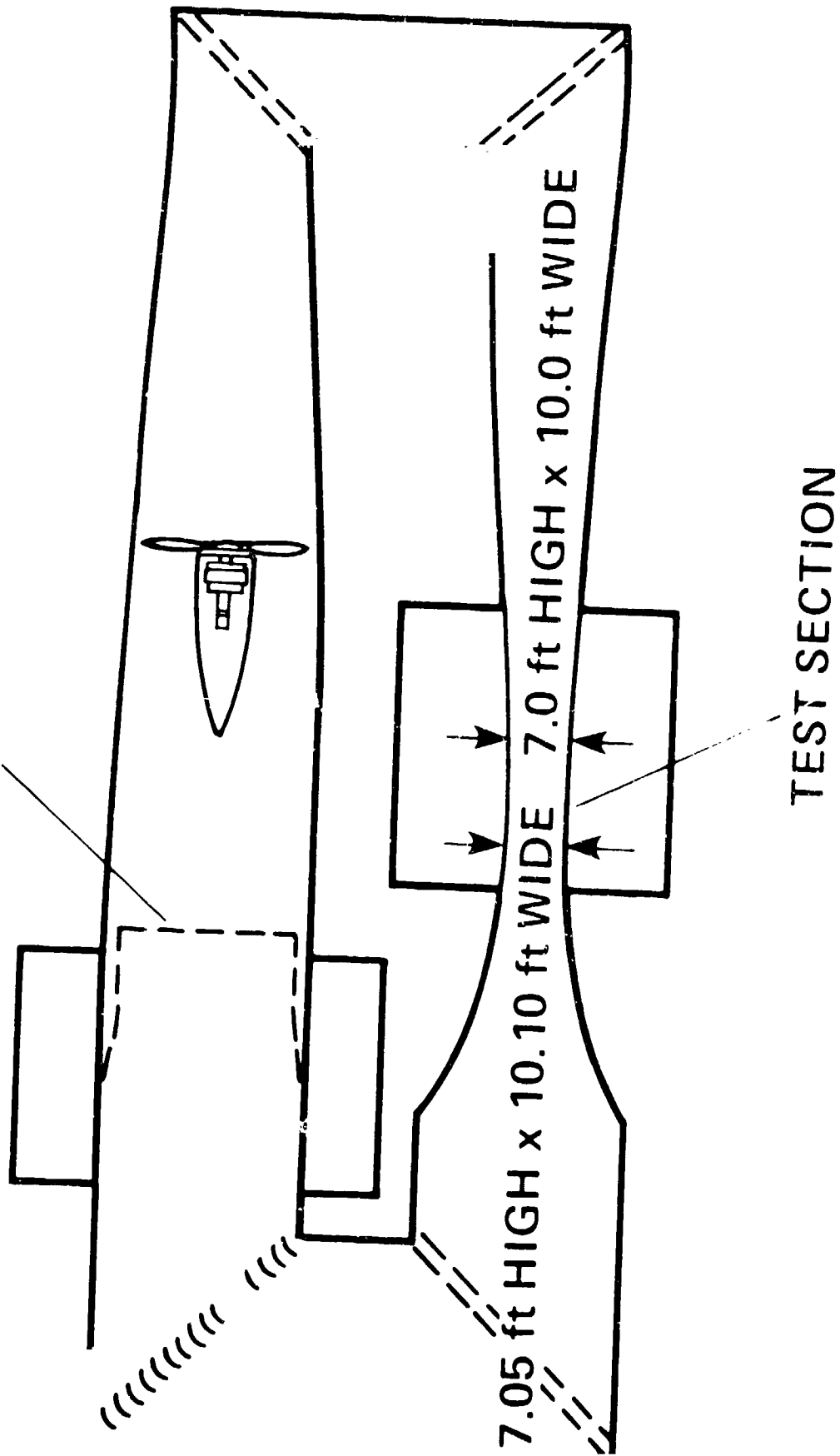


Figure 8.- Plan view of Ames 7- by 10-Foot Subsonic Wind Tunnel.

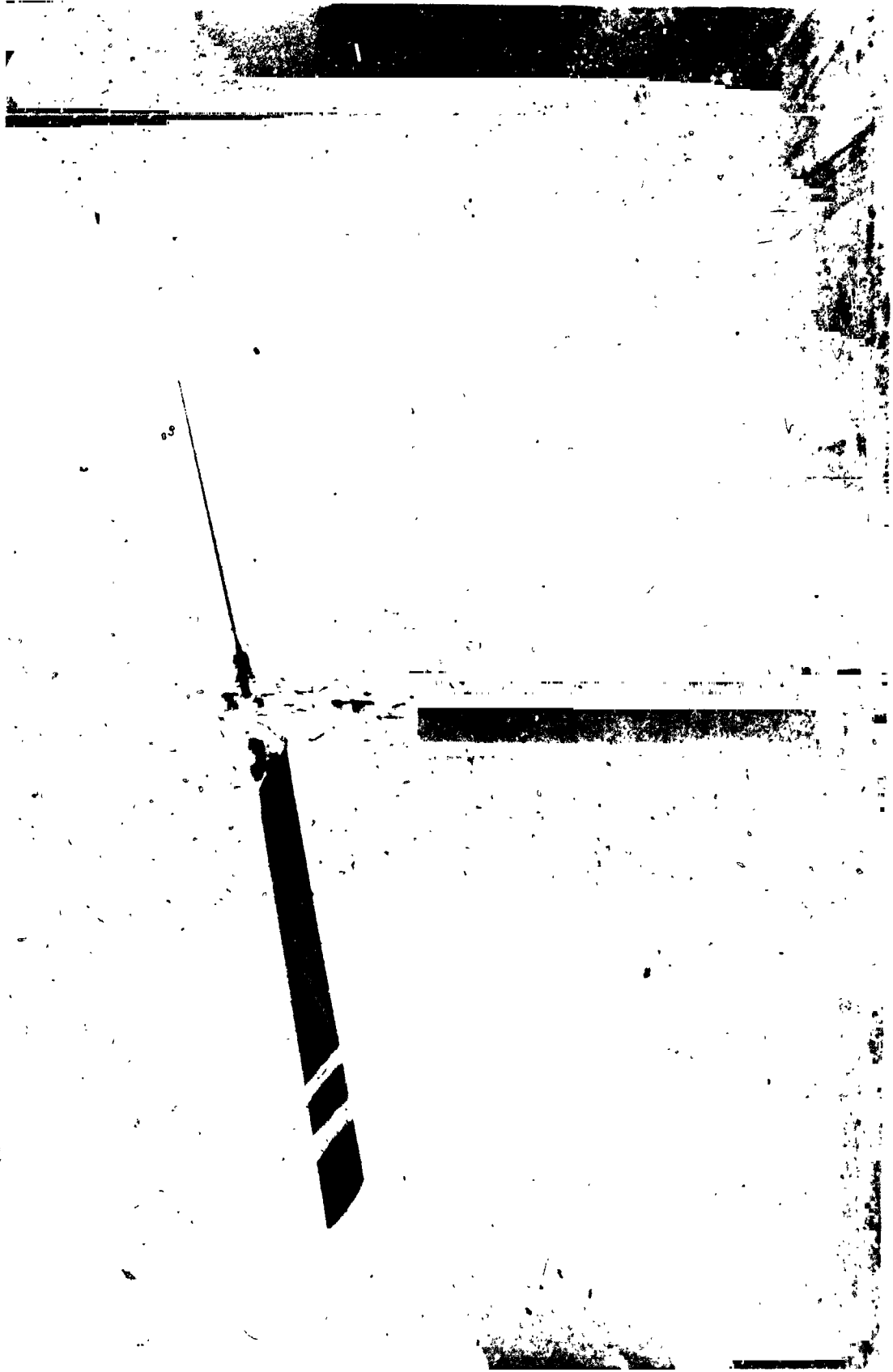


Figure 9.- Model rotor test in Ames 7- by 10-Foot Subsonic Wind Tunnel.

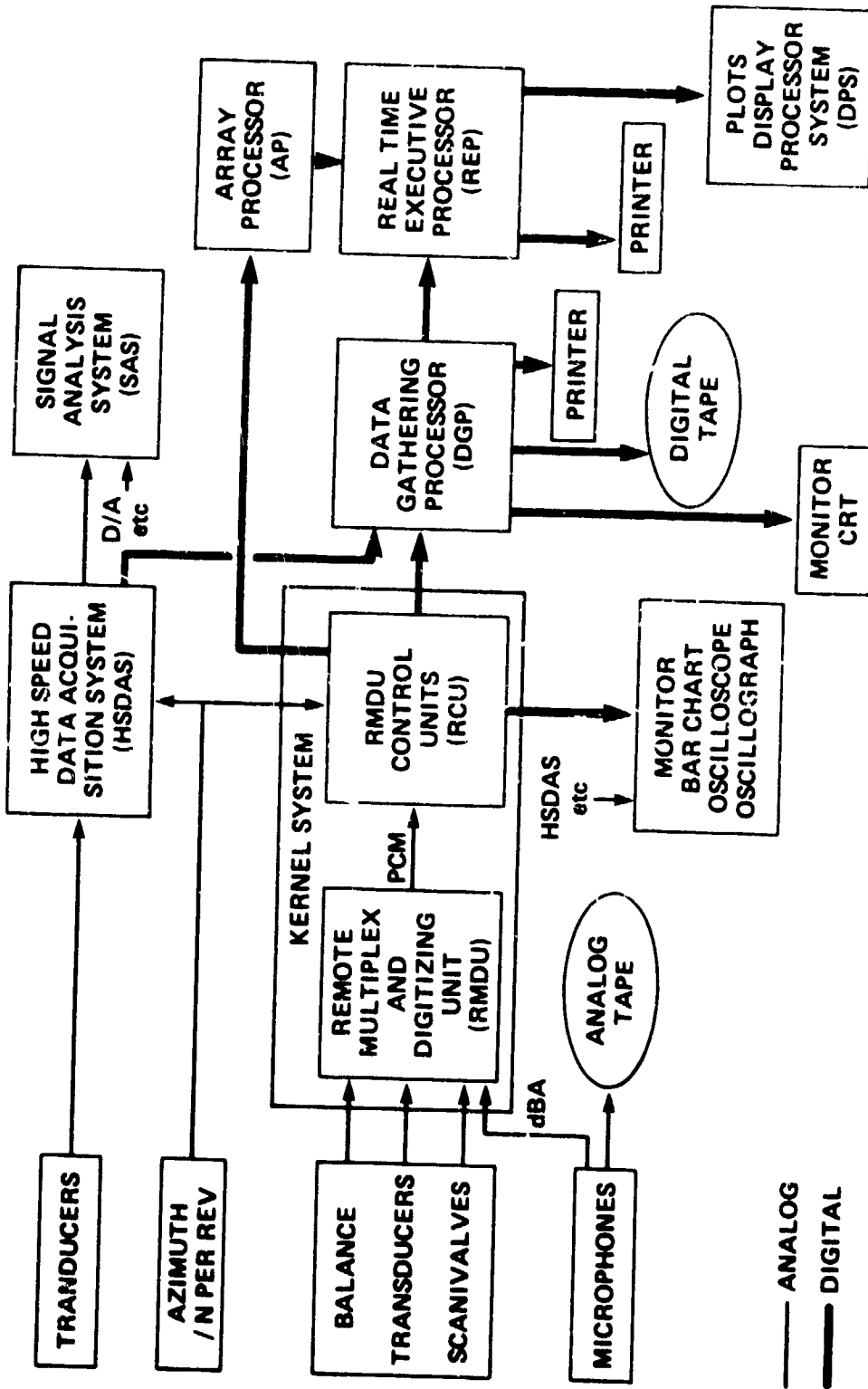


Figure 10.- Schematic of standard NFAC data-acquisition system.

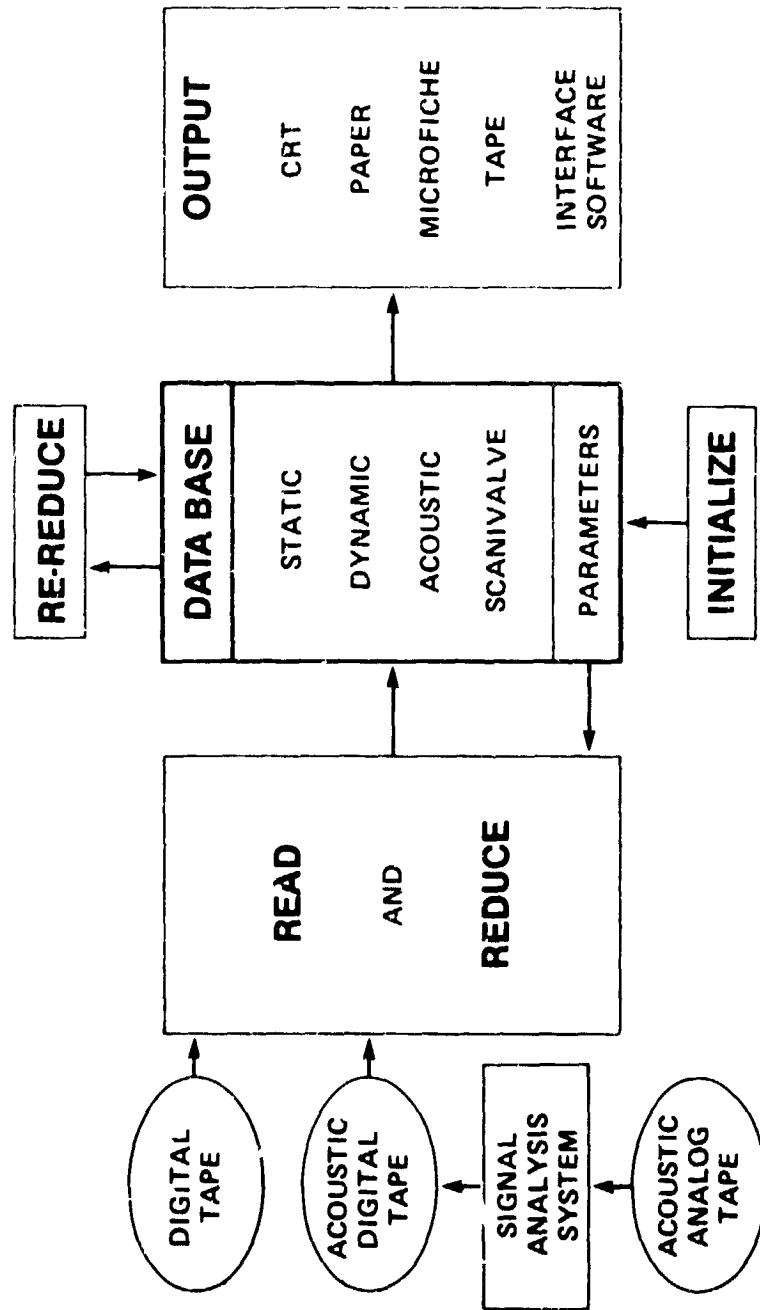


Figure 11.- Schematic of Rotor Data Reduction System.

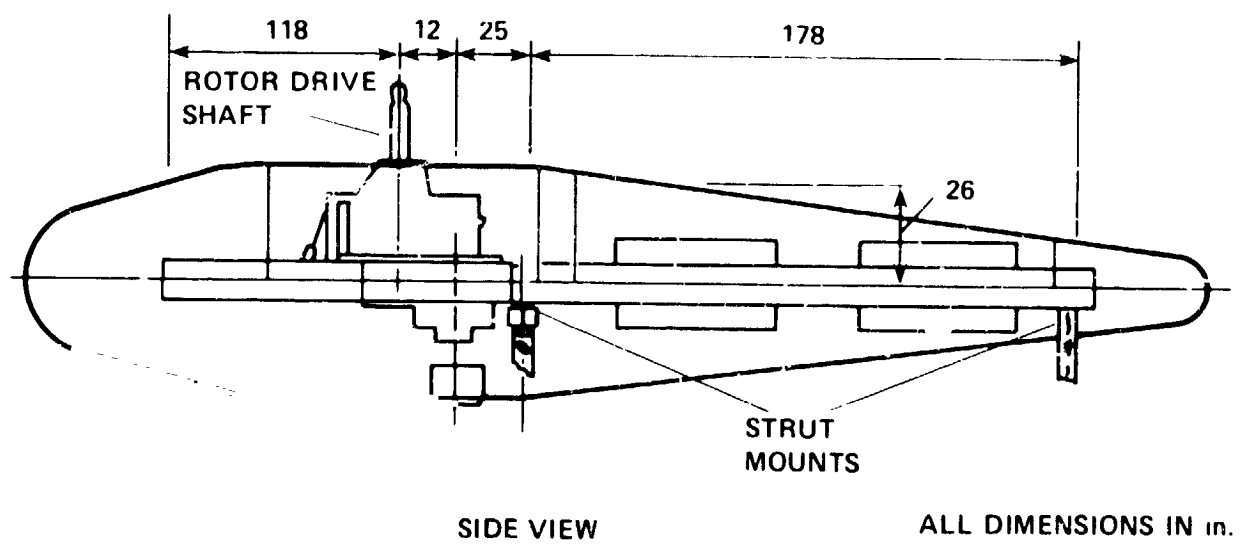
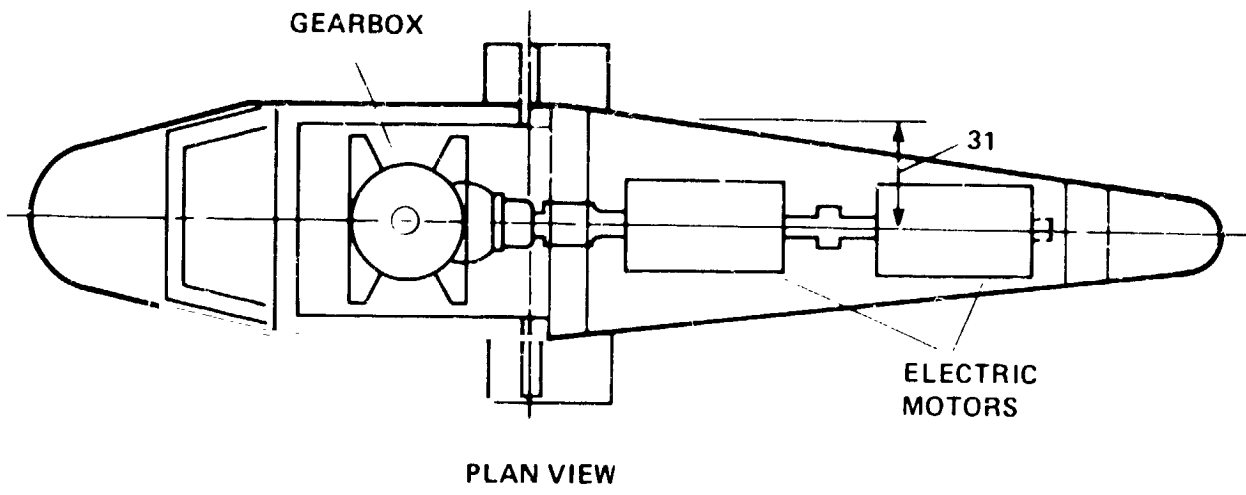


Figure 12.- Schematic of Ames Rotor Test Apparatus.

ORIGINAL PAGE IS  
OF POOR QUALITY.



Figure 13.- Installation of Ames Rotor Test Apparatus with Boeing Vertol Bearingless Main Rotor in 40- by 80-Foot Wind Tunnel.

ORIGINAL SIZE  
OF POOR QUALITY

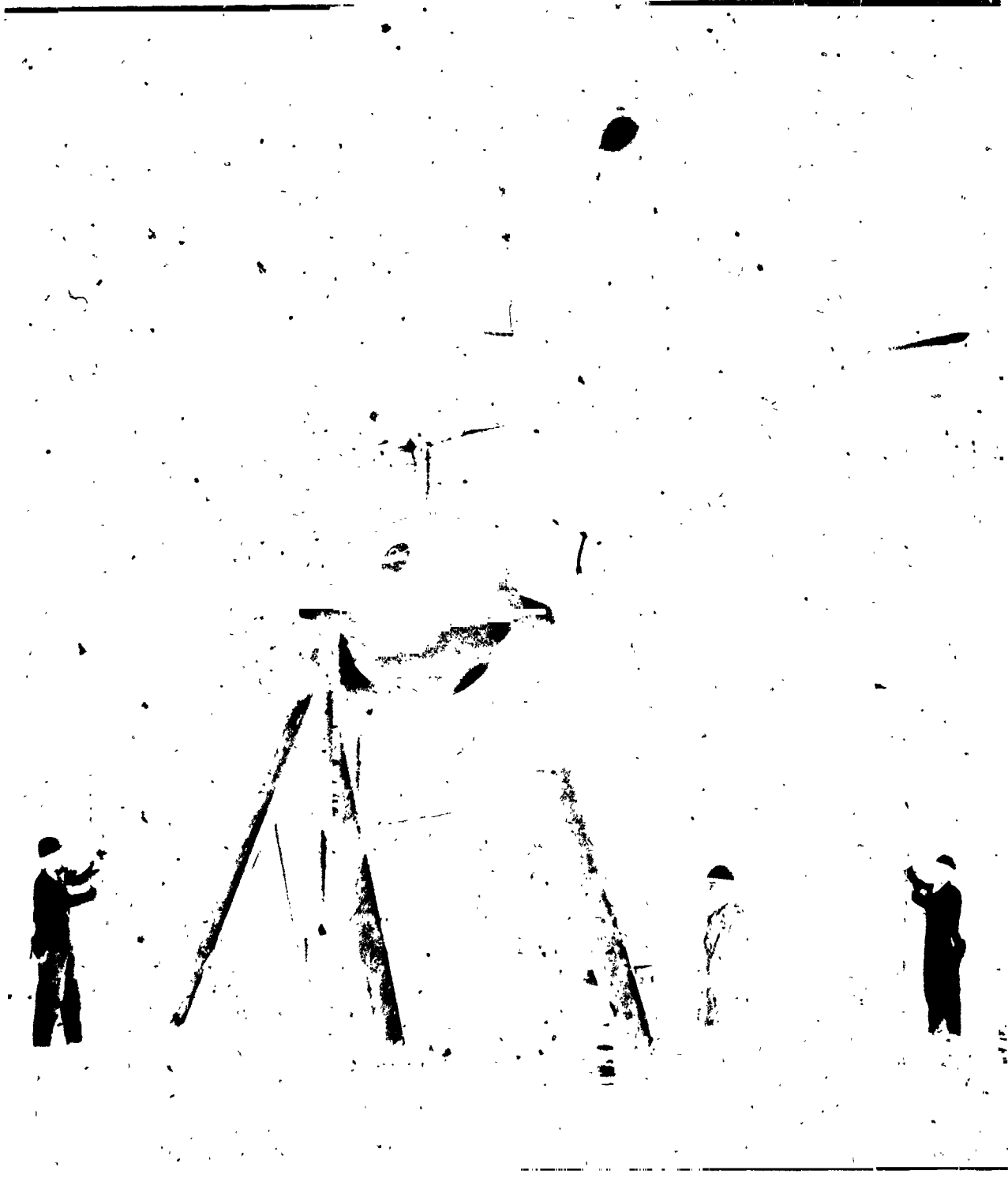


Figure 14.- Installation of Model 576 test stand (Easter Egg module) with Bell two-bladed rotor system in 40- by 80-foot Wind Tunnel.



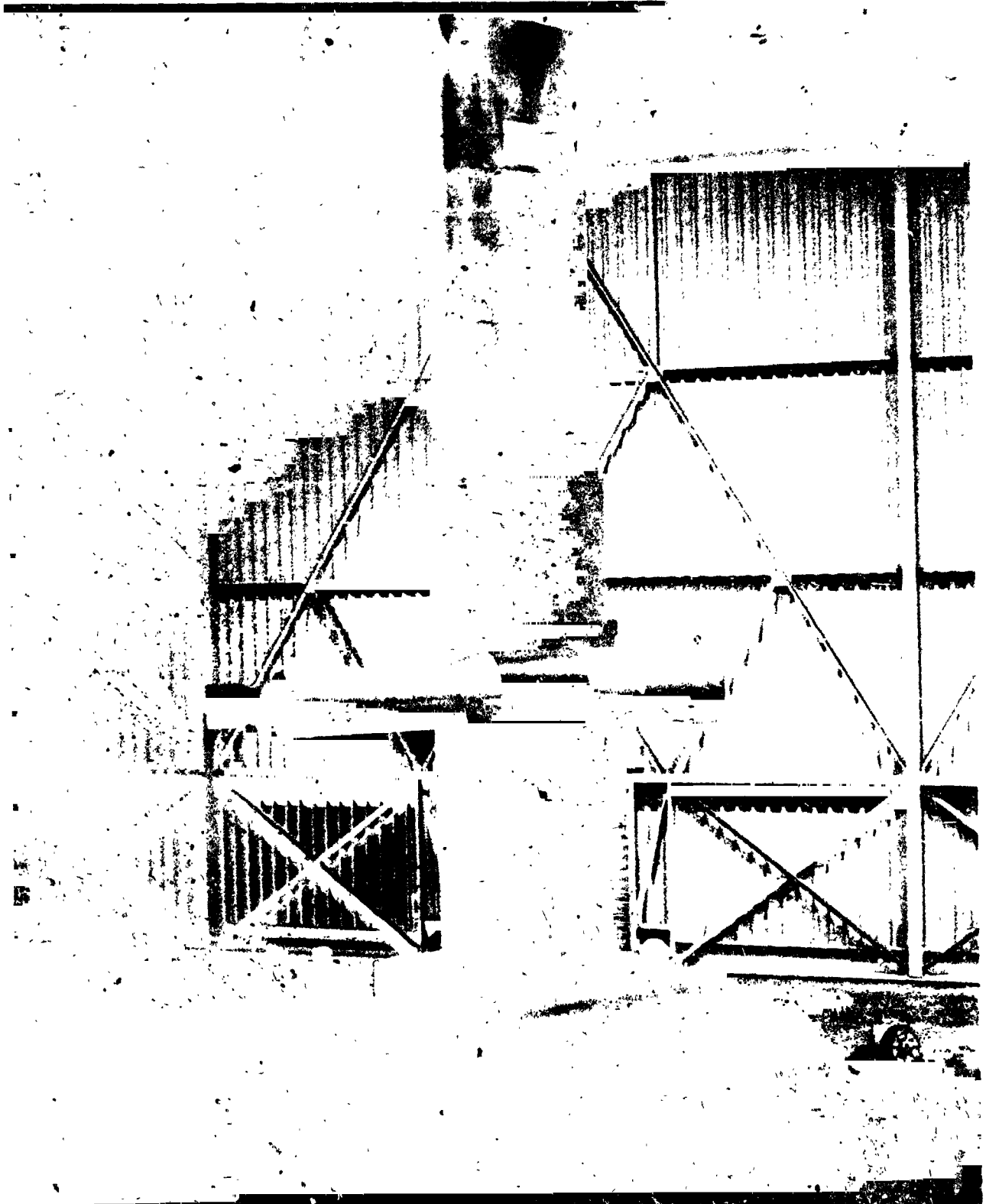


Figure 15.- Ames Tail Rotor Test Rig for testing full-scale tail rotors in the NFAC.

ORIGINAL PHOTOGRAPH  
OF POOR QUALITY



(a) 40- by 80-Foot Wind Tunnel.

Figure 16.- Installation of the Ames Prop Test Rig with XV-15 rotor system for forward flight and hover performance testing.

ORIGINAL PHOTOGRAPH  
OF POOR QUALITY



(b) Outdoor Aerodynamic Research Facility.

Figure 16.- Concluded.

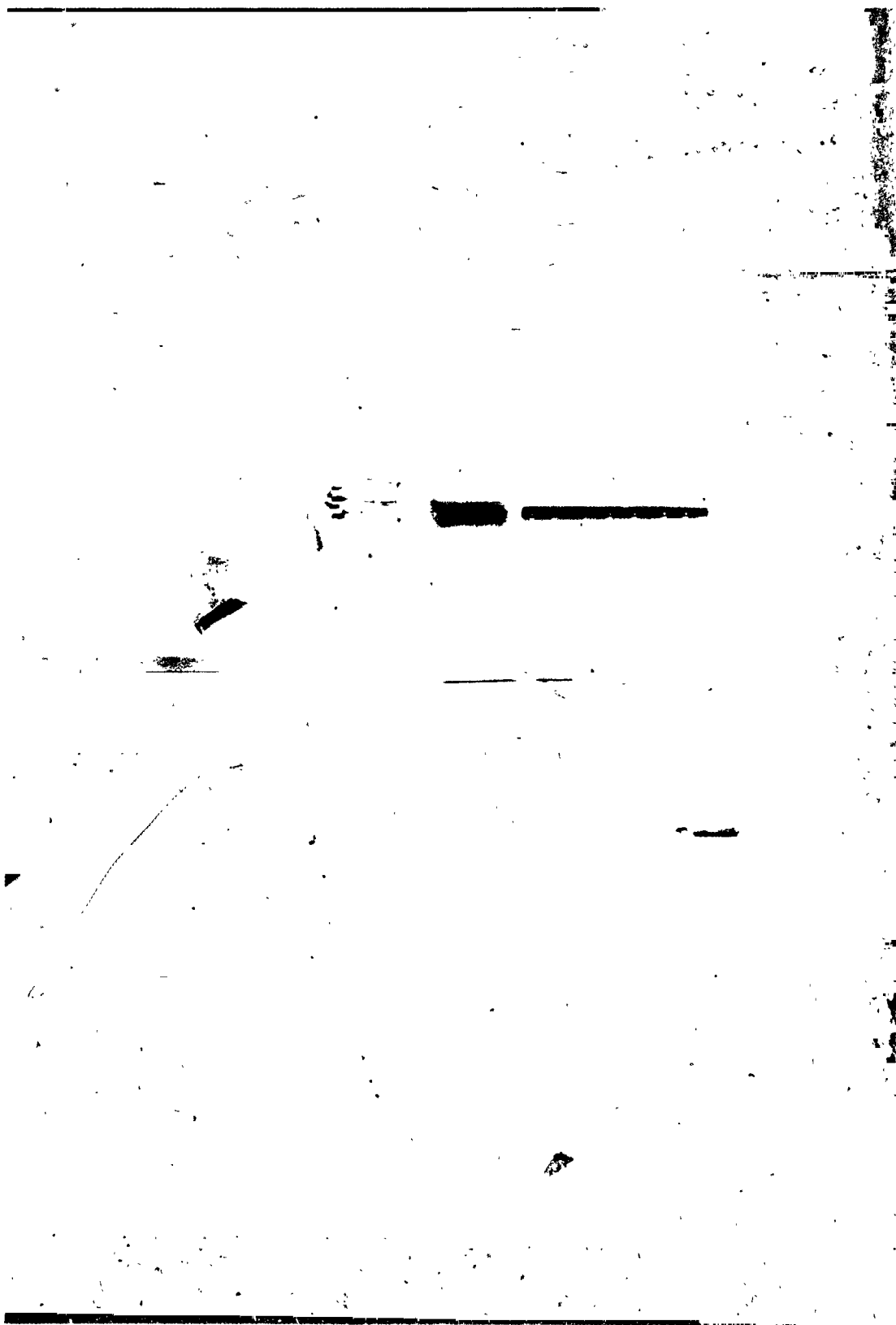
ORIGINAL COPY  
OF POOR QUALITY



(a) 40- by 8-Foot Wind Tunnel test section.

Figure 17.- Installation of the Ames Rotor Test Rig.

ORIGINAL FIGURE  
OF POOR QUALITY



(b) 7- by 10-Foot Subsonic Wind Tunnel.

Figure 17.- Concluded.

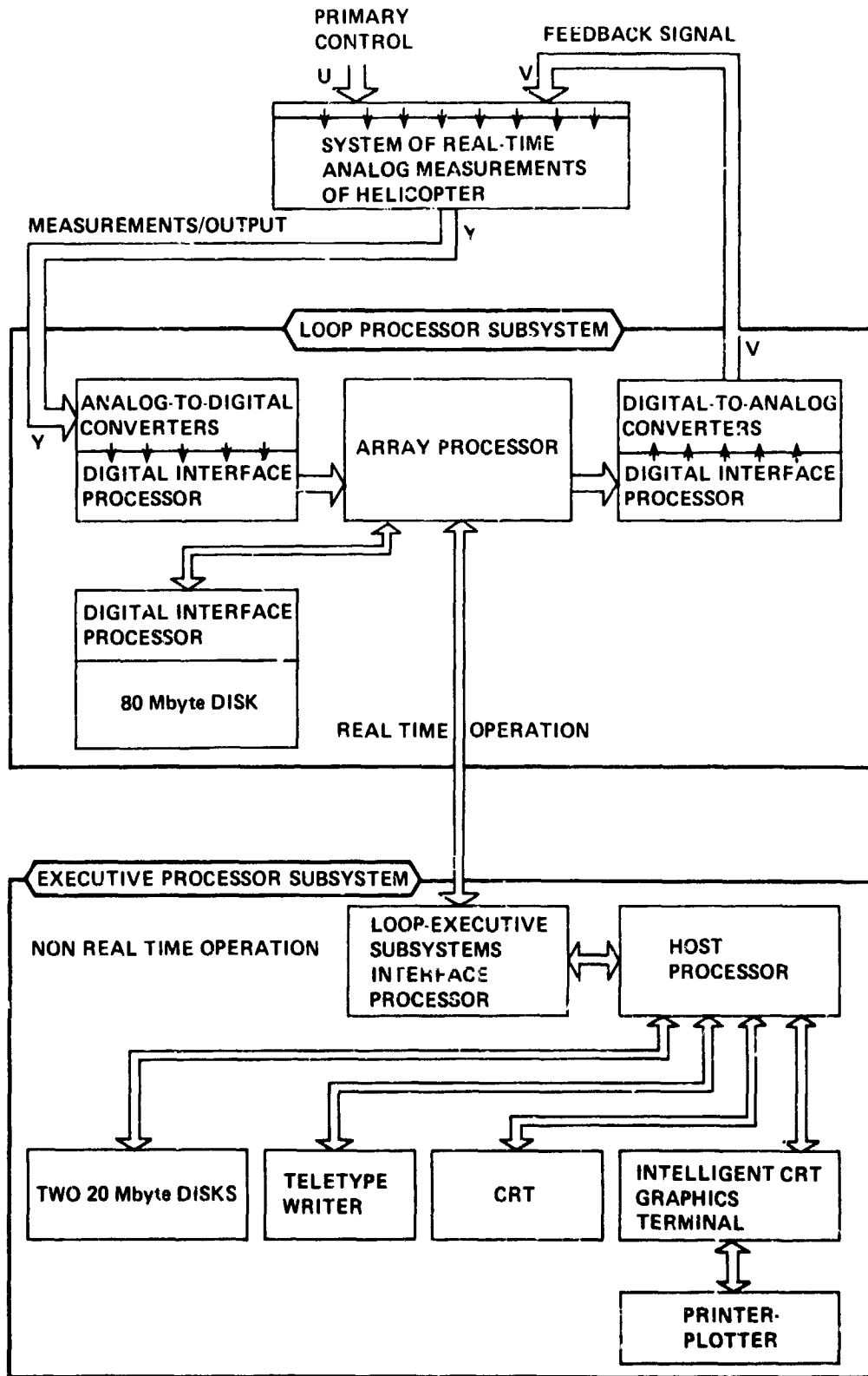


Figure 18.- Schematic of Multicyclic Computer Control System architecture.

ORIGINAL PAGE IS  
OF POOR QUALITY

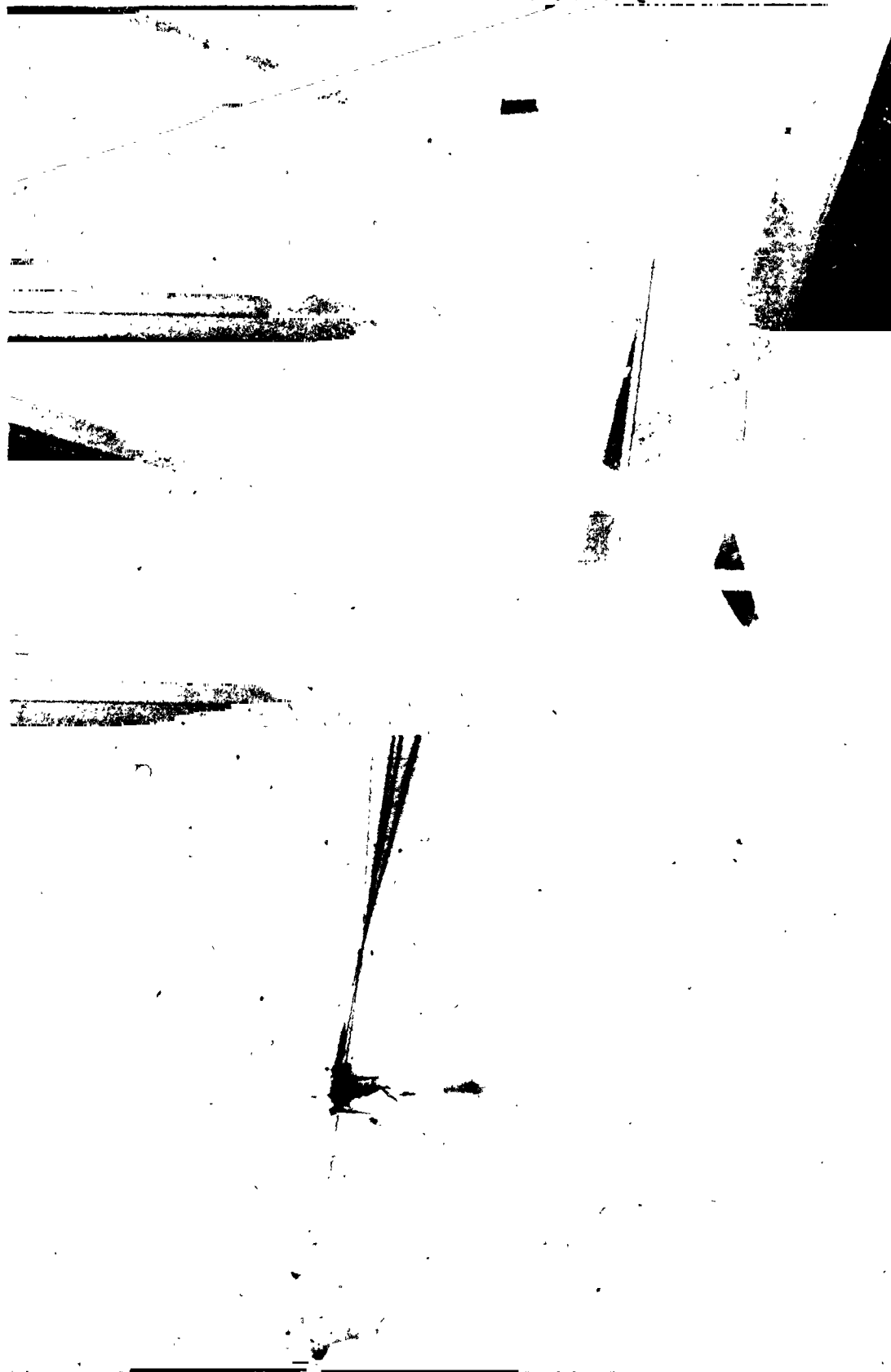
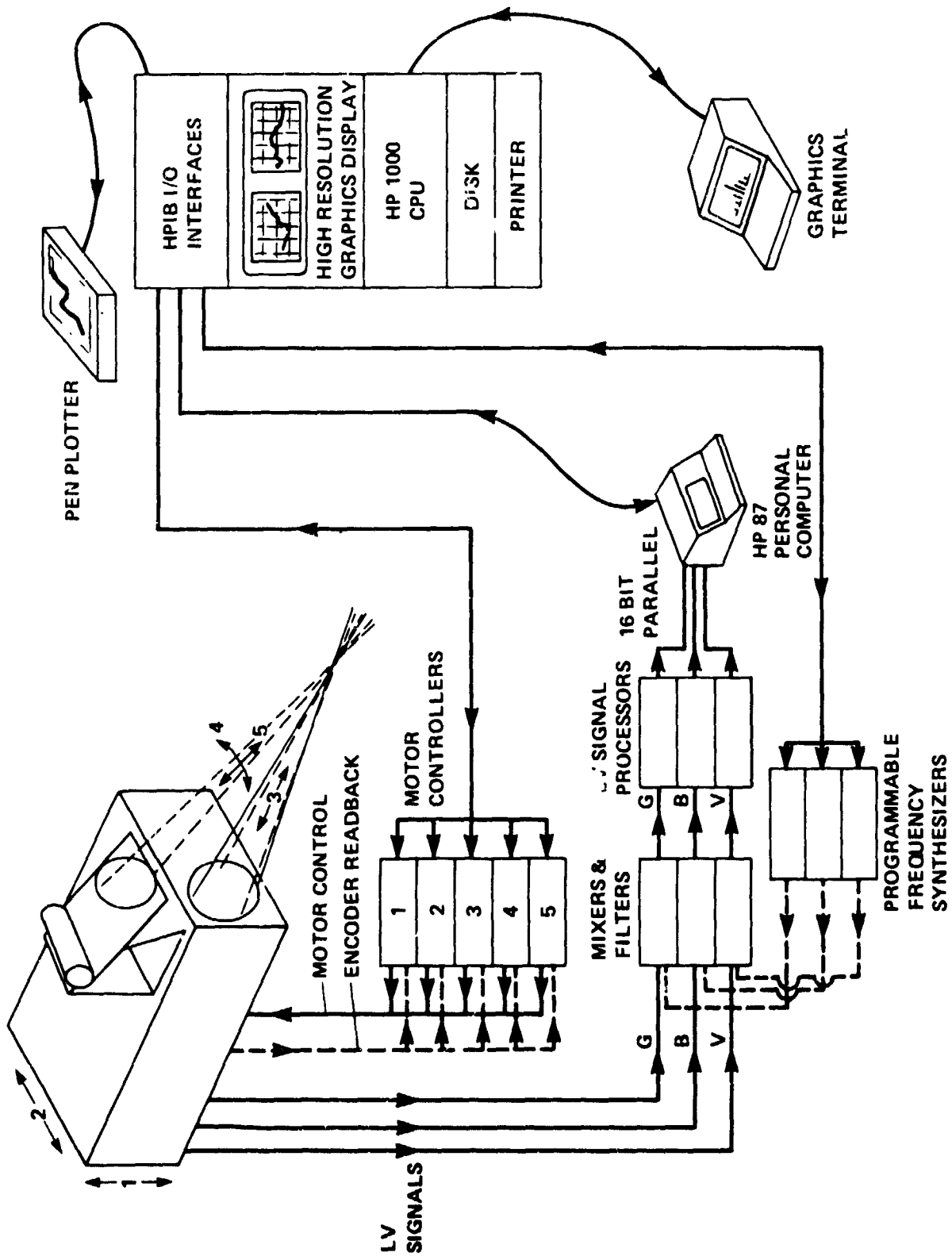


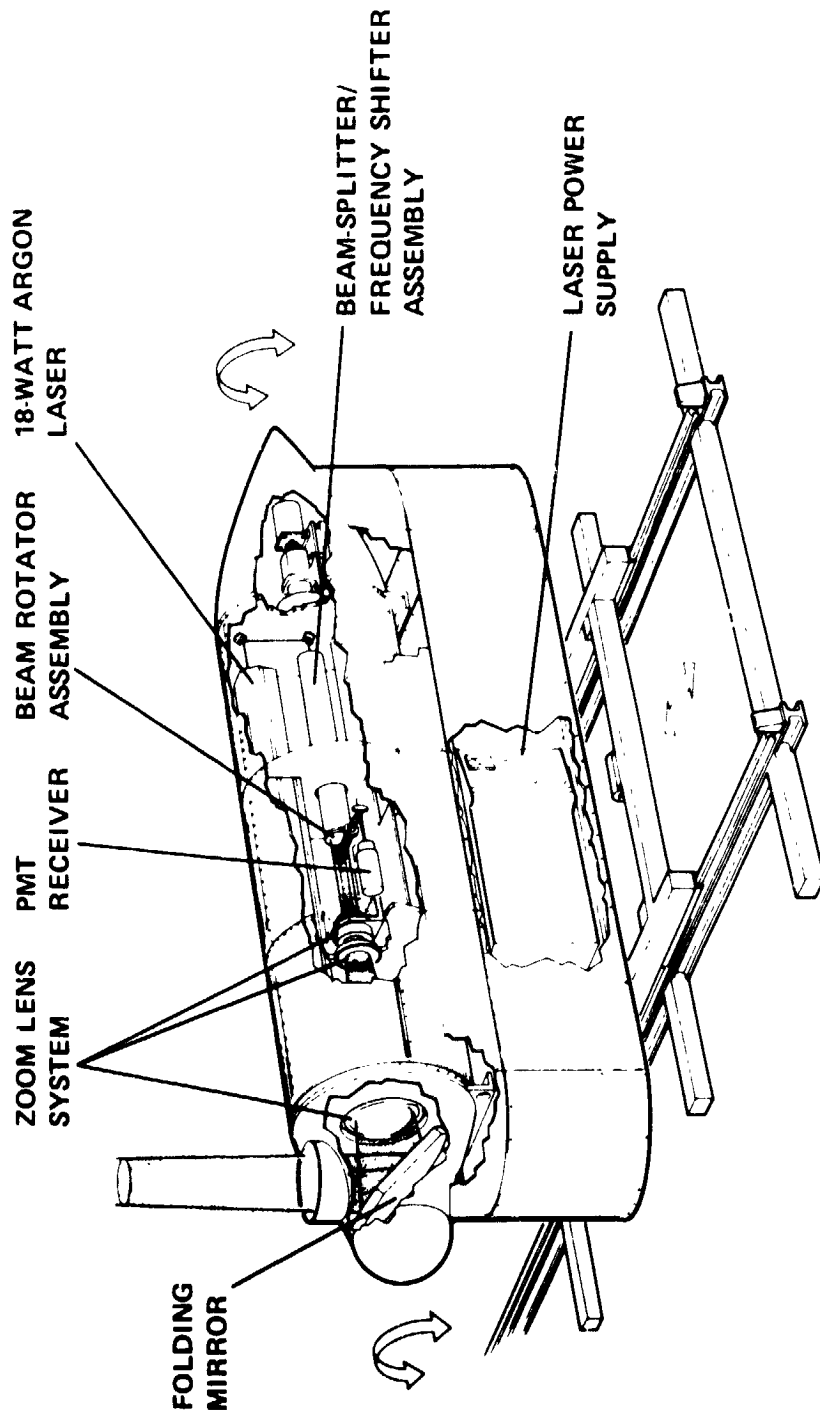
Figure 19.- Model rotor test using a two-dimensional LDV to measure hovering rotor-  
blade loading and wake velocities.



(a) Data-acquisition and control system.

Figure 20.- Recently developed laser velocimeter systems in the NFAC.





(b) Major components of 2-D long-range laser velocimeter.

Figure 20.- Concluded.



Figure 21.- Test installation of the Sikorsky S-76 rotor system on the Ames Rotor Test Apparatus in the 40- by 80-Foot Wind Tunnel.

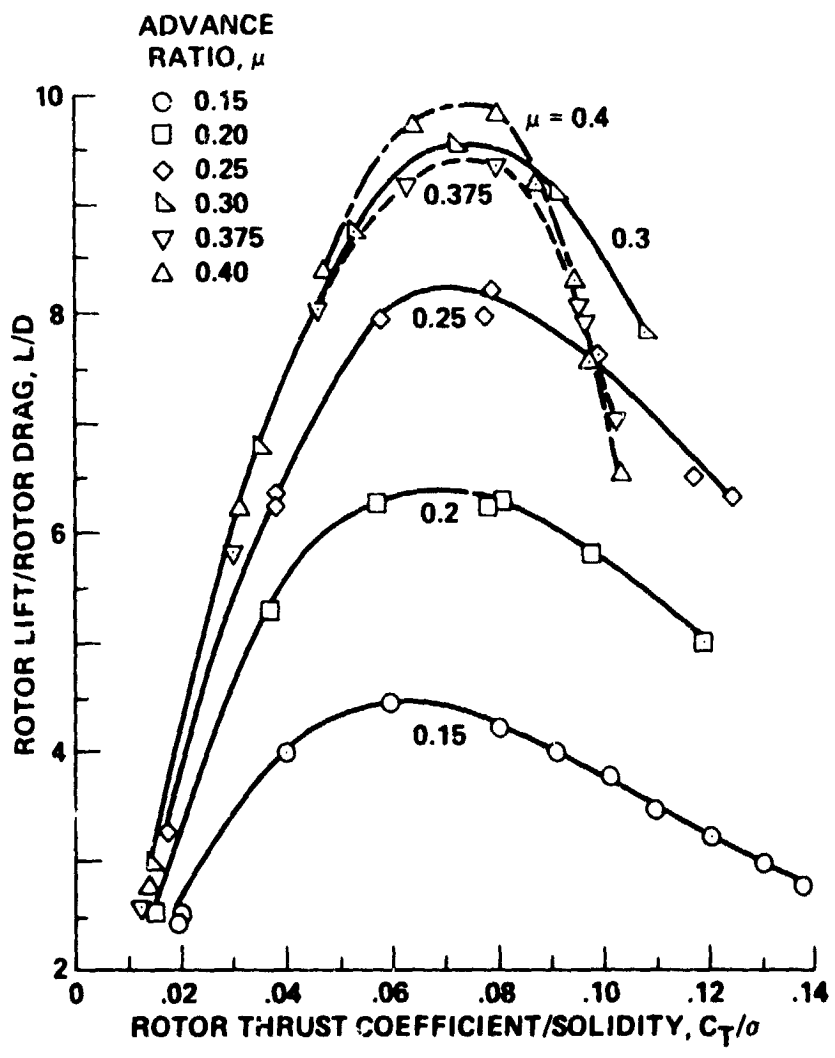
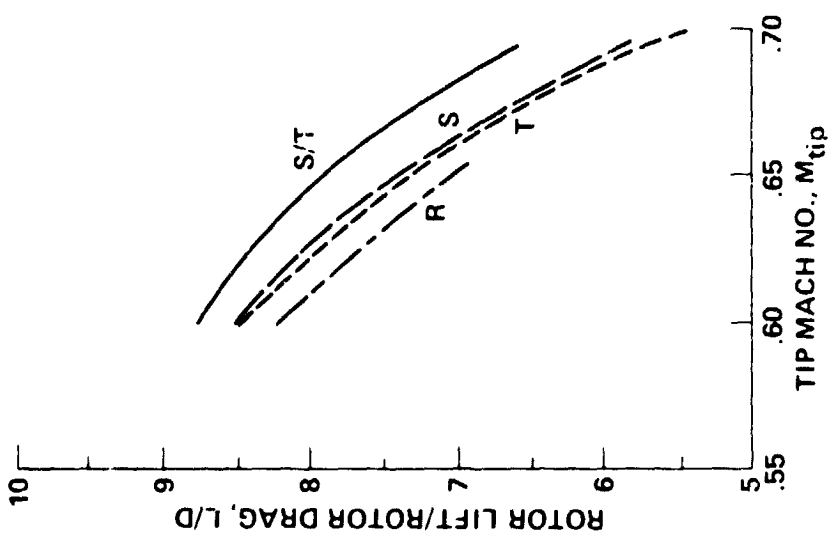
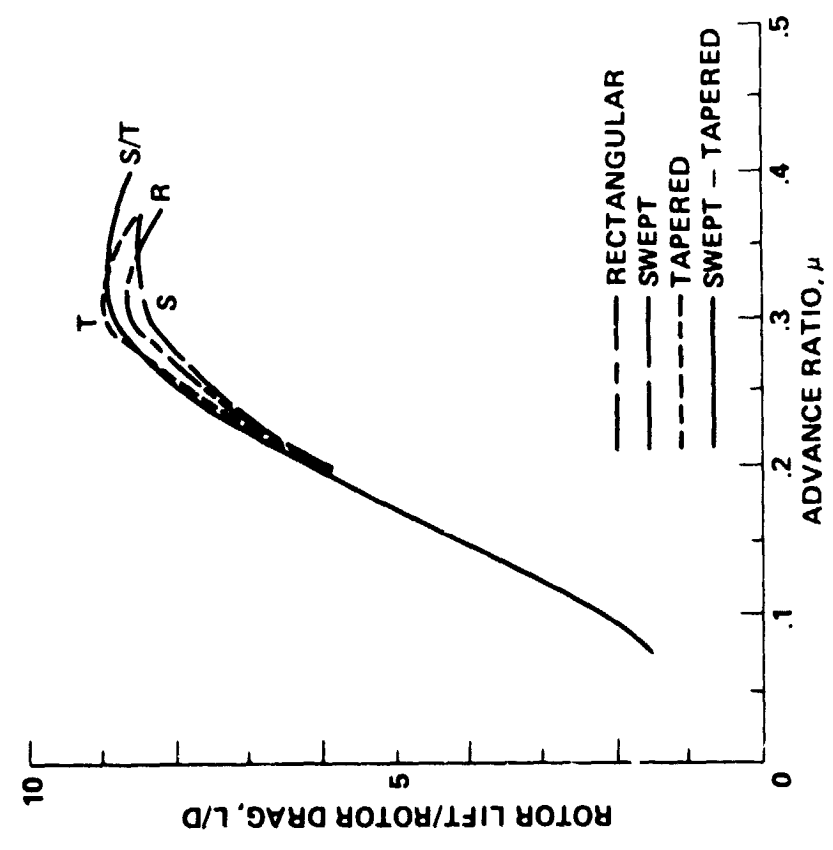


Figure 22.- Performance of S-76 rotor system with swept/tapered tips:  $\alpha_{TPP} = 0^\circ$ ,  $M_{tip} = 0.6$ .



(a)  $M_{tip} = 0.60$ .



(b)  $\mu = 0.375$ .

Figure 23.- Performance of S-76 rotor system with various tip shapes:  $C_T/\sigma = 0.07$ ,  
 $C_x/\sigma = v \cdot 0.043\mu^2$ .

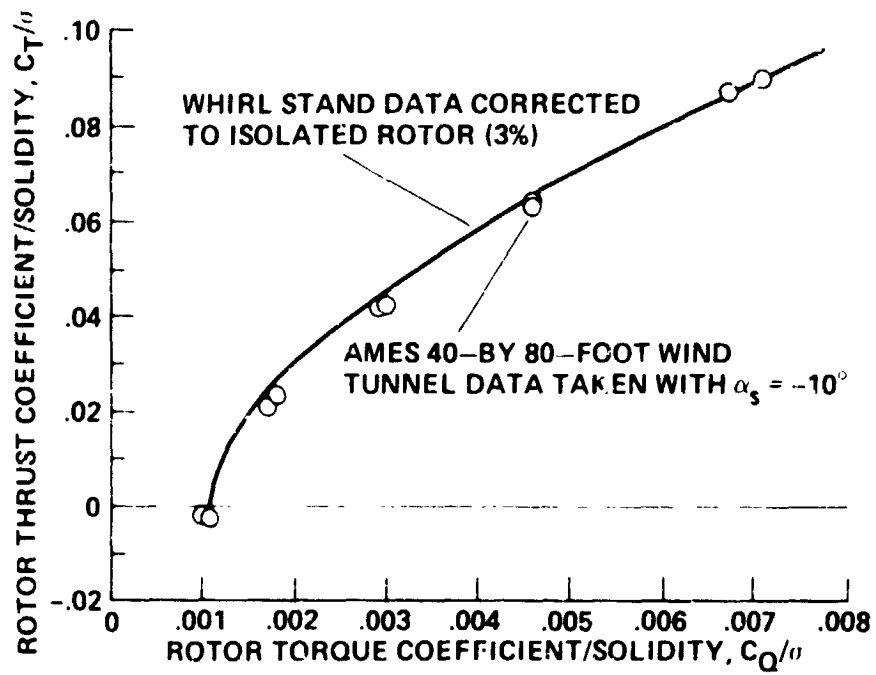
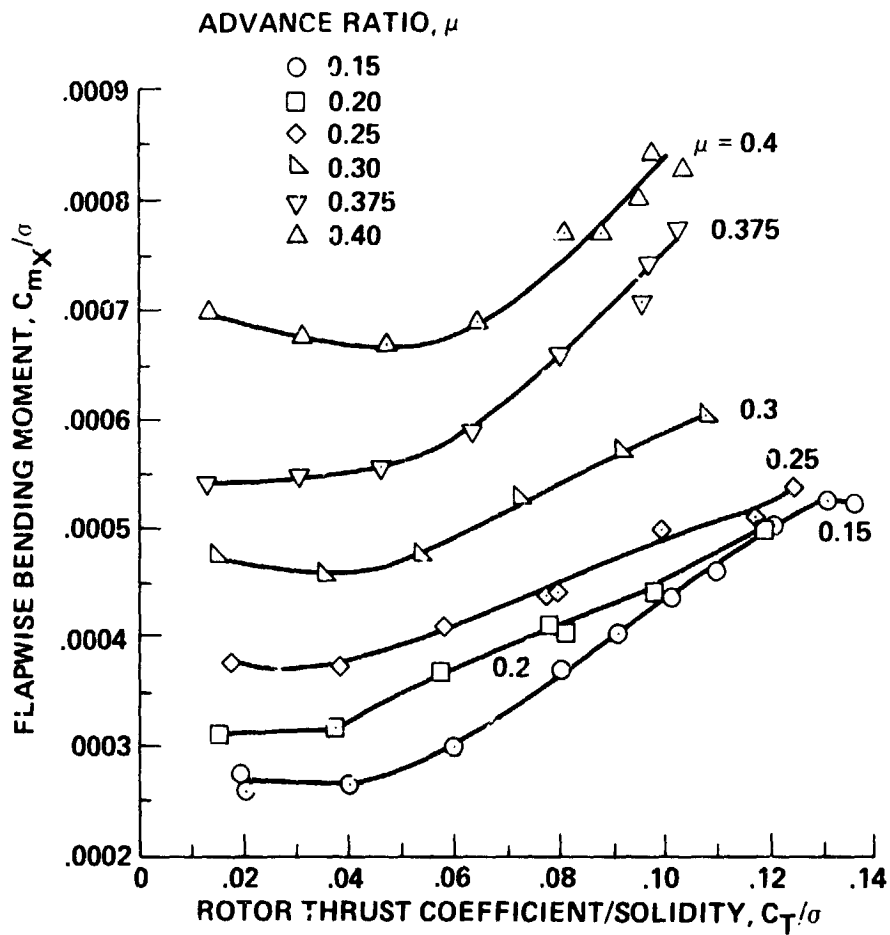
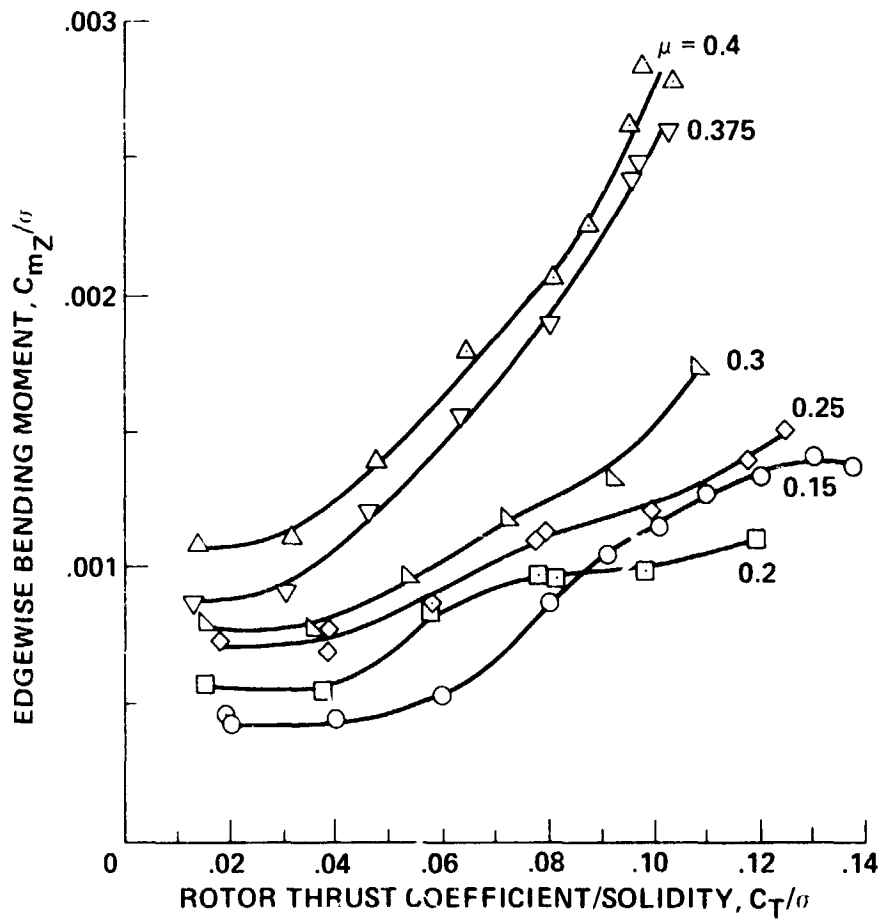


Figure 24.- Hover performance of S-76 rotor system.



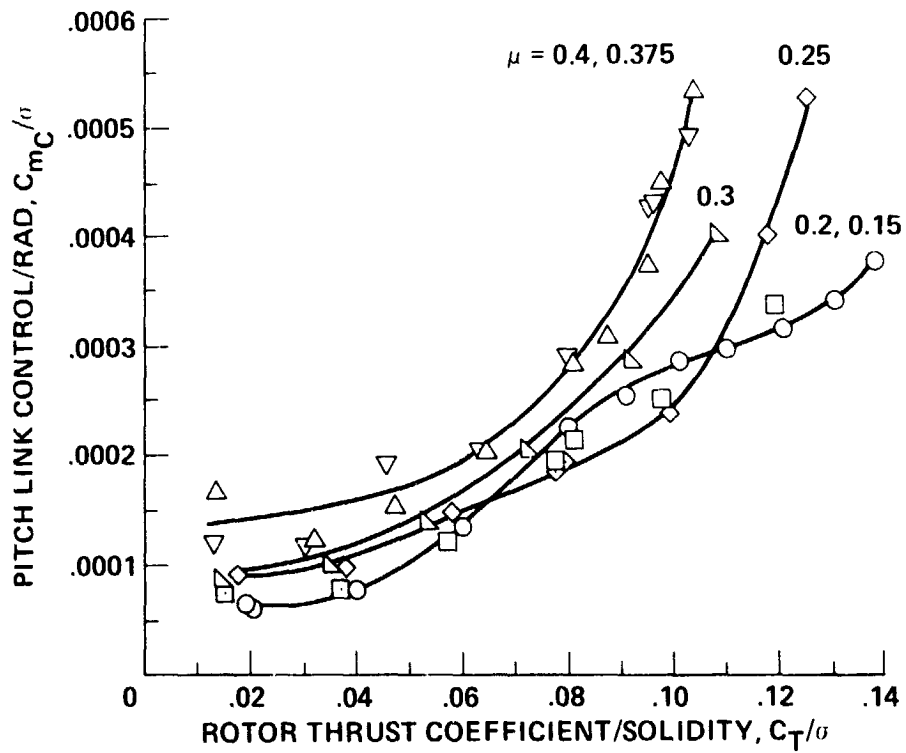
(a) Flapwise bending (1/2 peak-to-peak):  $r/R = 0.683$ .

Figure 25.- Rotor blade loads for S-76 rotor system, swept/tapered tip:  $\alpha_s = 0^\circ$ ,  $M_{tip} = 0.6$ .



(b) Edgewise bending (1/2 peak-to-peak):  $r/R = 0.604$ .

Figure 25.- Continued.



(c) Pitch-link control system load (1/2 peak-to-peak).

Figure 25.- Concluded.



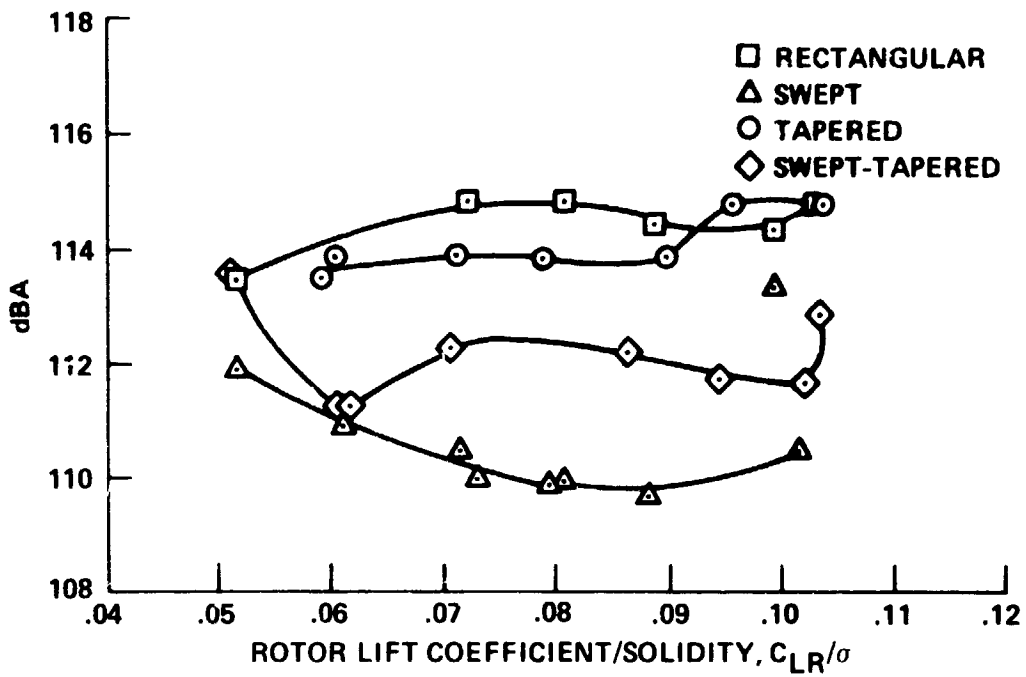


Figure 26.- Noise levels of S-76 rotor system at high wind-tunnel speeds:  
 $\alpha_s = -5^\circ$ ,  $\mu = 0.375$ ,  $M_{1,90} = 0.9$ .

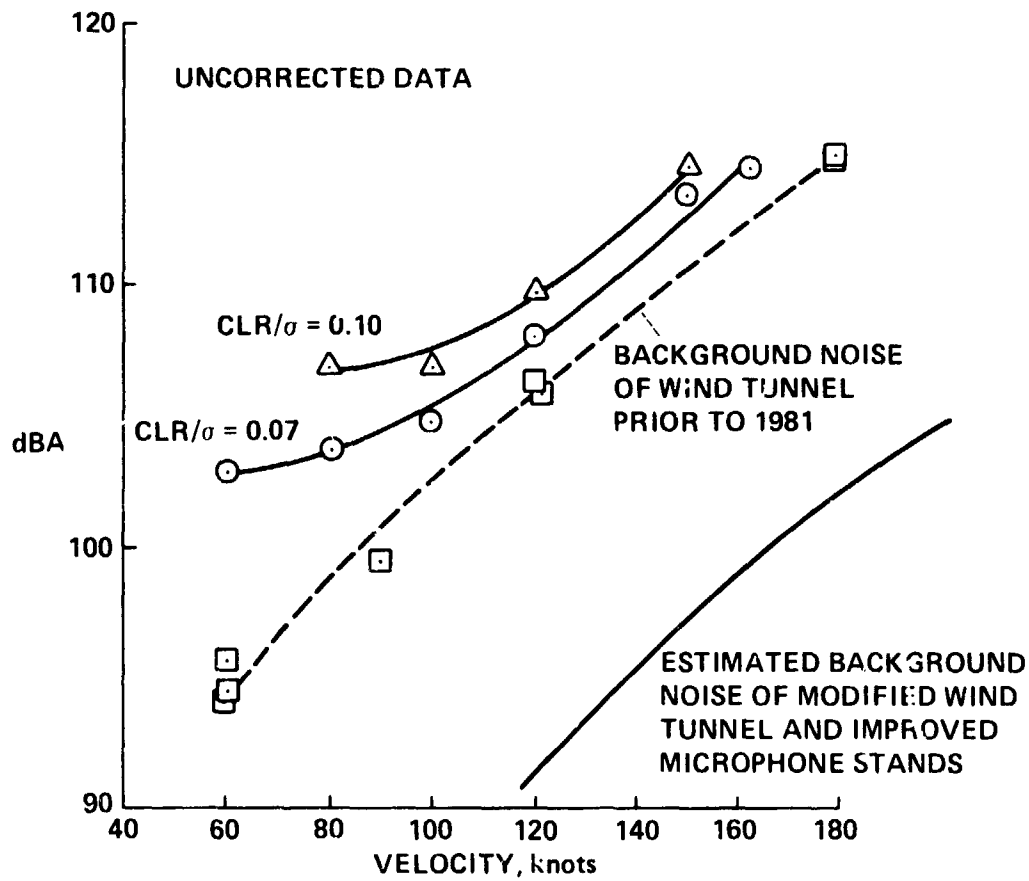
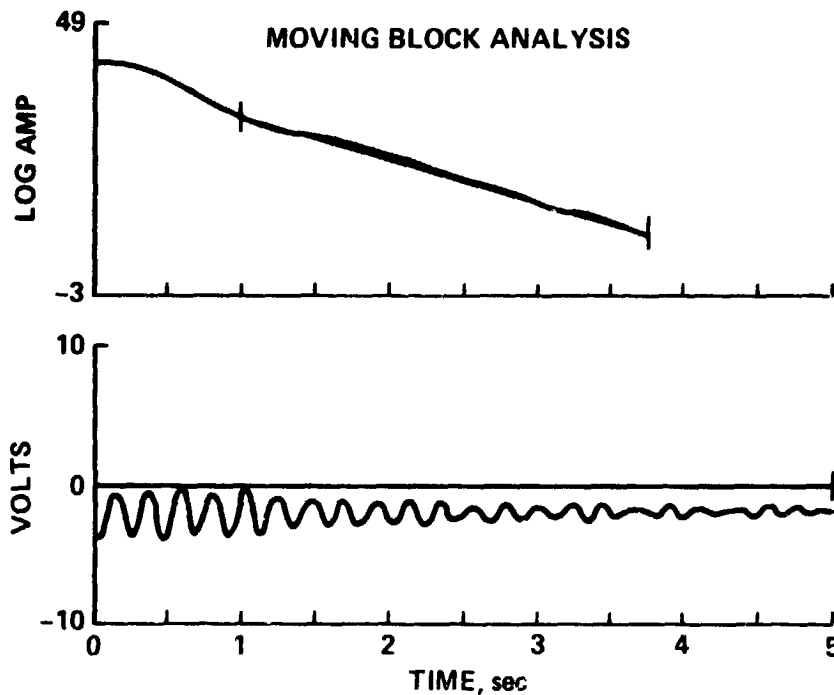
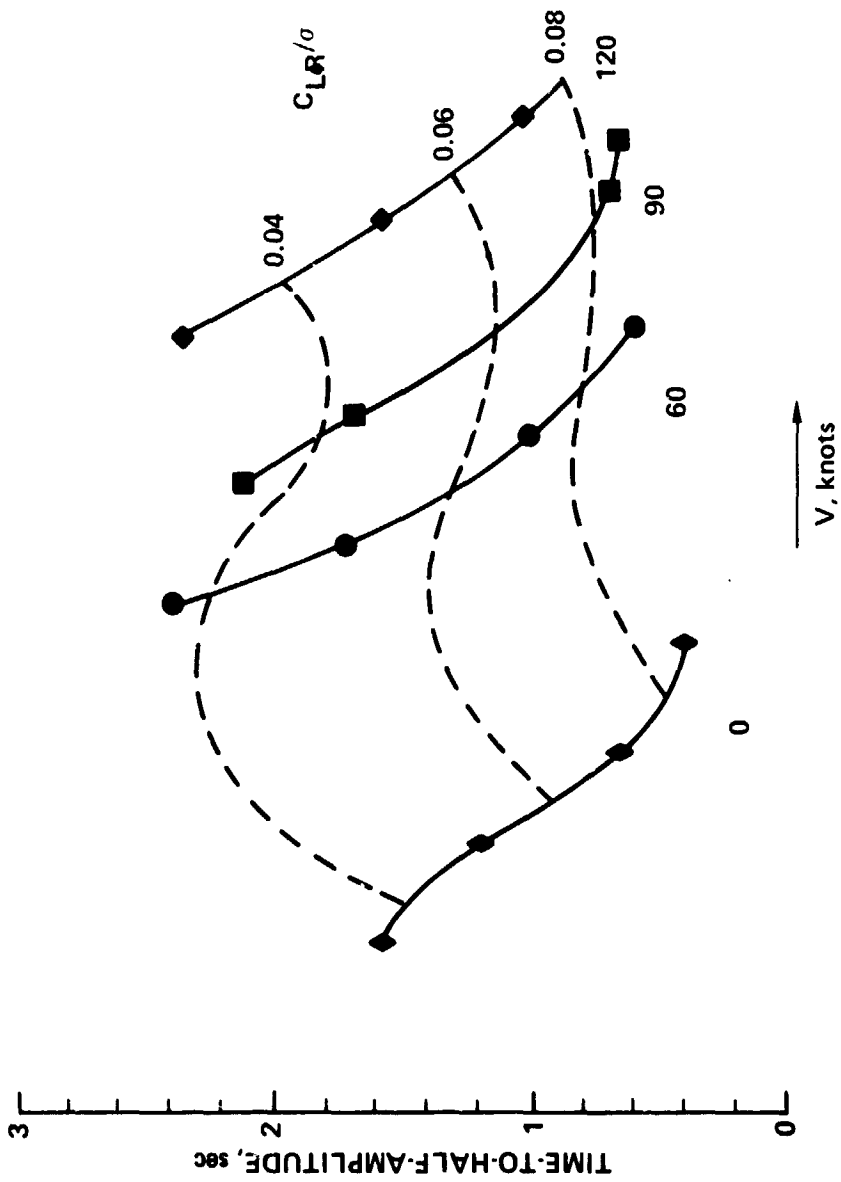


Figure 27.- Uncorrected noise levels of S-76 rotor system;  $\Omega R = 677$  ft/sec.



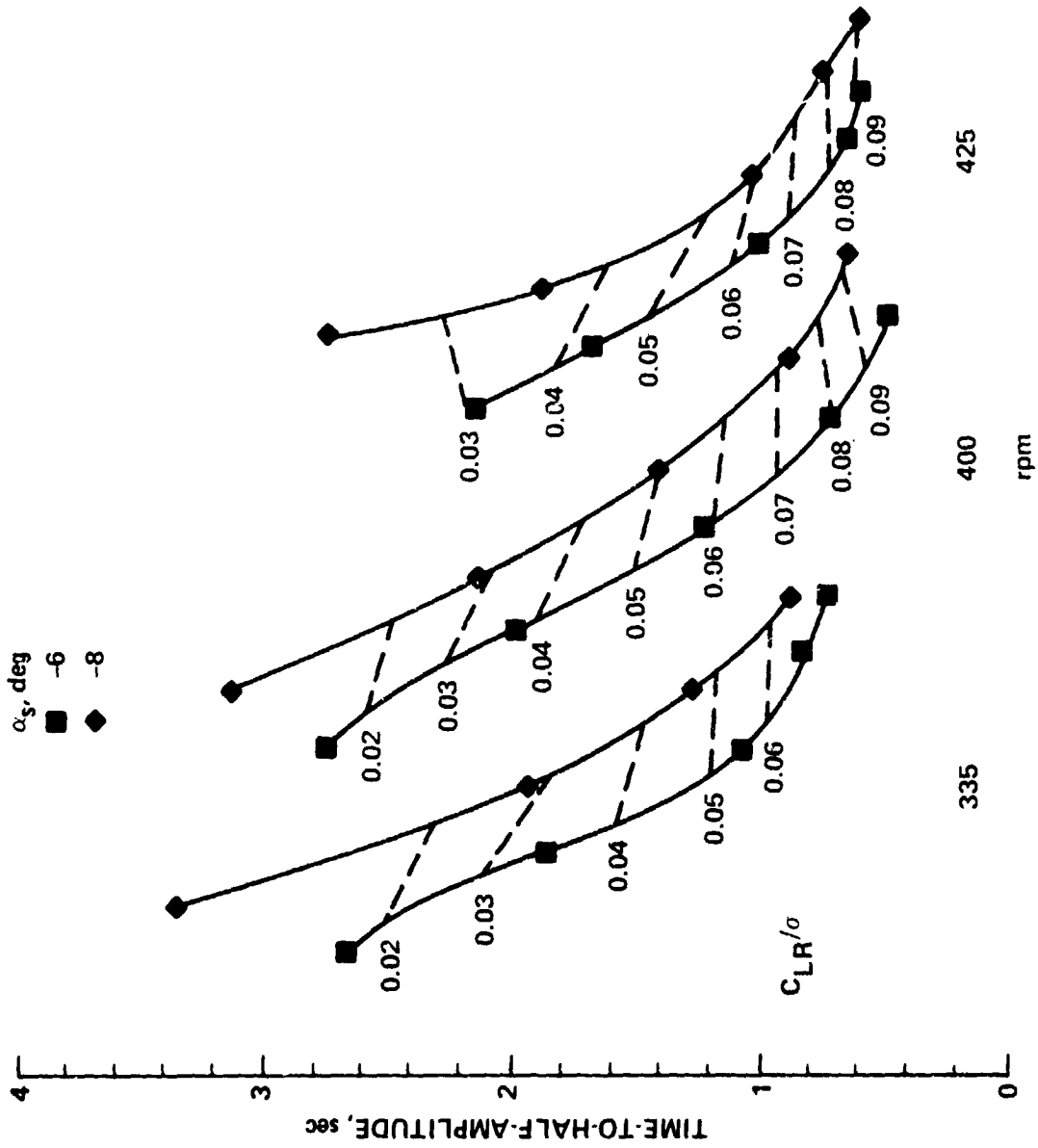
RUN= 7      POINT= 3  
 BLOCK SIZE=1/4      T 1/2= 1.4831 SEC.      1 PER REV= 6.25 HZ  
 R.FREQ.= 4.60 HZ R.DAMP.= 0.01617 F.FREQ.= 1.65 HZ F.DAMP.= 0.045081

Figure 28.- Typical displayed output during helicopter rotor stability testing using a moving-block analysis.



(a) Function of tunnel speed:  $\alpha_s = -6^\circ$ .

Figure 29.- Inplane rotor blade model damping data of the bearingless main rotor on the Ames Rotor Test Apparatus.



(b) Function of rotor shaft angle: 90 knots.

Figure 29.- Concluded.

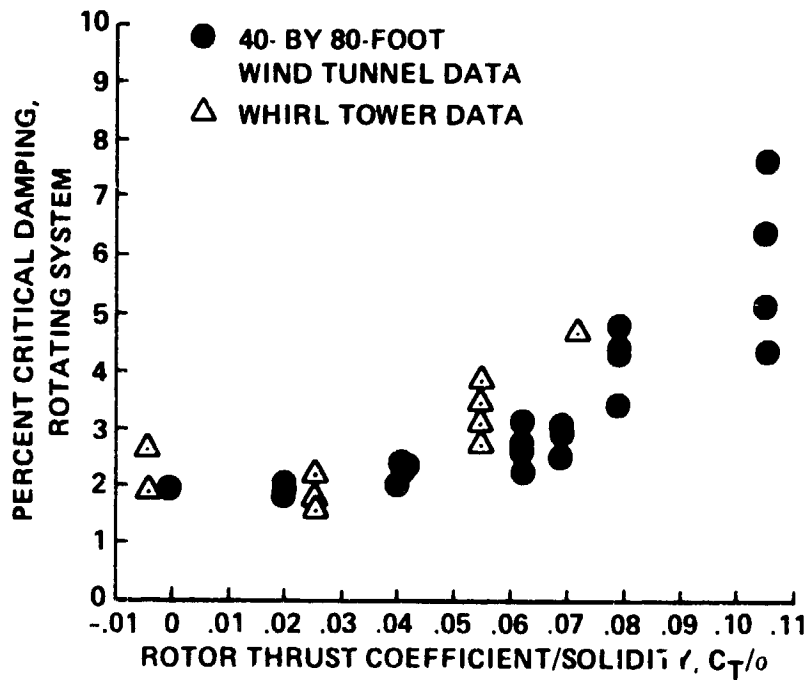


Figure 30.- Hover inplane modal damping of a B0-105 hingeless-rotor system on the Ames Rotor Test Apparatus: 425 rpm.

ORIGINAL PAGE IS  
OF POOR QUALITY



Figure 31.- Rotor/body installation for model interactional aerodynamics test in  
Ames 7- by 10-Foot Subsonic Wind Tunnel.

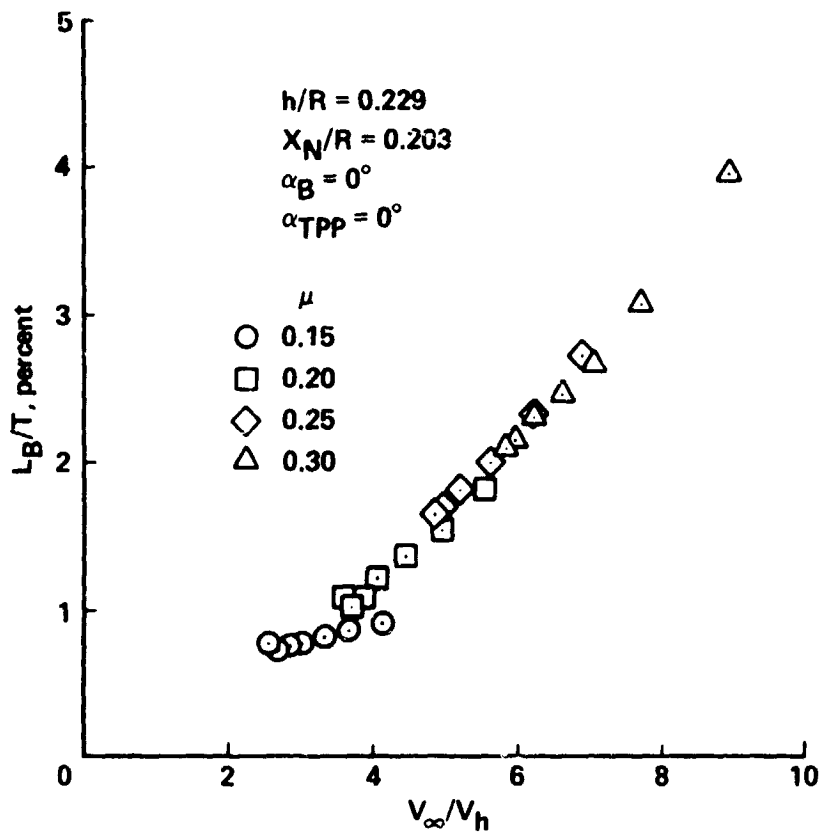


Figure 32.- Variation of fuselage lift with velocity ratio:  $\alpha_s = 0^\circ$ ,  $\alpha_{tip} = 0^\circ$ ,  $V_h = (T/2\rho A)^{1/2}$ .



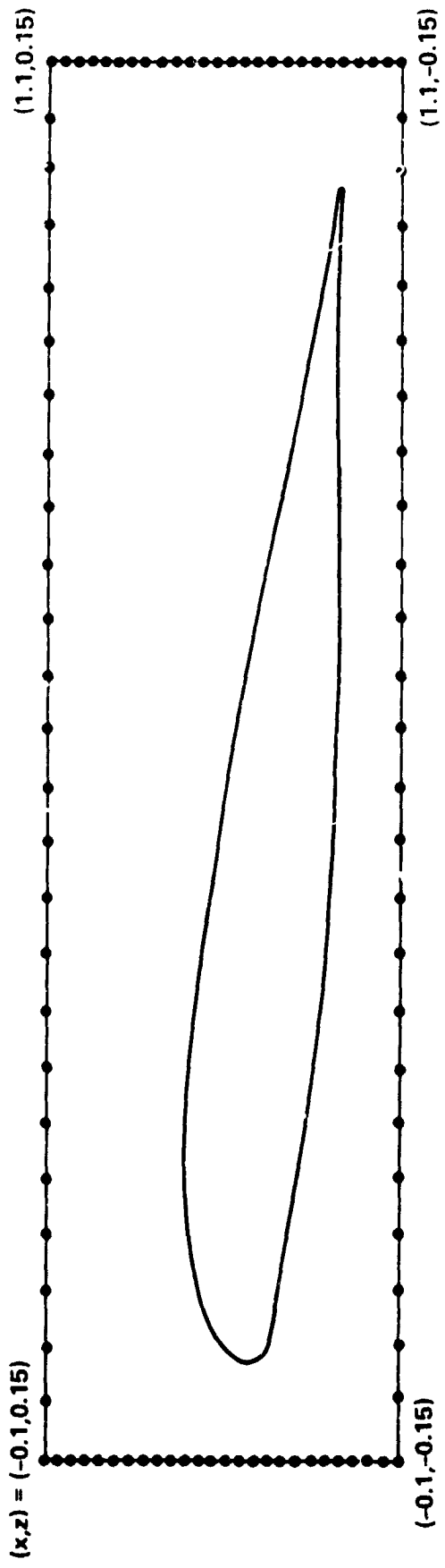


Figure 33.- Schematic of LDV circulation box for flow-velocity measurements.

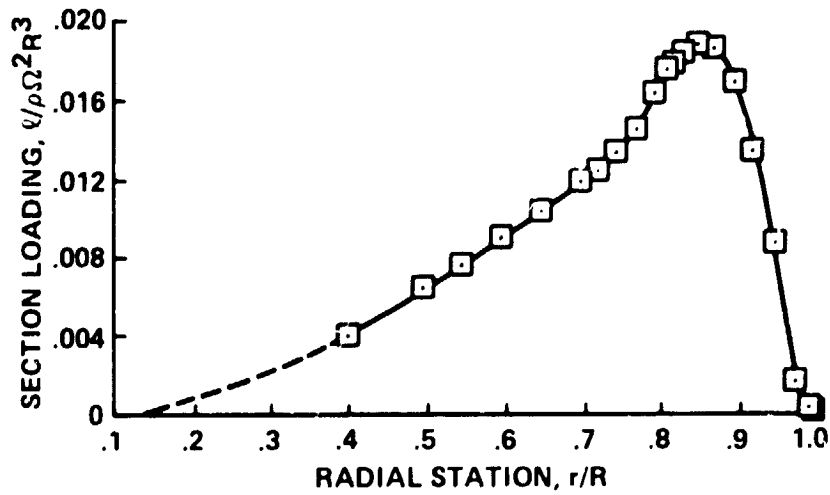


Figure 34.- Blade sectional loading in hover for a model ogee blade tip.

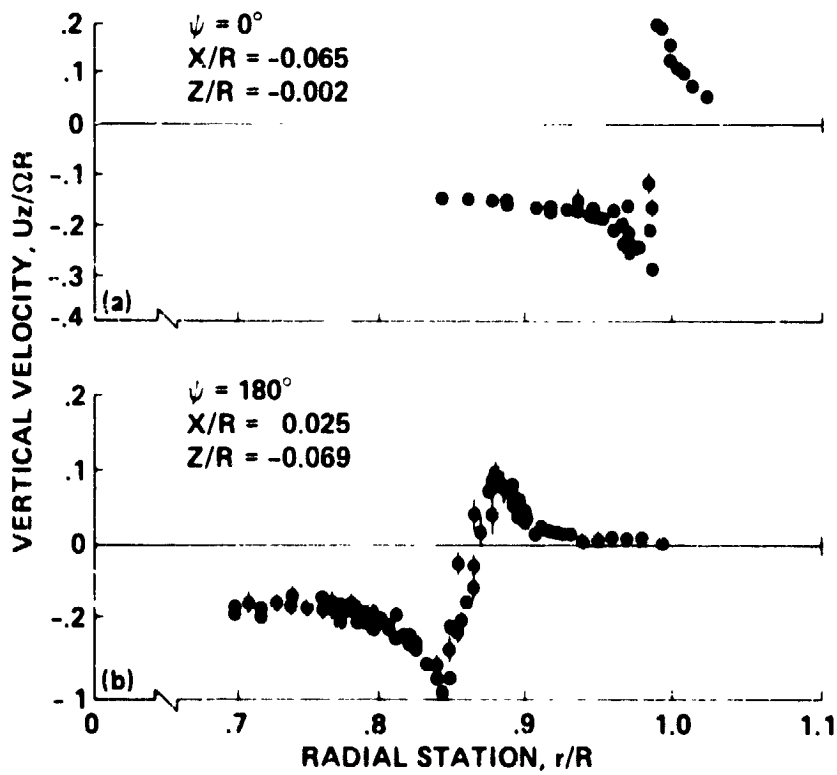


Figure 35.- Wake velocity radial distribution for a model rectangular blade tip.

ORIGINAL PAGE IS  
OF POOR QUALITY

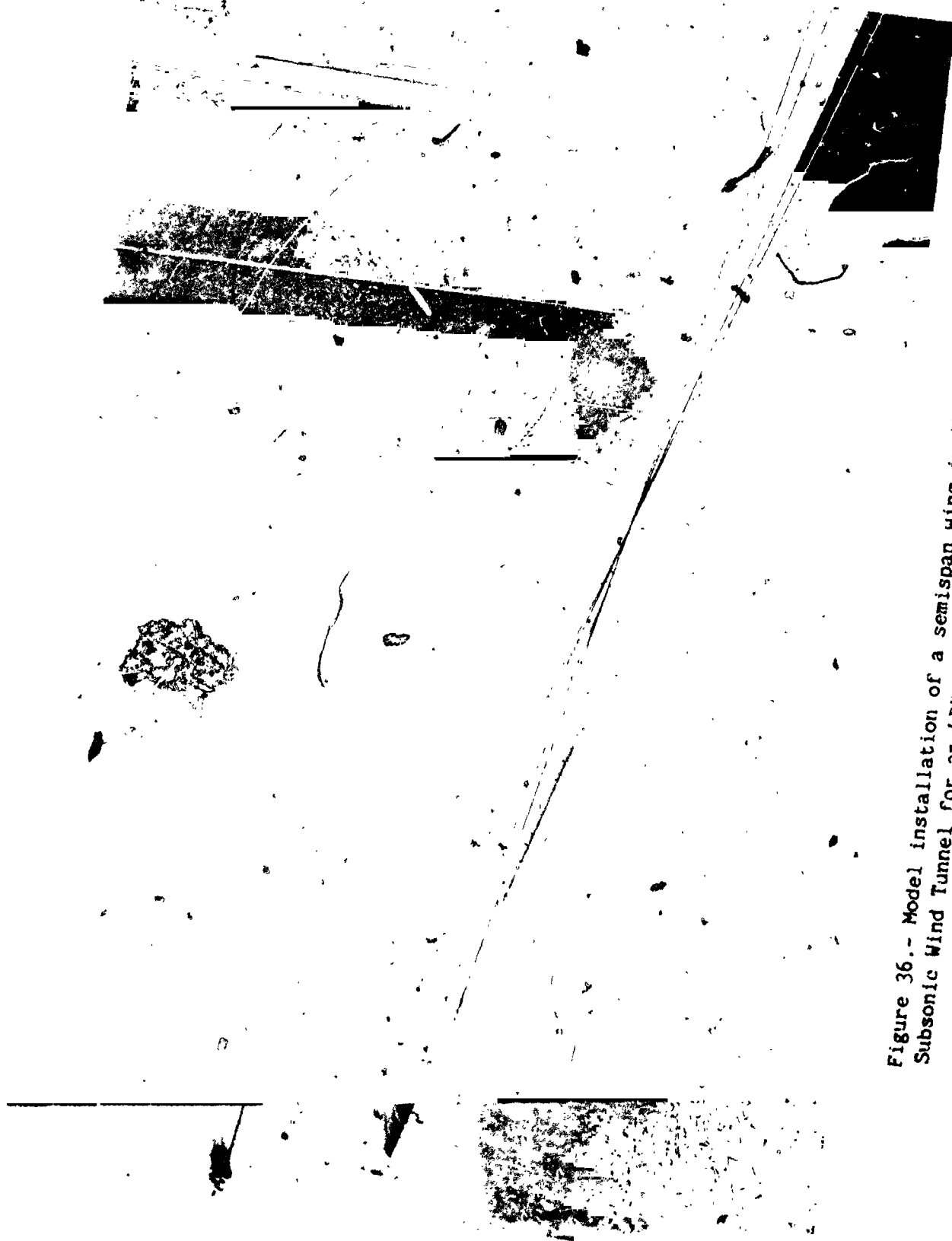


Figure 36.- Model installation of a semispan wing in the Ames 7- by 10-Foot Subsonic Wind Tunnel for an LDV spanwise loading/tip vortex formation test.

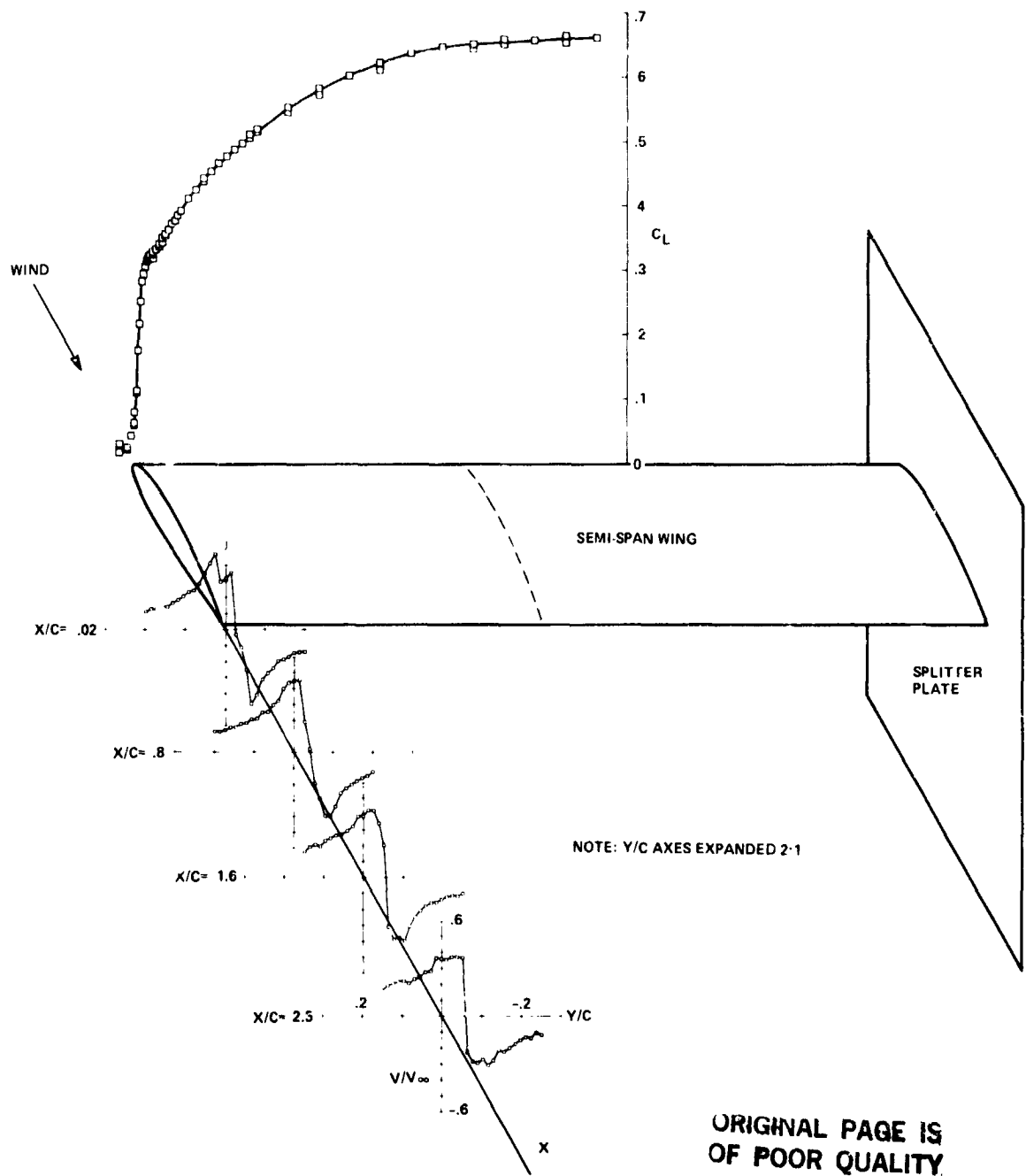


Figure 37.- Spanwise variation in section loading and wake-flow structure of tip vortex.



(a) Rotor/pylon/wing dynamics.

Figure 38.- Tilting prop-rotor tests in the 40- by 80-Foot Wind Tunnel.



(b) XV-15 performance/dynamics test.

Figure 38.- Concluded.

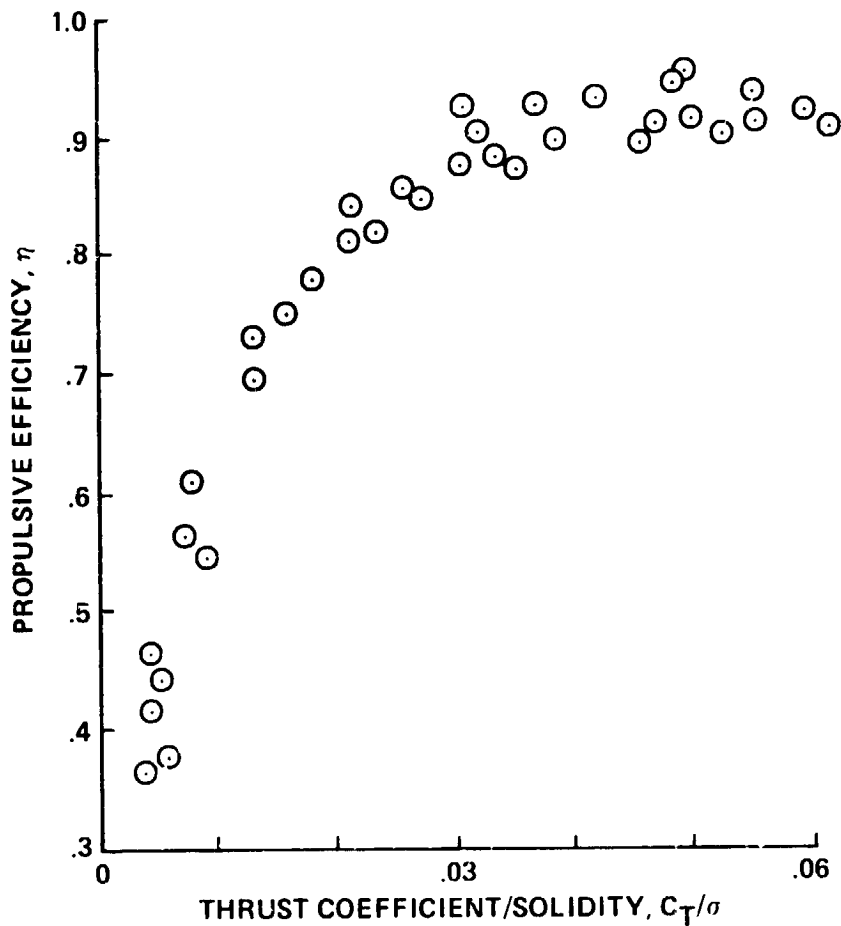


Figure 39.- XV-15 rotor propulsive efficiency as a function of thrust:  
 $0.35 < M_{tip} < 0.65$ ,  $0.34 < V/\Omega R < 0.68$ .

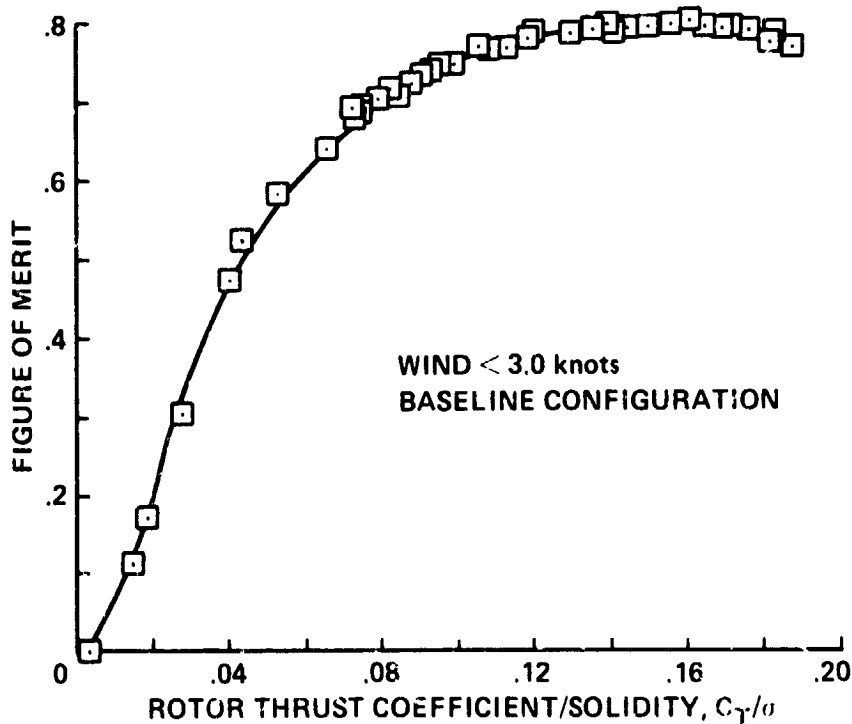


Figure 40.- Isolated tilting-prop rotor performance for XV-15 advanced technology rotor system.

ORIGINAL PAGE IS  
OF POOR QUALITY.



Figure 41.- X-Wing technology demonstrator in the 40- by 80-Foot Wind Tunnel.



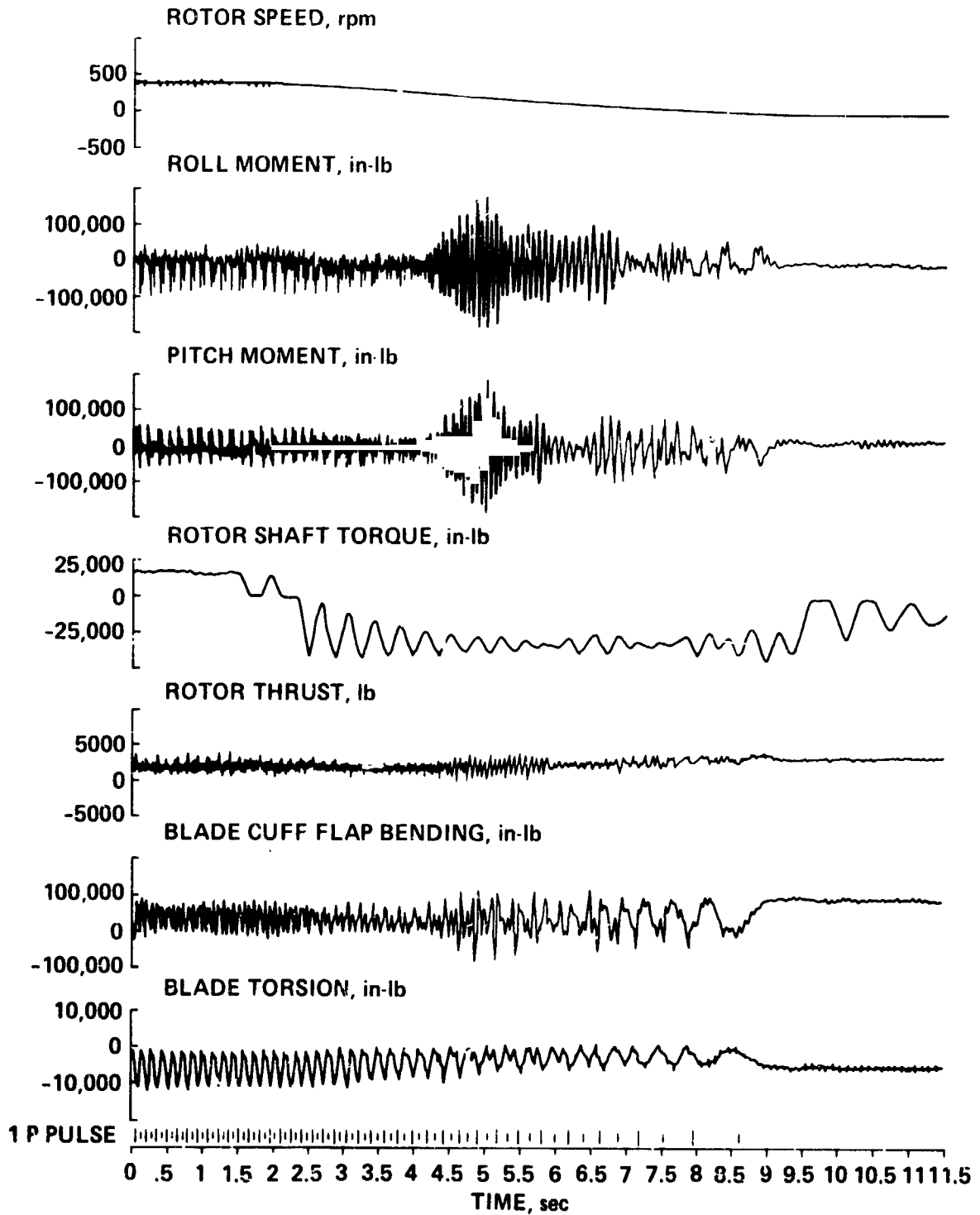


Figure 42.- Time-histories of X-Wing technology demonstrator during conversion from rotary-wing to fixed-wing operation:  $V = 180$  knots.

ORIGINAL SOURCE  
OF POOR QUALITY

1. Report No. NASA TM-86687	2. Government Accession No.	3. Recipient's Catalog No.	
4. Title and Subtitle ROTORCRAFT RESEARCH TESTING IN THE NATIONAL FULL-SCALE AERODYNAMICS COMPLEX AT NASA AMES RESEARCH CENTER		5. Report Date May 1985	6. Performing Organization Code
		8. Performing Organization Report No. 85140	10. Work Unit No.
7. Author(s) William Warmbrodt, Charles A. Smith, and Wayne Johnson		11. Contract or Grant No.	
9. Performing Organization Name and Address Ames Research Center Moffett Field, CA 94035		13. Type of Report and Period Covered Technical Memorandum	
		14. Sponsoring Agency Code 532-06-11	
12. Sponsoring Agency Name and Address National Aeronautics and Space Administration Washington, DC 20546		15. Supplementary Notes Point of Contact: William Warmbrodt, Ames Research Center, MS 247-1, Moffett Field, CA 94035. (415) 694-5642 or FTS 464-5642.	
16. Abstract The unique capabilities of the National Full-Scale Aerodynamics Complex (NFAC) for testing rotorcraft systems are described. The test facilities include the 40- by 80-Foot Wind Tunnel, the 80- by 120-Foot Wind Tunnel, and the Outdoor Aerodynamic Research Facility. The Ames 7- by 10-Foot Subsonic Wind Tunnel is also used in support of the rotor research programs conducted in the NFAC. Detailed descriptions of each of the facilities, with an emphasis on helicopter rotor test capability, are presented. The special purpose rotor test equipment used in conducting helicopter research is reviewed. Test rigs to operate full-scale helicopter main rotors, helicopter tail rotors, and tilting prop-rotors are available, as well as full-scale and small-scale rotor systems for use in various research programs. The specialized data-acquisition and analysis systems used in rotorcraft experiments in these facilities are reviewed. Special test equipment, including several laser Doppler velocimeters (LDVs), are briefly described. Lastly, the test procedures used in conducting rotor experiments are discussed together with representative data obtained from previous test programs. Specific examples are given for rotor performance, loads, acoustics, system interactions, dynamic and aeroelastic stability, and advanced technology and prototype demonstration models.			
17. Key Words (Suggested by Author(s)) Helicopter testing Test technology Wind tunnel testing		18. Distribution Statement Unlimited  Subject Category - 05	
19. Security Classif. (of this report) Unclassified	20. Security Classif. (of this page) Unclassified	21. No. of Pages 90	22. Price*